

January 2020

Development and Validation of a Simplified Transient Two-Phase Flow Model for Any Pipe Inclination

Ligia Tornisiello

Louisiana State University and Agricultural and Mechanical College

Follow this and additional works at: https://digitalcommons.lsu.edu/gradschool_theses



Part of the [Other Engineering Commons](#)

Recommended Citation

Tornisiello, Ligia, "Development and Validation of a Simplified Transient Two-Phase Flow Model for Any Pipe Inclination" (2020). *LSU Master's Theses*. 5045.

https://digitalcommons.lsu.edu/gradschool_theses/5045

This Thesis is brought to you for free and open access by the Graduate School at LSU Digital Commons. It has been accepted for inclusion in LSU Master's Theses by an authorized graduate school editor of LSU Digital Commons. For more information, please contact gradetd@lsu.edu.

DEVELOPMENT AND VALIDATION OF A SIMPLIFIED TRANSIENT TWO-PHASE FLOW MODEL FOR ANY PIPE INCLINATION

A Thesis

Submitted to the Graduate Faculty of the
Louisiana State University and
Agricultural and Mechanical College
in partial fulfillment of the
requirements for the degree of
Master of Science in Petroleum Engineering

in

The Craft & Hawkins Department of Petroleum Engineering

by
Ligia Tornisiello
B.S., Universidade Federal do Ceará, 2017
May 2020

Acknowledgements

I sincerely appreciate the opportunity provided by Dr. Waltrich of working on this project, and his willingness to help me and openness for discussions. I am grateful from the support I received during this period. My appreciation also goes to Dr. Ipsita Gupta and Dr. Mauricio Almeida for serving as committee members and providing valuable feedback.

Special thanks go to my parents, Jose Nivaldo Tornisiello and Leni Tornisiello, for always believing in my potential, providing guidance and encouragement, and supporting me in all decisions. Also thanks to my brother, Rodrigo Tornisiello, for his friendship and for closely looking after my parents. I am very thankful for the companionship and support from my boyfriend, Bruno Xavier. He deeply encouraged me to pursue this degree and was by my side in all the experiences during this period.

I also appreciate the support of my colleagues: Erika Pagan, Renato Coutinho, Valentina Rosales, Jack Blears, Sandeep Gupta, John Estrada, Nicolas Terselich, Nam Tram, Caitlyn Thiberville, Lidia Oliveira, Daniel Oliveira, Felipe Maciel, and Barbara Pontes, with whom I had many conversations and shared great moments.

Table of Contents

Acknowledgements	ii
List of Tables	iv
List of Figures	v
Abstract	ix
1. Introduction	10
1.1. Objectives	13
1.2. Thesis Outline	13
2. Literature Review	15
2.1. Flow Regimes for Two-Phase Flow in Pipes	15
2.2. Steady-State Models for Upward and Inclined Two-Phase Flow in Pipes	20
2.3. Steady-State Models for Downward Two-Phase Flow in Pipes	22
2.4. Transient Two-Phase Flow Modeling	24
3. Evaluation of Models for Steady-State Downward Two-Phase Flow in Vertical Pipe	
Annulus	29
3.1. Flow Regime Predictions	32
3.2. Liquid Holdup Predictions	36
3.3. Pressure Gradient Predictions	39
3.4. Evaluation Summary and Remarks	42
4. Description of the Simplified Transient Two-Phase Flow Model	43
4.1. Mathematical Modeling	44
4.2. Simulator Algorithm	51
5. Model Results and Discussions	55
5.1. Test Well Data for Vertical Downward Flow in the Pipe Annulus	55
5.2. Large-Scale Flow Loop for Vertical Upward Flow in the Tubing	65
5.3. Synthetic Data from OLGA Simulator	70
6. Conclusions and Recommendations for Future Work	96
Appendix A. Bhagwat and Ghajar (2014) Drift-Flux Distribution Parameter and Drift Velocity Correlations	98
References	101
Vita	106

List of Tables

Table 2.1. Review summary of published works on downward two-phase flow in pipes	23
Table 3.1. Flow regime transition criteria (Usui and Sato, 1989).....	31
Table 3.2. Void fraction correlations (Usui and Sato, 1989).....	32
Table 4.1. Range of the parameters of the experimental data used for the development of the correlations of Bhagwat and Ghajar (2014).....	47
Table 5.1. Experimental conditions of the data from Waltrich (2012).....	66
Table 5.2. Synthetic cases generated with the commercial simulator OLGA for vertical downward flow	71
Table 5.3. Synthetic cases generated with the commercial simulator OLGA for inclined downward flow	79
Table 5.4. Synthetic cases generated with the commercial simulator OLGA for horizontal flow	82
Table 5.5. Synthetic cases generated with the commercial simulator OLGA for vertical upward flow	86
Table 5.6. Synthetic cases generated with the commercial simulator OLGA for inclined upward flow	91
Table 5.7. Recommend range of applicability of the simulator developed in this work	95

List of Figures

Figure 2.1. Flow regimes for different inclination angles and flow direction	16
Figure 2.2. Flow regimes for gas-liquid flow in horizontal pipes	17
Figure 2.3. Flow regimes for gas-liquid upward flow in vertical pipes.....	18
Figure 3.1. Comparison of the flow regime map for downward two-phase flow in annulus experimentally obtained by Coutinho (2018) and the map for downward two-phase flow in a 1-in ID pipe obtained by Usui and Sato (1989)	33
Figure 3.2. Comparison of the flow regime map for downward flow in annulus experimentally obtained by Coutinho (2018) and the map for downward flow in a 1 in ID pipe developed by Beggs and Brill (1973) theoretical model	34
Figure 3.3. Comparison of the flow regime map for downward flow in annulus experimentally obtained by Coutinho (2018) and the map for downward flow in a 1 in ID pipe developed by Usui (1989) theoretical model.	35
Figure 3.4. Comparison of the flow regime map for downward flow in annulus experimentally obtained by Coutinho (2018) and the map for downward flow in a 1 in ID pipe obtained using OLGA.	35
Figure 3.5. Comparison of experimental liquid holdup for annulus (Coutinho, 2018) and tubing (Usui and Sato, 1989) with the same hydraulic diameter, and values calculated with Usui (1989), Beggs and Brill (1973), Bhagwat and Ghajar (2014), and OLGA	37
Figure 3.6. Comparison of experimental liquid holdup for downward vertical flow in annulus (Coutinho, 2018) on Y axis and liquid holdup calculated with (a) Bhagwat and Ghajar (2014) correlation and (b) Beggs and Brill (1973) model on X axis.....	39
Figure 3.7. Comparison of experimental pressure gradient for downward two-phase flow in annulus (Coutinho, 2018) and values calculated with Beggs and Brill (1973) model and OLGA	41
Figure 4.1. Schematic of time and space discretization for the model developed in this work....	49
Figure 4.2. Flowchart for the model algorithm.....	51
Figure 4.3. Screenshot of the input data section of the simulator developed in this work	53
Figure 5.1. Schematic of the field-scale test well used in Coutinho (2018)	56
Figure 5.2. Test matrix for Coutinho (2018) experimental data set for downward flow in the annulus	57

Figure 5.3. Boundary conditions (standard gas and water flowrates and pressure at the bottom of the tubing-casing annulus as a function of time) for a certain experimental run.	58
Figure 5.4. Injection pressure as a function of time. Comparison of results from the simulator of this work, OLGA and experimental data from Coutinho (2018).	59
Figure 5.5. Liquid holdup as a function of measured depth at different time steps.....	60
Figure 5.6. Liquid holdup as a function of time at the bottom of the well	61
Figure 5.7. Average error for pressure calculated with the model from this work in relation to the experimental data	62
Figure 5.8. Comparison of injection pressure predicted in this work, calculated with OLGA and experimental (Coutinho, 2018) for two different runs	63
Figure 5.9. Gas and water injection rates for a fast transient case and the comparison of injection pressure predicted in this work, calculated with OLGA and experimental	64
Figure 5.10. Schematic of TowerLab (Waltrich, 2012).....	66
Figure 5.11. Liquid holdup (a) at the top and (b) bottom of the test section - Case 1.....	67
Figure 5.12. Pressure at the inlet of the fluids (bottom of the test section) – Case 1.	68
Figure 5.13. Liquid holdup at (a) the top and (b) bottom of the test section – Case 2.	68
Figure 5.14. Pressure at the inlet of the fluids (bottom of the test section) – Case 2.	69
Figure 5.15. Liquid holdup at (a) the top and (b) bottom of the test section – Case 3.	69
Figure 5.16. Pressure at the inlet of the fluids (bottom of the test section) – Case 3.	69
Figure 5.17. Comparison of results using the simulator of this work and OLGA for liquid holdup and pressure at three locations in vertical downward flow in the annulus.	73
Figure 5.18. Errors for liquid holdup and pressure at the top, middle and bottom grid blocks for (a) Case 1, (b) Case 6, and (c) Case 7	74
Figure 5.19. Snapshots of the simultaneous video recording from Waltrich (2015) at three different axial locations in the test section at different times.	76
Figure 5.20. Maximum error for liquid holdup predictions for vertical downward flow ($\theta = -90^\circ$).....	77
Figure 5.21. Maximum error for pressure predictions for vertical downward flow ($\theta = -90^\circ$).....	77

Figure 5.22. Comparison of results using the simulator of this work and OLGA for liquid holdup and pressure at three locations in inclined downward flow in the annulus.	79
Figure 5.23. Errors for liquid holdup and pressure at the top, middle and bottom grid blocks for (a) Case 1, (b) Case 6, and (c) Case 7	80
Figure 5.24. Maximum error for liquid holdup prediction for Inclined downward flow ($\theta = -45^\circ$).....	81
Figure 5.25. Maximum error for pressure prediction for Inclined downward flow ($\theta = -45^\circ$).....	81
Figure 5.26. Comparison of results using the simplified model and OLGA for liquid holdup and pressure at three locations (inlet, middle and outlet of horizontal pipe) as a function of time, for (a) Case 1, (b) Case 2, (c) Case 3, and (d) Case 4.....	83
Figure 5.27. Comparison of results using the simplified model and OLGA for liquid holdup and pressure at three locations (inlet, middle and outlet of horizontal pipe) as a function of time, for (a) Case 5, (b) Case 6, and (c) Case 7.	84
Figure 5.28. Maximum error for liquid holdup predictions for horizontal flow ($\theta = 0^\circ$)	85
Figure 5.29. Maximum error for pressure predictions for horizontal flow ($\theta = 0^\circ$)	85
Figure 5.30. Comparison of results using the simulator of this work and OLGA for liquid holdup and pressure at three locations for a slug-bubbly flow regime case in vertical upward flow in the tubing.....	87
Figure 5.31. Comparison of results using the simulator of this work and OLGA for liquid holdup and pressure at three locations for a slug-annular flow regime case in vertical upward flow in the tubing.....	87
Figure 5.32. Errors for liquid holdup and pressure at the top, middle and bottom grid blocks for (a) Case 3, (b) Case 4, and (c) Case 5	88
Figure 5.33. Maximum error for holdup prediction for vertical upward flow ($\theta = 90^\circ$)	90
Figure 5.34. Maximum error for pressure predictions for vertical upward flow ($\theta = 90^\circ$).	90
Figure 5.35. Errors for liquid holdup and pressure at the top, middle and bottom grid blocks for (a) Case 1, (b) Case 2, (c) Case 3, (d) Case 4, and (e) Case 5.....	92
Figure 5.36. Maximum error for the liquid holdup predictions for inclined upward flow ($\theta = 45^\circ$)	93
Figure 5.37. Maximum error for pressure predictions for inclined upward flow ($\theta = 45^\circ$).....	93
Figure 5.38. Summary of maximum error for liquid holdup for all cases in all pipe inclinations.....	94

Figure 5.39. Summary of maximum error for pressure for all cases in all pipe inclinations. 94

Abstract

This study describes the development and validation of an improved simplified model for transient two-phase flow for any pipe inclination. The simplified model proposed has been validated with field-scale test well and laboratorial data, and also compared to the state-of-the-art commercial simulator for transient two-phase flow in pipes. The results of the simplified model showed an agreement within the range of $\pm 30\%$ for the holdup predictions for 65% of the scenarios, and an agreement within the range of $\pm 30\%$ for the pressure predictions for 82% of the scenarios considered in this work.

In the oil and gas industry, transient two-phase flow is present in many production and drilling operations, such as in well unloading, well control, and managed pressure drilling. There are many commercial transient multiphase flow simulators available, which use complex numerical procedures to describe multiphase flow in pipes and estimate variables of interest, such as pressure, temperature, phase fractions, and flow regimes discretized in space and time.

Many of the transient flow scenarios encountered in the industry are considered slow transients and a rigorous transient simulator may not be necessary in these cases. With a few simplifications of the fundamentals equations, less complex models can be deployed in such cases without significantly compromising the accuracy of the results. With this consideration, and taking the fact that acquiring a license of a commercial software can be prohibitive for small operators and consulting companies, an easy-to-use and open source simulator was implemented based on the simplified transient model discussed in this work.

1. Introduction

The understanding of fluid flow in pipes is fundamental for the oil and gas industry. There are processes that can be simulated as steady-state, and other more complex operation analysis that require transient simulations. Steady-state simulations are generally used for equipment sizing such as design of pipe diameters, and sizing of pumps and compressors. On the other hand, pipeline start-ups and shut-downs, line depressurization, terrain slugging, and ramp-up slugging require transient simulations.

Earliest studies on steady-state models date back from the 1950's, when some investigators started developing empirical correlations from experimental data (Hagedorn and Brown, 1965; Duns and Ros, 1963; Orkiszewski, 1967; Aziz et al., 1972; Beggs and Brill, 1973; Mukherjee and Brill, 1985). More recently, the popularization of personal computers in the 1980's facilitated the employment of these empirical models by the major oil companies for prediction of pressure drop and flow rates in wells and pipelines. However, the empirical models proved to be limited in accuracy. This issue could only be solved with the introduction of physical models. Fueled by this need, the industry invested in multiphase flow research consortiums and several test facilities were built. This led to the development of several mechanistic models (Ansari et al., 1994; Hasan and Kabir, 1988; Hasan and Kabir, 1990).

The necessity to simulate processes in which operational conditions change, such as inlet flow rates and outlet pressure, led to the development of transient models. A discussion on the evolution of multiphase steady-state and transient flow modeling is presented on Shippen and Bailey (2012). Analysis of transient flow though was pioneered by the nuclear industry because of the necessity to analyze the loss of coolant accidents related to nuclear reactor safety (Shoham, 2006). This phenomena consist of fast transients of steam and water in small diameter pipes (e.g.,

diameter of around 1 inch). However, unlike transient phenomena in the nuclear industry, most transient multiphase flows in the petroleum industry are slow (Danielson et al., 2000; Shoham, 2006). Slow transients are characterized by gradual changes in the operational conditions with time (for instance, changes in the liquid rate of the order of one barrel per day per second). They are common in oil and gas production systems because of the usual pipe sizes and the nature of the reservoir production changes. Typically, reservoir production rate changes are of the order of days or months. However, production start-ups or shut-downs may not fall in this range.

The industry efforts to attain models that can be used as design tools for transient processes resulted in the development of complex computer codes and commercial software, such as OLGA and LEDAFlow. On the opposite trend, there has been a recent movement for simpler models that can be applied to specific transient conditions. Several authors (Taitel et al., 1989; Lorentzen et al., 2001; Li et al., 2012; Choi et al., 2013; Ambrus et al., 2015) have developed simplified transient multiphase flow models, which have lower computational requirements and simpler codes.

As it will be discussed later, the majority of the simplified transient models available in the literature are for horizontal flow. The mathematical approaches and limitations of some simplified transient models for both horizontal and vertical flow are discussed in Chapter 2.

To the knowledge of the author, there is no simplified transient model that has been validated and proved to be capable of simulating transient two-phase flow for any inclination for a wide range of scenarios. Only simulators which include the transient conservations of mass, momentum and energy equations are capable of simulating these wide range of flow scenarios. However, the complexity of implementation, availability, and cost of acquiring a license of a commercial software is high (in the order of tens of thousands of dollars). For these reasons, the wide use of transient simulators is scarce, and consequently, only large operators and research

institutions are the primary users of such costly and sophisticated codes. Therefore, it may not be feasible for small operators and consulting companies to simulate and optimize their design of fluid flow for important transient scenarios.

These circumstances motivated the development of a simplified transient multiphase flow model that can represent the physics of transient phenomena, with lower implementation and computational costs, easy-to-use, and without jeopardizing much of the results accuracy.

Another advantage of the development of a simplified transient model is the possibility for continuous improvement of the code. The less complex the code, the easier is the implementation of modifications. For instance, part of this study included the implementation and validation of transient downward two-phase flow in annulus. To the knowledge of the authors, not even steady-state flow models are available for such case. The implementation and validation of the downward flow in annulus would probably not be possible in the timeframe of this study if using the more complex transient model available in the literature.

As it was mentioned earlier, the transient phenomena in the oil and gas industry are generally considered slow. Although there is no quantitative definition in the literature for what can be considered as fast or slow transient, several studies discuss the circumstances under which some inherently transient phenomena can be approximated as a sequence of steady states over short time periods (Danielson et al., 2000; Fan and Danielson, 2009; Al-Safran and Brill, 2017). The literature review also shows that for these slow transients, it is reasonably accurate to solve the mass conservation equations in time and space, but use a pseudo-steady-state approach for the momentum and energy equations.

1.1. Objectives

The objective of this thesis is to develop an improved simplified transient flow model, based on the formulation of a model available in the literature (Choi et al., 2012). The model developed and validated in this study should simulate transient flow for any pipe inclination (e.g., pipe inclinations from -90° to $+90^\circ$ with the horizontal direction). The model proposed by Choi et al. (2012) is limited for pipe inclinations from -30° to $+90^\circ$ with the horizontal direction, and to the knowledge of the author, it has not been validated for transient flow in a wide range of flowing conditions and pipe inclinations/geometries (such pipe annulus and vertical downward two-phase flow).

The desired characteristics of the simulator developed in this study should also include:

- Low computational cost;
- Open source (e.g., users are be able to easily modify the source code).
- Validated for transient downward two-phase flow in annulus.
- Provided of a generic method to determine slow transient in order to guide the user on the applicability of the simplified simulator.
- Verified for several pipe inclinations and flow directions. The verification database includes well test and experimental data, and simulation results from the state-of-the-art transient simulator OLGA.

1.2. Thesis Outline

This thesis is divided into six chapters. Chapter 1 describes the problem and the motivation of this thesis, as well as the importance of this research and its objectives. Chapter 2 reviews the flow regimes for two-phase flow in pipes, the differences between upward and downward flow, and steady-state multiphase flow models for both flow directions. In addition to that, it discusses

the methods of some simplified transient models and their limitations. Chapter 3 describes a comparison between experimental data in steady-state for vertical downward two-phase flow in annulus and theoretical models. Chapter 4 presents the mathematical formulation of the improved simplified transient model developed in this work, and discusses its implementation in Excel Visual Basics for Applications. Chapter 5 presents the validation of the model with experimental data and a commercial simulator. Finally, Chapter 6 presents the conclusions and lists recommendations for future work.

2. Literature Review

This chapter is subdivided into four main sections:

- i. The first section outlines the flow regimes observed for two-phase flow in different pipe inclinations.
- ii. The second outlines the steady-state models available in the literature for upward two-phase flow in pipes.
- iii. Third section outlines the steady-state models available in the literature for downward two-phase flow in pipes. The focus of the second and third sections is to summarize the findings from other authors in regards to the main differences between upward and downward two-phase flow.
- iv. The fourth section briefly discusses the development of transient models for two-phase flow, including the main two modelling approaches (two-fluid model and drift-flux model), and reviews some simplified transient models available in the literature. The main focus of this section is to compare the formulations and approaches and to list the limitations of these models.

Since the simplified transient model of this work aims at being applicable to any pipe inclination, the main goal of the literature review is to search steady-state flow models that can be applied to any pipe inclination that are most appropriate to be utilized in the formulation.

2.1. Flow Regimes for Two-Phase Flow in Pipes

Most models have different procedures for the calculation of liquid holdup and pressure drop for each flow regime. For mechanistic models (Shoham, 2006), once the flow regime is predicted, the models determine the liquid holdup, which is typically the central problem in multiphase flow in pipes. Liquid holdup is the most fundamental parameter in two-phase flow in

pipes, since it is a required input for many important parameters such as the two-phase mixture density, two-phase mixture viscosity, actual velocities of each phase, and, most importantly for the oil and gas industry analysis, for the determination of the two-phase pressure drop.

The prediction of the flow regime is key in multiphase flow. As shown in Figure 2.1, the flow regimes can be considerably different depending on the pipe inclination and geometry, and flow direction. Multiphase flow is governed by liquid inertia, buoyancy, gravity and surface tension forces. The resultant of these forces determine the main characteristics of the flow regimes.

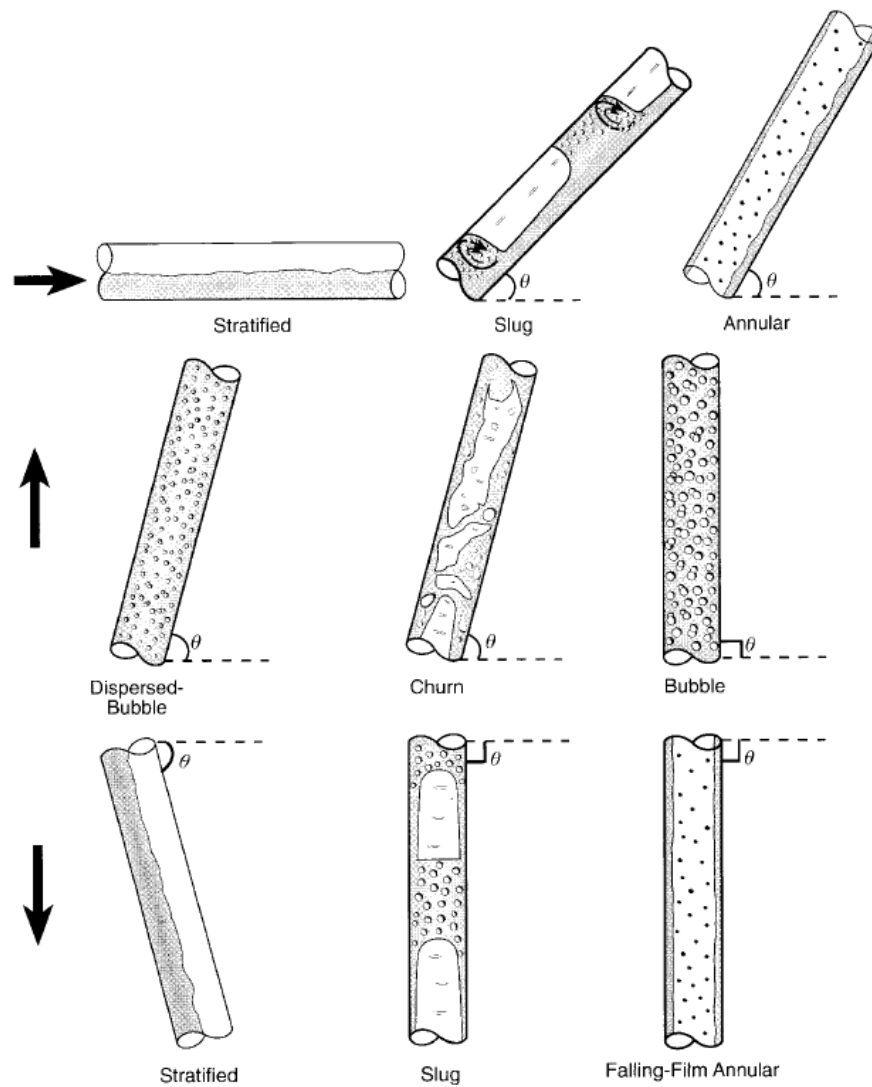


Figure 2.1. Flow regimes for different inclination angles and flow direction (Shoham, 2006).

For horizontal flow, the major flow regimes observed are stratified (smooth or wavy), intermittent (slug or elongated-bubble), annular and dispersed-bubble (Figure 2.2). Stratified flow regime occurs at low gas and liquid flow rates, for which the two phases are separated by gravity. Stratified-wavy occurs at higher gas rates than stratified-smooth. In intermittent flow regime, there is alternate flow of gas and liquid. Both elongated-bubble and slug are characterized by the same flow mechanism, but in the former the liquid slug is free of entrained bubble, because it occurs for relatively lower gas rates. For very high gas and liquid rates, the flow regime is annular, with the gas flowing with high velocity in the core and liquid flowing in a thin film around the pipe wall. For very high liquid rates, the flow regime is dispersed-bubble, which is characterized by a continuous phase of liquid with gas dispersed as discrete bubbles (Shoham, 2006).

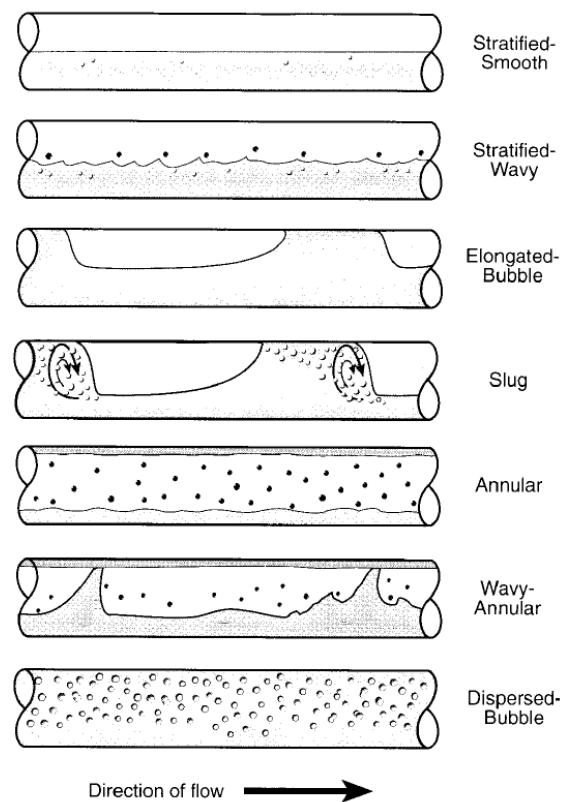


Figure 2.2. Flow regimes for gas-liquid flow in horizontal pipes (Shoham, 2006).

For vertical and inclined upward two-phase flow in pipes, the stratified flow regime disappears, and the major flow regimes observed are dispersed-bubble, bubble, slug, churn and annular (Figure 2.3). For inclined downward flow, stratified is the dominant flow regime, occurring for a wide range of downward inclination angles (0 to -80°) and for a wide range of gas and liquid flow rates (Shoham, 2006). For vertical downward flow (-90°), the stratified flow regime disappears and the flow regimes observed are bubble, slug, falling film and annular (Figure 2.1).

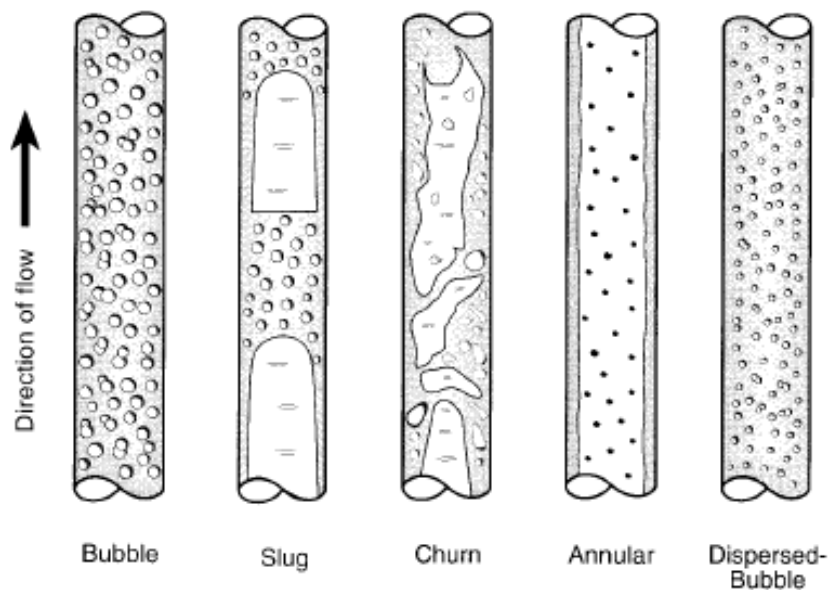


Figure 2.3. Flow regimes for gas-liquid upward flow in vertical pipes (Shoham, 2006).

For vertical upward flow in pipes, bubbly flow pattern is observed at low gas and high liquid flow rates. The liquid inertia and buoyancy force act in the same direction, assisting the gas bubbles to rise in the vertical upward direction. In contrast, in downward flow in pipes, these forces act in opposite directions to each other, and then the gas phase resists the liquid flow. Oshinowo and Charles (1974) and Bhagwat and Ghajar (2012), observed that the bubbles concentrate in the axis region in downward flow.

Slug flow regime in upward flow in pipes is characterized by elongated gas bubble (called Taylor slugs) oriented in the direction of the mean flow and by a film of liquid falling on the walls. For downward flow in pipes, some authors have reported appearance of slug flow, however the slugs have different shapes, with blunt nose shape or flat ends (Bhagwat and Ghajar, 2012).

Churn flow regime is observed in upward flow when the gas flow rate is increased, from the condition for slug flow regime, so that the slugs are disintegrated. Authors report that churn flow regime is unique to upward flow (Oshinowo and Charles, 1974; Bhagwat and Ghajar, 2012).

Falling film flow pattern is characterized by a wavy liquid film flowing down the pipe surface and gas flowing in the core region. It is unique to vertical downward two-phase flow and it is observed for low gas and liquid flowrates.

Annular flow regime appears for high gas and liquid flowrates in upward flow in pipes. In upward flow, gas phase in the core moves faster than the surrounding liquid film, while in downward flow the liquid phase moves faster than the gas phase because of the influence of gravity and high inertia. Bhagwat and Ghajar (2012) says that there is no quantitative distinction between falling film and annular flow.

This discussion points out the main differences between upward and downward flow in pipes. The development of the simplified transient model of this work required a deeper understanding on flow in the annulus. The content of this thesis include such more extensive discussion on experimental and modeling studies for downward flow in annulus, a study on the validity of correlations for liquid holdup or void fraction and pressure gradient developed for downward flow in pipes when used for predicting these variables in downward flow in annulus, and the description of the mathematical formulation of the proposed model, along with its validation.

2.2. Steady-State Models for Upward and Inclined Two-Phase Flow in Pipes

The first developed models for two-phase systems were referred to as “black box” models, since they ignored the different two-phase flow regimes. Among these models is the drift-flux approach, which treats the two-phase flow as a homogenous mixture but allows slippage between the gas and liquid phases (Shoham, 2006).

The concept of drift-flux was originally developed by Zuber and Findlay (1965), and later improved by Wallis (1969) and Ishii (1977). The drift-flux model correlates the void fraction (the complement of the liquid holdup) with the superficial velocity of the gas phase (v_{SG}), the two-phase mixture velocity (v_m), the distribution parameter (C_o), and the drift velocity (v_d).

The distribution parameter (C_o) accounts for the distribution of the gas phase across the pipe cross section and acts as a correction factor for the assumption of no local slippage between the liquid and gas phases. The drift velocity (v_d) represents the cross sectional void fraction weighted average of the local relative velocity of the gas phase with respect to the two-phase mixture velocity at the pipe volume center. Several authors have developed correlations for prediction of the distribution parameter and the drift velocity as a function of pipe diameter and inclination, and fluid properties (Hasan, 1995; Hibiki and Ishii, 2002; Goda et al., 2003; Bhagwat and Ghajar, 2014; Rassame and Hibiki, 2018).

Starting at early 1960s, empirical correlations from experimental data (Hagedorn and Brown, 1965; Duns and Ros, 1963; Orkiszewski, 1967; Aziz et al., 1972; Beggs and Brill, 1973; Mukherjee and Brill, 1985) were developed. Since these models were derived by fitting experimental data, theoretically they may not give accurate predictions for conditions outside of the experimental data used for developing the model. However, over the years these empirical correlations have proven to be as accurate as mechanistic models. Therefore, there is still debates

to this date if mechanistic models are more accurate than empirical correlations for two-phase flow in pipes (Shippen and Bailey, 2012).

One of the most well-known empirical model is Beggs and Brill (1973). Although it was developed to the entire range of inclination angles, based on comparisons with data and the results from other models, the model is not recommended for vertical upward flow because it under predicts the pressure loss for this case (Shoham, 2006). Hagedorn and Brown (1965) is better suited for vertical upward flow. A discussion on the applicability of these models is presented in Mukherjee and Brill (1985).

With the allegedly accuracy limitation of empirical models, there was a motivation to introduce more physics in the models, and several mechanistic models (Ansari et al., 1994; Hasan and Kabir, 1988; Hasan and Kabir, 1990) were developed. In these models, transition criteria are defined as functions of the flow regimes, and the liquid holdup and pressure gradient are calculated differently for each flow regime.

Several factors need to be considered when choosing a model for two-phase flow in pipes. The first would be based on the type of fluids, flow direction, and pipe inclination, preferably within the range of the values that the models were developed for. A second factor to be considered relates to complexity. Empirical models are indeed much simpler than mechanistic models and might be faster if used for the pseudo-steady-state approach for the momentum conservation equations, considering a simplified transient model.

As it will be discussed in Chapter 4, for the simplified transient model of this work, the drift-flux model from Bhagwat and Ghajar (2014) is used. As Chapter 3 will show, this decision was based on the wide range of the variables used for the development of these correlations, its

simplicity, which allows for easy implementation and low computational cost, and its accuracy when evaluated with field-scale test well and laboratorial experimental data.

2.3. Steady-State Models for Downward Two-Phase Flow in Pipes

Downward two-phase flow has not been studied as extensively as upward flow. Studies found on the literature include the investigations by Golan and Stenning (1969), Oshinowo and Charles (1974), Yamazaki and Yamaguchi (1979), Barnea et al. (1982), Usui (1989), Usui and Sato (1989), Hernandez et al. (2002), Bhagwat and Ghajar (2012), and Almabrok et al. (2016). Table 2.1 summarizes the experimental conditions included in the investigation of these authors. These studies consider downward two-phase flow in pipes, and, to the knowledge of the author, there are no studies available for downward two-phase flow in annulus.

Golan and Stenning (1969) developed the first empirical flow regime map for vertical downward two-phase flow in pipes. Based on their investigation, they concluded that the void fraction correlations developed for vertical upward flow would not result in accurate predictions when used for downward flow. Later, Barnea et al. (1982) developed a mechanistic flow map based on the approaches presented by Taitel and Dukler (1976) for horizontal flow, and Taitel et al. (1980) for vertical flow. Barnea et al. (1982) suggested modifications to the transition criteria proposed by Taitel and Dukler (1976) and Taitel et al. (1980) in order to extend the applicability of the mechanistic flow map to downward inclined pipes.

The first flow regime independent correlations for void fraction and pressure drop in downward flow were empirically derived and proposed by Yamazaki and Yamaguchi (1979). The proposed correlations predicted void fraction within $\pm 20\%$ error and pressure drop within $\pm 30\%$ error for the experimental data. Later, Usui and Sato (1989) proposed criteria for flow regime

transition based on mechanisms of flow transition and experimental data, and derived flow regime dependent correlations for the prediction of the void fraction.

Table 2.1. Review summary of published works on downward two-phase flow in pipes

Study	Pipe ID (in)	Fluids	Observed flow regimes	Liquid/gas superficial velocities
Golan and Stenning, 1969	1 ½	Water-air	Bubble, slug, annular, annular-mist	v_{SL} 1 – 5 ft/s v_{SG} 1 – 170 ft/s
Oshinowo and Charles, 1974	1	Water-air Glycerol-air	Coring bubble, bubbly-slug, falling film, falling bubbly-film, froth, annular	v_{SL} up to 5.5 ft/s v_{SG} up to 160 ft/s
Yamazaki and Yamaguchi, 1979	1	Water-air	Slug, wispy annular, annular, wetted wall flow	v_{SL} 0.2 – 4.3 ft/s v_{SG} 0.03 – 84 ft/s
Barnea et al., 1982	1, 2	Water - air	Stratified (smooth/wavy), intermittent (elongated bubble, slug), annular, dispersed bubble	v_{SL} 0.30 – 30.0 ft/s v_{SG} 0.3 – 80 ft/s
Usui, 1989	5/8, 1	Water - air	Bubbly, slug, falling film, annular	v_{SL} 0.20 – 5 ft/s v_{SG} 0.3 – 46 ft/s
Hernandez et al., 2002	2	Water - air	Bubbly, slug, annular	v_{SL} 0.15 – 13 ft/s v_{SG} 1.5 – 45 ft/s
Bhagwat and Ghajar, 2012	0.5	Water - air	Bubbly, slug, froth, falling film, annular	v_{SL} 0.40 – 2.0 ft/s v_{SG} 1.3 – 50 ft/s
Almabrok et al., 2016	4	Water-air	Bubbly, intermittent, annular	v_{SL} 0.07 – 1.5 ft/s v_{SG} 0.15 – 30 ft/s

Hernandez et al. (2002) evaluated how accurate Beggs and Brill (1973) correlation predicts holdup and total pressure drop in downward flow. As a result, Beggs and Brill (1973) was found to over predict liquid holdup by 31% in annular flow, 18% in slug flow and 12% in bubble flow. As the holdup predicted is higher, so is the hydrostatic pressure drop. On the comparison of total pressure drop, Hernandez et al. (2002) found that Beggs and Brill (1973) over predict total pressure drop in bubble flow; for slug flow it predicts pressure drop accurately; for annular flow, Beggs and Brill (1973) predict well for high gas velocity but it under predicts for low gas velocity.

Bhagwat and Ghajar (2012) investigated 52 void fraction correlations for upward flow and 26 correlations for downward orientation. They verified the performance of these correlations with

a comprehensive data set, which included results for pipe orientation from $+90^\circ$ to -90° . From the performance analysis of the different correlations for void fraction, Bhagwat and Ghajar (2012) observed that the correlations for upward flow obtained by data fitting failed to predict the void fraction for downward flow. On the other hand, the correlations based on drift-flux could be used to predict void fraction in downward flow by changing the sign of the drift velocity term. Based on this evaluation, these authors later developed drift-flux model based correlations that can be applied to a wide range of pipe orientations, diameters and geometries, for both upward and downward flow (Bhagwat and Ghajar, 2014).

It is important to note that the works mentioned in this section, besides the work by Bhagwat and Ghajar (2014), were conducted for pipe diameter up to 2 in. Almabrok et al. (2016) has shown that some of the correlations mentioned in this literature review, such as Barnea et al. (1982) and Usui and Sato (1989), might not give accurate predictions when used for large diameter pipes.

2.4. Transient Two-Phase Flow Modeling

Since the 1980's, several authors have been investigating transient multiphase flow in pipes (Taitel et al., 1989; Bendiksen et al., 1991; Minami, 1991; Minami and Shoham, 1994; Pauchon et al., 1994; Vigneron et al., 1995; Henriot et al., 1997). These efforts resulted in the development of complex computer codes and commercial simulators, such as OLGA and LEDAFlow.

Fundamentally, there are two types of modeling approaches: the two-fluid model and the drift-flux model. The two-fluid model treats the gas and the liquid as two phases, each flowing in a separate channel. The commercial software OLGA, for example, is a dynamic, one-dimensional,

extended two-fluid model. On the other hand, the drift-flux model treats the two-phase flow mixture as a pseudo single phase, with the relative motion of one phase with respect to the mixture.

The two-fluid model approach consists of six conservation equations: three conservation of mass (one for the gas phase, another for the continuous liquid phase, and another for liquid droplets entrained in the gas phase), two conservation of momentum (combined momentum for the gas phase and liquid droplets, and combined momentum for the continuous hydrocarbon phase), and one conservation of energy for the two phases. In the mathematical formulation of OLGA, nine closure relationships are used to close the hydrodynamic model, and a finite difference method on a staggered mesh for the spatial discretization and a semi-implicit time integration method are employed to solve the system of equations (Bendiksen, 1991).

The drift-flux approach is essentially an approximate formulation compared to the more detailed two-fluid flow model. The drift-flux model consists of four equations: one conservation of mass for the mixture, one conservation of mass for the gas phase, one conservation of momentum for the mixture, and one conservation of energy for the mixture. This approach is usually preferred over the two-fluid model due to its simplicity and flexibility. It is important to note that the drift-flux model is better suited for cases when there is strong coupling and local relative motion between the liquid and gas phases, which is typically the case for bubbly and slug flow regimes (Ishii, 1977). For stratified or annular flow regimes, the two-fluid model approach provides better predictions.

2.4.1. Simplified Transient Models

Considering the complexity and the high computational requirements of the transient models currently available, several authors felt motivated to work on the development of simplified transient two-phase flow models, for specific applications.

Taitel et al. (1989) were one of the first authors to develop a simplified transient multiphase flow model. Their model is based on local equilibrium momentum balance of the gas and liquid and a quasi-steady state flow for the gas. To complete the set of equations, they use an interfacial friction factor correlation and a steady-state flow pattern dependent pressure gradient model. The model is valid for small angles of inclination from the horizontal direction and cannot be applied to cases with very low velocities of gas and liquid. Later, Minami et al. (1994) improved Taitel et al. (1989) model by proposing a new flow pattern transition criteria for transient two-phase flow, which is based on the stability of the slug flow structure. Vigneron et al. (1995) also proposed a modification for Taitel et al. (1989) model, by adding a pigging model. Thus, the models of the latter authors are limited to very specific cases.

Lorentzen et al. (2001) developed a model based on the classic drift-flux set of conservation equations and measured data for closure of the system. The purpose of the model is to accurately predict downhole pressure and returning flow rates in under-balanced drilling operations. Mechanistic steady-state models are integrated into the model for obtaining the phase velocities and pressure loss terms. The Kalman filter is used for estimating unknown parameters from measured data acquired during drilling operations. The main limitation of their model is that the quality of the model predictions depend on the type of measurement used for closing the system. For instance, this model cannot be used for design of new systems since data would not be available to be used for the closure relationships.

Choi et al. (2013) developed a flow pattern independent simplified transient model for horizontal flow that utilizes drift-flux approach to calculate the liquid holdup and a power law correlation for the pressure drop. The model was tested with experimental data and OLGA. The comparison showed that the model reasonably predicts liquid holdups and pressures for some

cases, but it over predicts holdup at low liquid loading cases because of the constants values of the distribution parameter and drift velocity. Besides the discrepancies between the results with the proposed model and with commercial software, the authors emphasize the speediness of the simulations when compared to the latter.

Ambrus et al. (2015) developed a simplified transient model suited for real-time decision making and automated well control applications. The model consists of a lumped parameter model of the pressure dynamics, a transport equation for gas bubble migration and associated closure relations. The main assumptions are: no solubility of gas in the liquid phase; negligible variation of the liquid density along the length of the well; frictional pressure drop is negligible compared to gravitational pressure drop. They adopted an explicit numerical solution algorithm that significantly reduces computational time. However, the model is only applicable to vertical and low-inclination well sections and to water-gas systems (because of the assumption of negligible solubility of gas in the liquid phase).

Malekzadeh et al. (2012) developed a transient drift flux model with the objective of simulating severe slugging phenomena in pipeline-riser systems. Their model consists of two mass balance equation, a mixture momentum balance equation and the correlation of Shi et al. (2005) for the drift-flux slip. Using finite differences discretization, the equations are written as a system of ordinary differential equation that can be solved for the unknown variables (void fraction, pressure, volumetric rate of gas and liquid). An algorithm based on fourth and fifth order Runge-Kutta is used for the time discretization. The authors demonstrate the performance of the model for a severe slugging case by comparing its result with OLGA and experimental data.

This literature review points out the fact that most simplified transient models were developed for specific cases (e.g., to simulate slugging), and for certain inclination angles (for

most of the models, either only horizontal or only vertical). None of the studies presented in this section include validation for the full range of pipe inclinations (-90° to 90°), and covering a wide range of conditions (e.g. wide range of velocities, flow regimes, and pressures).

3. Evaluation of Models for Steady-State Downward Two-Phase Flow in Vertical Pipe Annulus

As previously discussed, the simplified transient model of this work adopts a pseudo-steady-state approach for the momentum equation and it aims at being applicable to any pipe inclination, for flow in both pipe annulus and tubing. To the knowledge of the author, there is no model in the literature that has been developed or evaluated for vertical downward two-phase flow in pipe annulus, even in steady-state. Therefore, the evaluation presented in this chapter is useful for understanding if models developed for downward flow in pipes can be used for simulating flow in the pipe annulus and for selecting the most appropriate model to be utilized in the formulation for the simplified transient model developed in this study. This evaluation also shows how easily new improvements can be added to the simplified transient model of this work for new flow scenarios.

To determine the differences and similarities between downward flow in pipe and annulus, Coutinho (2018) carried out an experimental investigation of downward two-phase flow in pipe annulus and compared his data to the experimental observations of Usui and Sato (1989). The latter authors generated and analyzed experimental data for downward flow in a vertical pipe with similar flowing conditions (e.g., similar hydraulic diameter, gas and liquid velocities) of Coutinho (2018).

To understand if currently available models for downward two-phase flow in pipes can be used to describe downward two-phase flow in annulus, the experimental data of Coutinho (2018) was used to evaluate the applicability of the models of Beggs and Brill (1973), Usui (1989), and Bhagwat and Ghajar (2014). The results also include a comparison with the commercial software OLGA (Bendiksen, 1991). This chapter presents this comparison in terms of flow regimes, liquid holdup and pressure gradient.

Coutinho (2018) used air and water as his working fluids. Water and air flow downward in a 16.4-ft long pipe annulus test section, composed by a 3.98-in ID transparent PVC outer pipe and a 2.88-in OD aluminum inner pipe. A high speed camera was used to visually observe the different flow regimes. For the holdup measurement, the volume of collected water was considered in relation to the total volume of the annulus portion of the pipe. Pressure gradient was obtained from measurements of four pressure transducers located along the test section.

The full description of the experimental setup and test procedures used to obtain the visual observations of the flow regime and the measurements of liquid holdup and pressure gradient for the experimental runs is described in Coutinho (2018).

The literature review on steady-state models for downward flow in pipes presented in Chapter 2 was used in this study to select numerical models for comparison with the experimental data for downward two-phase flow in annulus from Coutinho (2018). From the literature review, Beggs and Brill (1973) model was chosen for this comparison because it was developed for flow in pipes with inclination angles ranging from -90° to $+90^\circ$ (with the horizontal direction), it has been vastly validated, and it is widely used. Beggs and Brill (1973) model is available in many different commercial software and its full description is available in the literature.

Usui (1989) model was chosen since it was developed more recently to specifically characterize downward two-phase flow in vertical pipes. Table 3.1 gives the flow regime transition criteria developed by the author. Table 3.2 gives the void fraction correlations for each flow regime. For the comparison of this study, equations on Table 3.1 and Table 3.2 were implemented in Excel.

The flow pattern independent drift-flux model based void fraction correlation developed by Bhagwat and Ghajar (2014) was also used in this study. This correlation was chosen for the

comparison since it was developed for gas-liquid two-phase flow covering a wide range of pipe orientations, diameters and geometries. The Bhagwat and Ghajar (2014) model is briefly discussed in Chapter 4 and presented in details in Appendix A.

Table 3.1. Flow regime transition criteria (Usui and Sato, 1989)

Transition from bubbly to slug flow:

$$3.76 \left(\frac{v_{SG}}{v_{SL}} \right) + \frac{1.28}{(Fr_L E_o^{1/4})} = 1 \quad (3.1)$$

where v_{SG} is the gas superficial velocity, v_{SL} is the liquid superficial velocity, Fr_L is the Froude number, and E_o is the Eotvos number.

$$Fr_L = \frac{v_{sl}}{\sqrt{gD \frac{(\rho_L - \rho_G)}{\rho_L}}} \quad (3.2)$$

where g is the gravity acceleration, D is the pipe diameter, ρ_L is the liquid density, and ρ_G is the gas density.

$$E_o = \frac{(\rho_L - \rho_G)gD^2}{\sigma} \quad (3.3)$$

where σ is the interfacial tension.

Transition from slug to annular flow:

$$\frac{C_1}{Fr_L C_o} + \left[\frac{1}{\{1 - (2C_w Fr_L^2)^{7/23} C_o\}} - 1 \right] \left(\frac{v_{SG}}{v_{SL}} \right) = 1 \quad (3.4)$$

where

$$C_1 = 0.345[1 - \exp\{(3.37 - E_o)/10\}] \quad (3.5)$$

$$C_o = 1.2 - 1/(2.95 + 350E_o^{-1.3}) \quad (3.6)$$

$$C_w = 0.005$$

Transition from falling film to slug flow:

$$Fr_L = \left(\frac{K_1 - K_2}{E_o} \right)^{23/18} \quad (3.7)$$

where K_1 and K_2 are experimentally derived constants. For their study, $K_1 = 0.92$ and $K_2 = 7.0$.

Transition from falling film to annular flow:

$$Fr_L = 1.5 \left(\frac{v_{SG}}{v_{SL}} \right)^{-1.1} \quad (3.8)$$

Table 3.2. Void fraction correlations (Usui and Sato, 1989)

Bubbly flow:	
$(1 - C_o \alpha) \left(\frac{v_{SG}}{v_{SL}} \right) - C_o \alpha + \frac{1.53 \alpha}{\left(Fr_L E_o^{\frac{1}{4}} \right)} = 0 \quad (3.9)$	
Slug flow:	
$(1 - C_o \alpha) \left(\frac{v_{SG}}{v_{SL}} \right) - C_o \alpha + \frac{C_1 \alpha}{Fr_L} = 0 \quad (3.10)$	
Annular flow:	
$(1 - \alpha)^{23/7} - 2C_w Fr_L^2 \left[1 - \frac{C_1}{C_w} \frac{(1 - \alpha)^{16/7}}{\alpha^{5/2}} \frac{\rho_g}{\rho_l} \left(\frac{v_{SG}}{v_{SL}} \right)^2 \right] = 0 \quad (3.11)$	
where	
$C_i = 0.005[1 + 75(1 - \alpha)] \quad (3.12)$	
Falling film flow:	
$1 - \alpha = (2C_w Fr_L^2)^{7/23} \quad (3.13)$	

A comparison with OLGA is also included in this study. OLGA is the industry standard tool for transient simulation of multiphase flow in the oil and gas industry.

To compare the experimental data from Coutinho (2018) with these models, the hydraulic diameter concept was used, which defines the hydraulic diameter as the difference between the inner diameter of the outer pipe and the outer diameter of the inner pipe.

3.1. Flow Regime Predictions

The experimental data of Coutinho (2018) consists of 114 points, for gas superficial velocities ranging from 0.05 to 26 *ft/s*, and liquid superficial velocities from 1.3 to 4.5 *ft/s*. The flow regimes observed were bubbly, intermittent and annular flow. Figure 3.1 presents the flow regime map with the experimental observations from Coutinho (2018) (pipe annulus) and Usui and Sato (1989) (circular pipe).

The experimental data from Usui and Sato (1989) is represented by the background-shaded areas and dotted lines indicating the transitions between the flow regimes in Figure 3.1. For the purpose of this comparison, the experimental observations for slug and churn flow regime in Usui and Sato (1989) work are combined as intermittent flow regime.

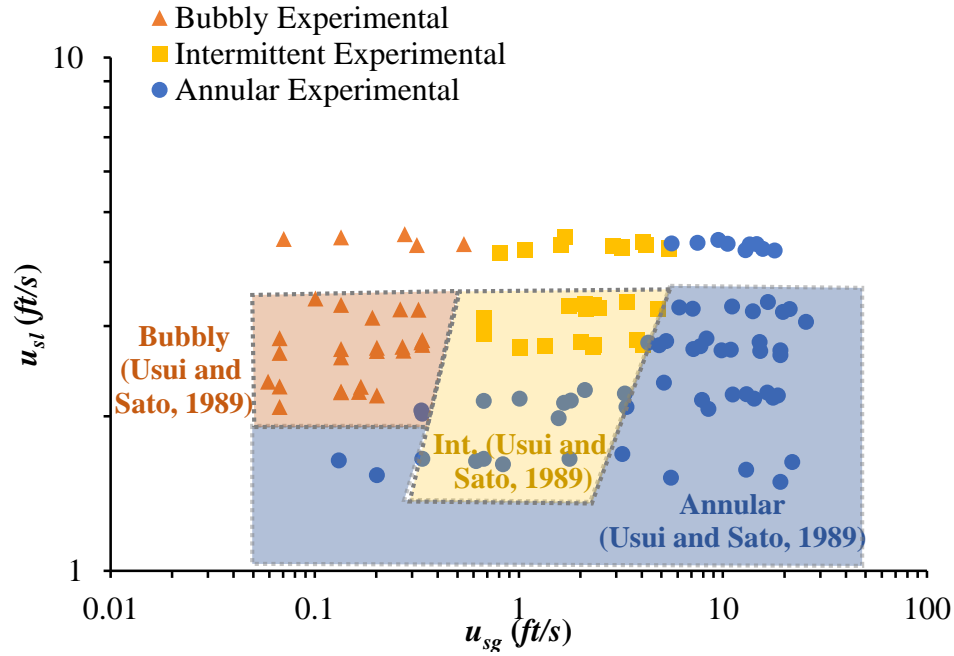


Figure 3.1. Comparison of the flow regime map for downward two-phase flow in annulus experimentally obtained by Coutinho (2018) and the map for downward two-phase flow in a 1-in ID pipe obtained by Usui and Sato (1989).

Figure 3.1 shows that the bubbly flow region is very similar for flow in both pipes and annulus. It also shows that the annular flow region is mostly in agreement for both pipe geometries. It can be seen that the annular flow region is wider, which is in agreement with the observations from Yamazaki and Yamaguchi (1979) and Barnea et al. (1982). Intermittent flow is observed for lower superficial liquid velocities for flow in pipes. It is important to note that there is also certain subjectivity in the visual identification of flow regimes, since different authors may classify flow regimes differently.

On Figure 3.2, Figure 3.3 and Figure 3.4, the experimental observations from Coutinho (2018) are grouped according to flow regime and are compared with flow regime transition criteria of Beggs and Brill (1973), Usui (1989) and OLGA. It is important to note that Beggs and Brill (1973) model describes the flow regimes as separated, intermittent and distributed flow. For this study, the separated flow regime is named as annular flow, and the distributed flow regime is named as bubbly flow. The model of Bhagwat and Ghajar (2014) was not used in the predictions for flow regimes in this study because their model is flow regime independent.

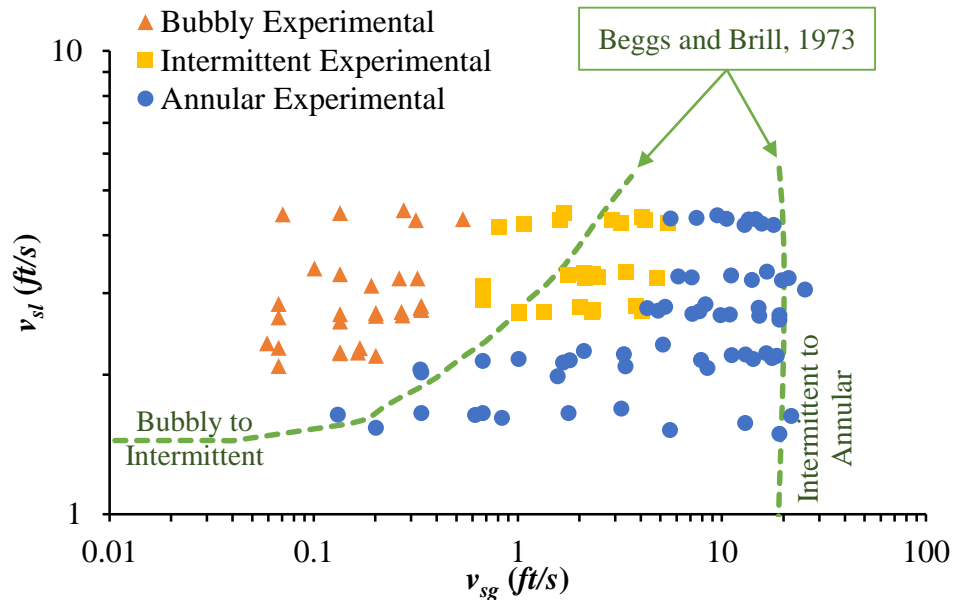


Figure 3.2. Comparison of the flow regime map for downward flow in annulus experimentally obtained by Coutinho (2018) and the map for downward flow in a 1 in ID pipe developed by Beggs and Brill (1973) theoretical model.

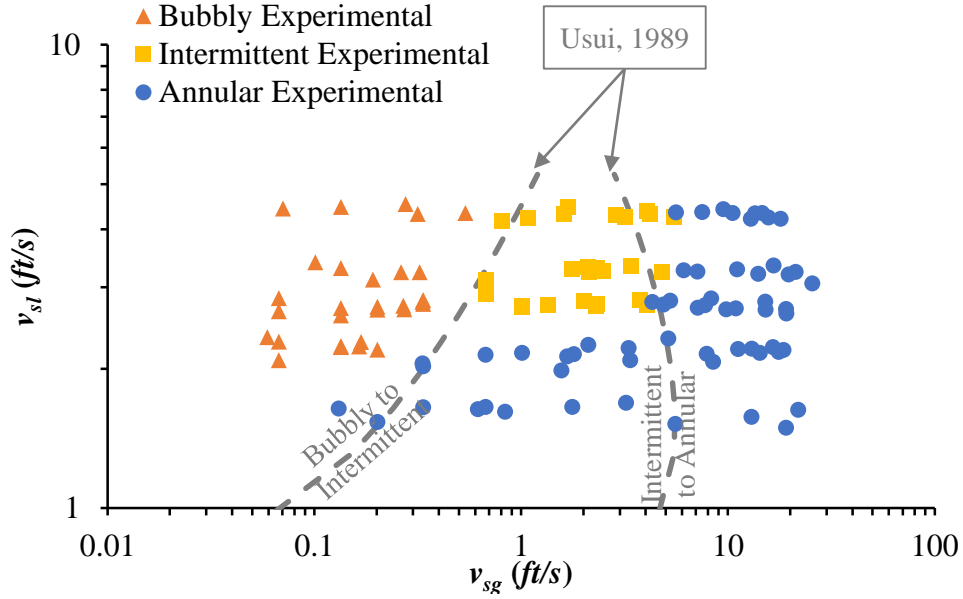


Figure 3.3. Comparison of the flow regime map for downward flow in annulus experimentally obtained by Coutinho (2018) and the map for downward flow in a 1 in ID pipe developed by Usui (1989) theoretical model.

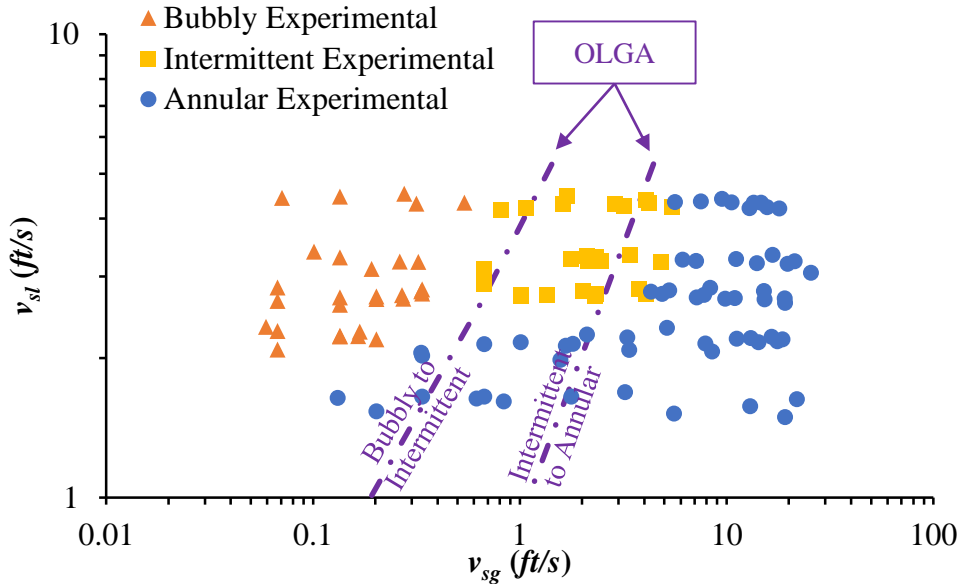


Figure 3.4. Comparison of the flow regime map for downward flow in annulus experimentally obtained by Coutinho (2018) and the map for downward flow in a 1 in ID pipe obtained using OLGA.

The differences between the experimental observations from Coutinho (2018), the models of Beggs and Brill (1973), Usui (1989) and OLGA indicate different behavior for downward flow in pipes and annulus. From Figure 3.2, Figure 3.3 and Figure 3.4, it can be seen that the predictions obtained using Usui (1989) model and OLGA have a better agreement with the experimental data than that obtained with Beggs and Brill (1973) model. This is expected since the literature has shown that Beggs and Brill (1973) model yields higher prediction errors for vertical flow in comparison to other models. Therefore, it would be recommended to use either Usui (1989) model or OLGA for flow regime prediction in downward two-phase flow in annulus.

3.2. Liquid Holdup Predictions

Experimental liquid holdup obtained in the experiments by Coutinho (2018) was compared to experimental liquid holdup for downward two-phase flow in vertical pipe obtained by Usui and Sato (1989), and with calculated values using Beggs and Brill (1973), Usui (1989), and Bhagwat and Ghajar (2014) correlation, and OLGA commercial simulator. Figure 3.5 shows the results for two liquid superficial velocities.

The experimental data from Usui and Sato (1989), obtained for downward flow in a 1-in ID vertical pipe, is also included in Figure 3.5. The dotted vertical lines represent the flow regime transitions observed by Usui and Sato (1989). The experimental data from Coutinho (2018), obtained for a pipe annulus with hydraulic diameter of 1 inch, is represented by triangles, yellow squares and circles for bubbly, intermittent and annular flow regimes, respectively. The error bars represent the calculated uncertainty (approximately ± 0.12) for the liquid holdup. Values calculated with Beggs and Brill (1973) model, Usui (1989) model, Bhagwat and Ghajar (2014) correlation, and OLGA are represented by the continuous green line, gray dashed line, cyan dashed line, and purple dashed line, respectively.

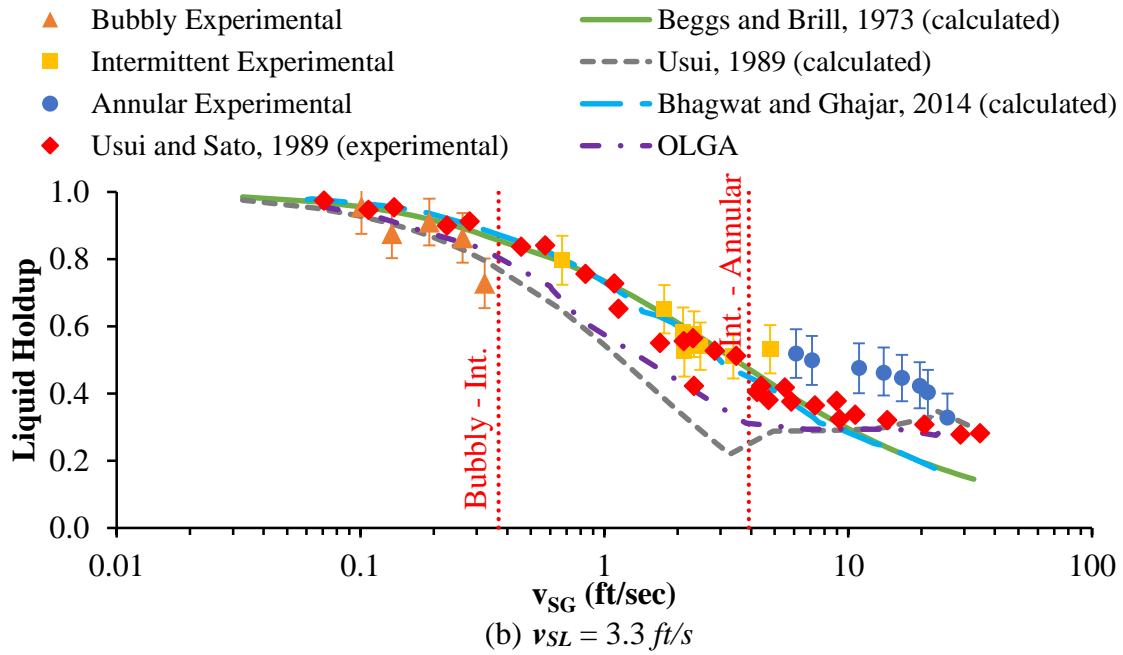
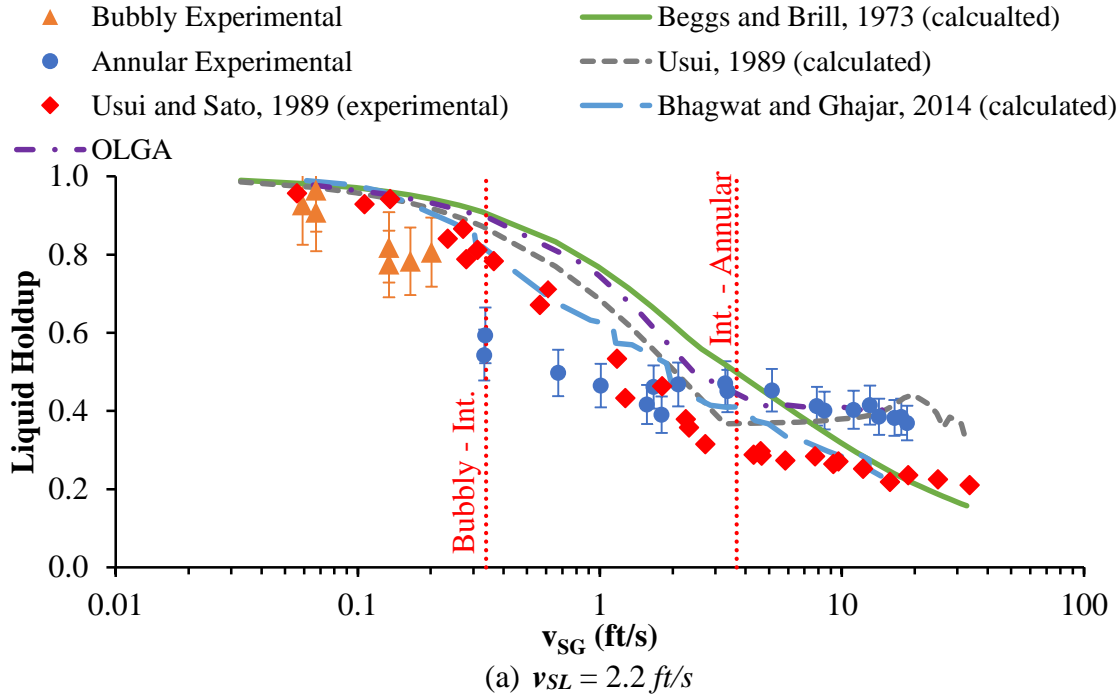


Figure 3.5. Comparison of experimental liquid holdup for annulus (Coutinho, 2018) and tubing (Usui and Sato, 1989) with the same hydraulic diameter, and values calculated with Usui (1989), Beggs and Brill (1973), Bhagwat and Ghajar (2014), and OLGA, as a function of gas superficial velocity for two liquid superficial velocities.

The comparison of experimental liquid holdup for downward flow in the annulus and the downward flow in the tubing from Usui and Sato (1989) shows that there are inherent differences between flow in annulus and tubing. There is a good agreement for experimental liquid holdup results for tubing and annulus in the bubbly flow regime. For higher liquid superficial velocities, as a consequence of the better agreement between the flow regime observations for flow in pipe and annulus (see Figure 3.1), the liquid holdup results for intermittent flow regime are also in reasonable agreement. From Figure 3.5, it can be seen that, for annular flow regime, the liquid holdup for flow in the annulus is consistently higher than for flow in the tubing.

In summary, for bubbly flow regime, all models considered give predictions within the accuracy of the experimental data. For intermittent and annular flow regime, however, the models considered in the comparison had different prediction performance for different liquid superficial velocities. The discrepancy between the experimental data and the numerical predictions of liquid holdup for Beggs and Brill (1973), Usui (1989) and OLGA models is probably related to inaccurate flow regime prediction.

Figure 3.6 shows a comparison of the experimental liquid holdup from Coutinho (2018) with the liquid holdup results calculated with Bhagwat and Ghajar (2014) correlation, in comparison with results obtained with Beggs and Brill (1973) model. On Figure 3.6, reference is made to the flow regimes visualized in the experiments of Coutinho (2018), as in the previous comparisons. It is important to note, however, that Bhagwat and Ghajar (2014) correlation is flow regime independent, meaning it does not rely on the prediction of flow regimes to estimate liquid holdup.

The comparison with the liquid holdup results calculated with Bhagwat and Ghajar (2014) correlation shows that for the experimental data classified as bubbly there is very good agreement

(9% average error in the prediction of liquid holdup). For the intermittent experimental data, the average error for the liquid holdup prediction is 21%. For the experimental data classified as annular flow regime, the average error for the liquid holdup prediction goes to 41%. The error increases for low liquid holdup values (which is the case for annular flow), since a small absolute difference between the predicted and measured values of liquid holdup corresponds to a high percentage error. The results from this comparison follow what is expected since the correlation is based on drift-flux model and the drift-flux approach is more appropriate for dispersed and intermittent flow regimes. The literature recommends separated flow models for shear driven flow such as annular flow.

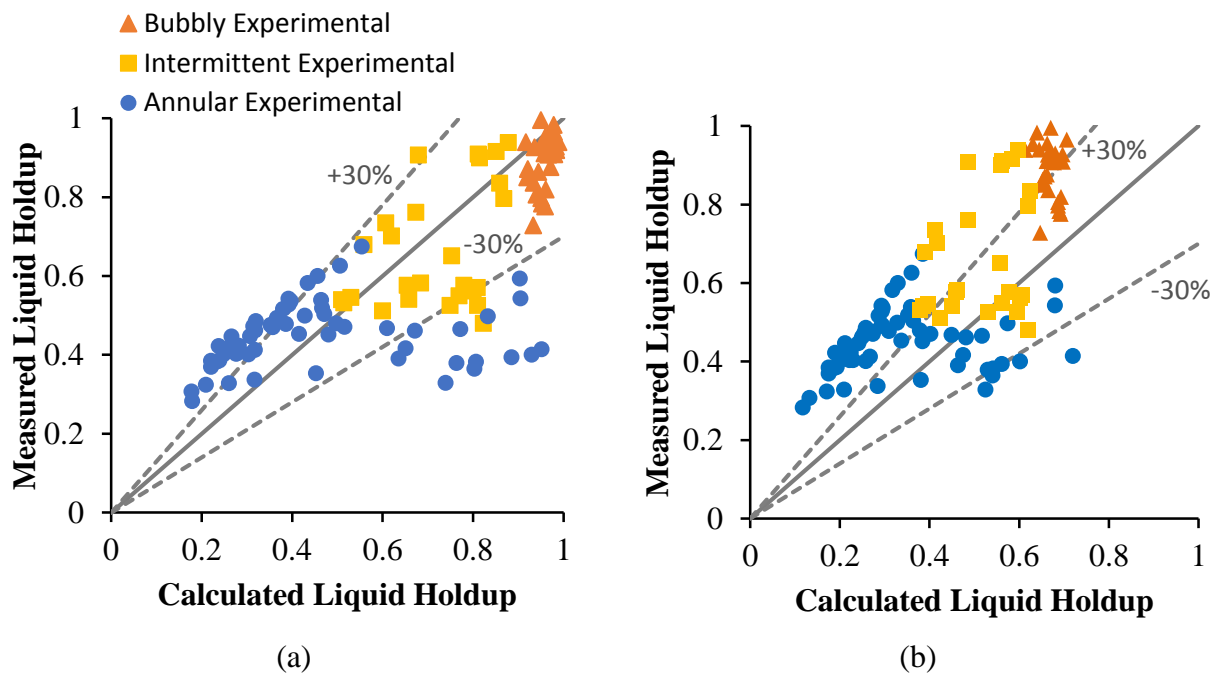


Figure 3.6. Comparison of experimental liquid holdup for downward vertical flow in annulus (Coutinho, 2018) on Y axis and liquid holdup calculated with (a) Bhagwat and Ghajar (2014) correlation and (b) Beggs and Brill (1973) model on X axis.

3.3. Pressure Gradient Predictions

The comparison for pressure gradient is shown on Figure 3.7. This figure includes the experimental pressure gradient from Coutinho (2018), and results calculated using Beggs and Brill

(1973) model and OLGA simulator. This comparison does not include Usui (1989) and Bhagwat and Ghajar (2014) models, as these authors did not propose a model to calculate pressure gradient.

As can be seen in Figure 3.7, neither Beggs and Brill (1973) model nor OLGA present a reasonable match with the experimental data for the full range of superficial velocities in this study. This is possibly a consequence of diverging prediction of flow regime by the models.

For liquid superficial velocity between 1.97 and 3.38 *ft/s*, Beggs and Brill (1973) model and OLGA present a reasonable prediction of pressure gradient for bubbly flow regime. As the gas superficial velocity increases, Beggs and Brill (1973) model and OLGA predict bubbly and intermittent flow when annular flow is experimentally observed. Due to this divergence in flow regime transition, and consequently differences in the liquid holdup, the total pressure gradient calculated with Beggs and Brill (1973) model and OLGA differ significantly. For OLGA results, the discrepancy to the experimental data gets lower as the gas superficial velocity reaches values closer to the transition to annular flow.

Overall, Figure 3.7 shows that for liquid velocities higher than 4 *ft/s*, the difference between the experimental total pressure gradient and values calculated with both models decreases, and reasonable agreement is achieved for all flow regimes.

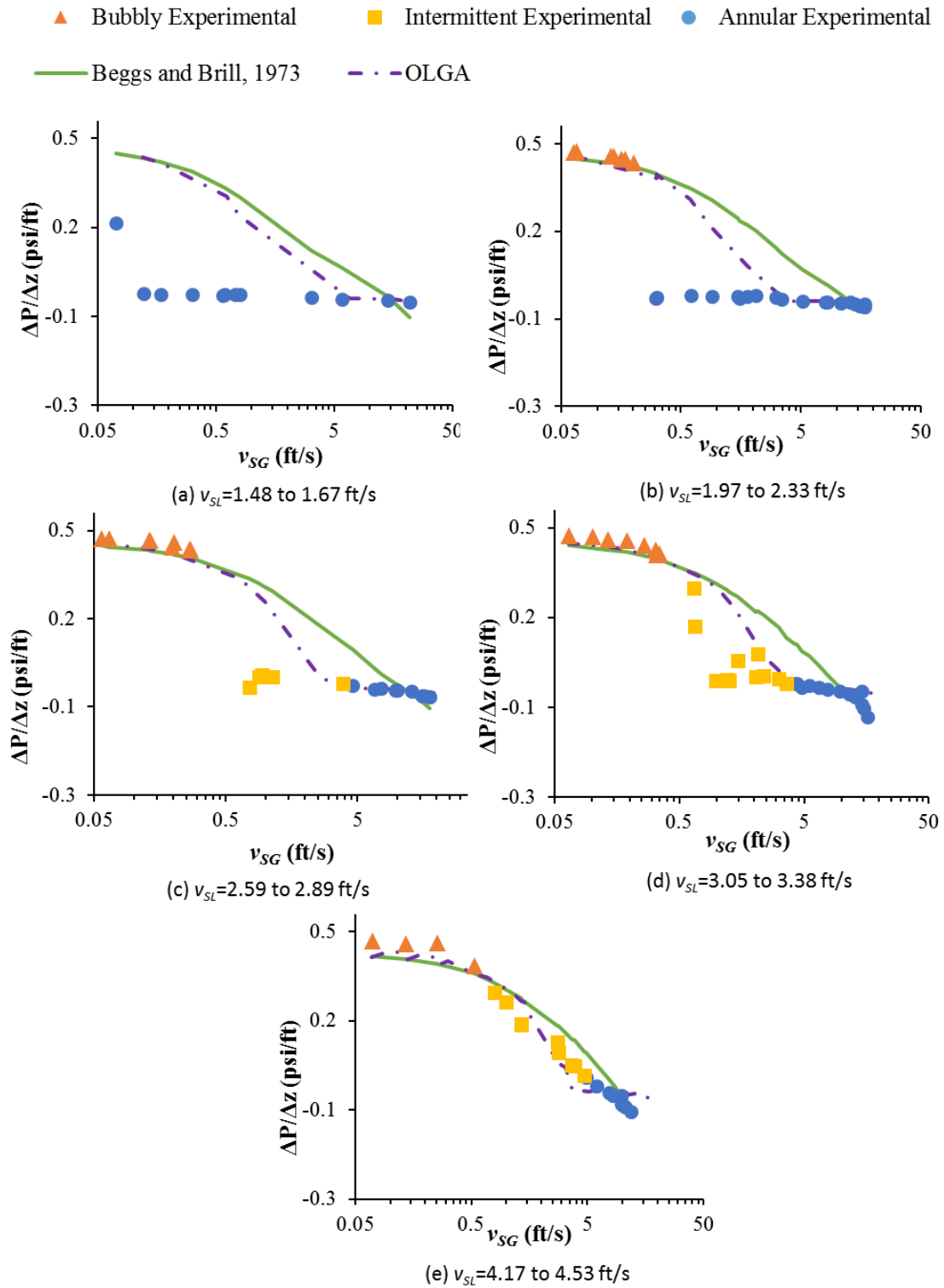


Figure 3.7. Comparison of experimental pressure gradient for downward two-phase flow in annulus (Coutinho, 2018) and values calculated with Beggs and Brill (1973) model and OLGA, as a function of gas superficial velocity for five liquid superficial velocities.

3.4. Evaluation Summary and Remarks

The results from the evaluation presented in this chapter show that:

- All models adopted in the comparison with experimental data for vertical downward flow in pipe annulus seem to provide an error of liquid holdup of $\pm 55\%$, and $\pm 150\%$ for pressure gradient for low liquid superficial velocities, and an error of liquid holdup of $\pm 35\%$, and $\pm 30\%$ for pressure gradient for high liquid superficial velocities.
- The results obtained with the simulator OLGA seem to have a better agreement with the experimental data, overall. However, OLGA is a proprietary model and its formulation is not accessible. Therefore it cannot be used for the pseudo-steady-state approach for the momentum in the simplified transient model of this work.
- Usui (1989) model was specifically developed for vertical downward flow in pipes and it is not the best choice for using in the simplified transient model, since the model is to be used for simulating transient flow in any pipe inclination.
- Bhagwat and Ghajar (2014) has a better match than Beggs and Brill (1973) model for all pipe inclinations.
- Thus, from this evaluation, the model by Bhagwat and Ghajar (2014) shows to be the most reasonable for downward two-phase flow in vertical pipe annulus, and the most appropriate for adoption in the simplified transient model of this work.

4. Description of the Simplified Transient Two-Phase Flow Model

This chapter describes the simplified transient model developed in this work. The model is based on the formulation proposed by Choi et al. (2013). It is a hybrid approach consisting of a two-fluid approach for transient continuity equation, and a pseudo-steady-state drift-flux approach for the momentum equation. The model is flow regime independent, which makes it simpler, since there is no need to implement separate models for different flow regimes. In addition to that, flow regime independent models are also more robust numerically, because they don't suffer from the numerical discontinuity for flow regime transitions. However, the model developed in this study is not fully continuous, because of the discontinuity in the distribution parameter (C_o) and drift velocity (v_d) correlations. The model considers adiabatic flow, and pseudo-steady-state mass transfer from liquid to gas phase.

Based on these assumptions, the model is expected to be applicable to slow transient flow, in which there are no significant changes in temperature, and for low gas-oil-ratio fluids (e.g., black oil fluids) with no sudden pipe diameter changes.

The main contributions of this work related to the model developed are:

- Adoption of the Bhagwat and Ghajar (2014) correlations for the drift-flux parameters in the simplified transient model, which enables the utilization of the model for simulating transient flow scenarios for any pipe inclination. These correlations were developed for a wide range of conditions, and proved to perform better than several other correlations available in the literature.
- Extensive validation of the model for the full range of pipe inclinations (-90° to 90°), for a wide range of conditions (all flow regimes, superficial liquid velocities from 0.01

to 10 *ft/s*, gas superficial velocities from 0.01 to 60 *ft/s*, pressures from 20 to 1400 *psig*), using different data sets (well test, experimental and synthetic data).

- Development of a more rigorous criterion to the definition of “slow transient”, which in turn defines the applicability of the simplified transient model.

Another objective of this work is to also develop a simulator that is simple to use and user-friendly. Thus, Excel Visual Basic for Applications (VBA) was opted as the programming platform to implement the simulator. This platform is compatible with Microsoft Excel and most engineers should be familiar with this software tool.

4.1. Mathematical Modeling

The modeling procedure developed in this study is based on the work of Choi et al. (2013). This decision was mainly influenced by the simplicity of Choi et al. (2013) model, which proposes a model for transient two-phase flow in pipes using a transient solution for the mass conservation equations for the gas and liquid phases, and a pseudo-steady-state approach for the momentum conservation. However, Choi et al. (2013) model does not cover the full range of pipe inclinations, being limited to $+90^\circ$ to -30° (Tang, 2019). This means it cannot be used for simulating inclined downward flow for pipes with inclinations greater than -30° to vertical direction, which can be the case when simulating drilling, gas-lift, and unloading operations.

One of the major contributions of the present study is to include the utilization of the drift-flux correlations for the distribution parameter and drift velocity given by Bhagwat and Ghajar (2014) to the approach originally proposed by Choi et al. (2013). This modification extends the applicability of the formulation proposed by Choi et al. (2013) and enables this new simplified transient model to be applied to any pipe inclination.

4.1.1. Conservation Equations

The one-dimensional transient liquid continuity equation that describes the time rate of change of liquid mass at any time and location is given by:

$$\frac{\partial(\rho_L A_L)}{\partial t} = \frac{\partial(\rho_L v_L A_p)}{\partial x} + \Gamma_L A_p \quad (4.1)$$

where ρ_L is the liquid phase density, A_L is the cross sectional area of the pipe occupied by liquid, v_L is the actual liquid velocity, A_p is the cross sectional pipe area, Γ_L is the liquid mass generation rate per control volume.

Assuming no liquid mass generation ($\Gamma_L = 0$), incompressible liquid and substituting $A_L = A_p H_L$ and $v_{SL} = v_L H_L$:

$$\frac{dH_L}{dt} = -\frac{dv_{SL}}{dx} \quad (4.2)$$

where v_{SL} is the liquid superficial velocity and H_L is the liquid holdup.

Similarly, for the gas phase:

$$\frac{\partial(\rho_G A_G)}{\partial t} = \frac{\partial(\rho_G v_G A_G)}{\partial x} + \Gamma_G A_p \quad (4.3)$$

where ρ_G is the gas phase density, A_G is the cross sectional area of the pipe occupied by gas, v_G is the actual gas velocity, Γ_G is the gas mass generation rate per control volume.

Assuming no mass transfer between phases ($\Gamma_G = -\Gamma_L = 0$), and substituting $A_G = A_p(1 - H_L)$ and $v_{SG} = v_G(1 - H_L)$:

$$\frac{d[\rho_G(1 - H_L)]}{dt} = -\rho_G \frac{dv_{SG}}{dx} \quad (4.4)$$

where v_{SG} is the gas superficial velocity.

The assumption of no mass transfer between phases is fairly reasonable when using immiscible fluids such as air and water, at pressures and temperatures that no phase change is present for neither fluids. For hydrocarbon fluids, this assumption is fair if gas “flashing” is not excessive (gas flashing would occur, for instance, for hydrocarbon fluid flow through sudden pipe area changes). This means that this assumption should be fairly reasonable if the model is to be used for simulating flows of black oil fluids without sudden pipe restrictions or expansions. According to McCain (1973), black oil fluids are characterized as having initial producing gas-oil ratios of 2000 scf/STB or lower, and stock-tank gravity usually below 45° API. Low gas-oil-ratios would typically imply that considerable amounts of gas may not come out from the liquid phase for slow transients, small time increments (time steps smaller than 1 seconds), small pipe discretization (length increments smaller than 10 *feet*), and small temperature changes (less than 1 °F per second).

Thus, Eq. (4.4) can be simplified to:

$$-\frac{dv_{SL}}{dx} - \frac{dv_{SG}}{dx} = 0 \quad (4.5)$$

One closure relationship is needed for the liquid holdup (H_L) to solve Eq. (4.4) and (4.5).

Liquid holdup is given by:

$$H_L = 1 - \frac{\overline{v_{SG}}}{v_G} \quad (4.6)$$

and the drift velocity (v_G) given by (Nicklin et al., 1962):

$$v_G = C_o(\overline{v_{SG}} + \overline{v_{SL}}) + v_d \quad (4.7)$$

In Choi et al. (2013) model, the distribution coefficient and the drift velocity are constant and given by $C_o = 1.2$ and $v_d = 0.3583$. In this work, C_o and v_d are calculated with the correlations proposed by Bhagwat and Ghajar (2014). These correlations were developed for a wide range of fluid combinations, pipe diameters and inclinations, and are flow regime independent. Table 4.1 summarizes the conditions for which the correlations were developed. The correlations for the drift velocity and the distribution coefficient proposed by these authors are presented as a function of variables such as pipe diameter, pipe orientation, fluid properties and the void fraction. The correlations proposed by Bhagwat and Ghajar (2014) for the distribution coefficient and the drift velocity are described in more details in Appendix A.

Table 4.1. Range of the parameters of the experimental data used for the development of the correlations of Bhagwat and Ghajar (2014)

Parameter	Range
Fluid combinations	air–water, argon–water, natural gas–water, air–kerosene, air–glycerin, argon–acetone, argon–ethanol, argon–alcohol, refrigerants, steam–water and air–oil fluid combinations
Hydraulic pipe diameter	0.02 – 12 in
Pipe orientation	$-90^\circ \leq \theta \leq 90^\circ$
Pipe geometries	Circular, annular and rectangular
Liquid viscosity	0.1 – 600 cp
System pressure	14.5 – 2625 psi
Two-phase Reynolds number	$10 - 5 \cdot 10^6$

The calculation of the distribution parameter and the drift velocity for the correlations of Bhagwat and Ghajar (2014) are implicit functions of the void fraction ($1 - H_L$). Therefore, based on an initial guess for void fraction, C_o and v_d are calculated and the numerical value of Eq. (4.7) is obtained.

The momentum balance is given by:

$$\begin{aligned} \frac{\partial}{\partial t}(\alpha_L v_L \rho_L + \alpha_G v_G \rho_G) + \frac{\partial}{\partial x}(P + \alpha_L v_L^2 \rho_L + \alpha_G v_G^2 \rho_G) \\ = -\rho_m g \sin \theta - \frac{f_{TP} \rho_m v_m^2}{2D_h} \end{aligned} \quad (4.8)$$

Neglecting the convection terms and taking a pseudo-steady-state approach ($\partial/\partial t \approx 0$), Eq. (4.8) is simplified as:

$$\frac{dP}{dx} = -\rho_m g \sin \theta - \frac{f_{TP} \rho_m v_m^2}{2D_h} \quad (4.9)$$

where ρ_m is the mixture density calculated based on the liquid holdup from the solution of the mass conservation and f_{TP} is the two-phase friction factor (calculated using Colebrook (1939) correlation).

It is generally reasonable to neglect the convection term in the conservation of momentum equation, since the magnitude of the accelerational pressure gradient is usually small compared to the contribution of the gravitational and frictional pressure gradients (Shoham, 2006).

The pseudo-steady-state approach taken for simplifying the model should be reasonable when:

$$\frac{\partial}{\partial t}(\alpha_L v_L \rho_L + \alpha_G v_G \rho_G) \ll \frac{\partial P}{\partial x} \quad (4.10)$$

Writing in terms of flow rates, deriving the terms on the left-hand side, assuming negligible variation in the liquid density across the length of the well, and rearranging the terms, Eq. (4.10) can be written as:

$$\frac{\partial q_L}{\partial t} + \frac{\rho_G}{\rho_L} \frac{\partial q_G}{\partial t} + \frac{q_G}{\rho_L} \frac{\partial \rho_G}{\partial t} \ll \frac{A}{\rho_L} \frac{\partial P}{\partial x} \quad (4.11)$$

Equation (4.11) represents a powerful tool for the definition of slow transients, in a quantitatively manner. In the simulator implemented in this work, Eq. (4.11) is used as a validation tool to indicate to the user, based on the given input data, if the simulation to be performed satisfies the criterion of Eq. (4.11) (in other words, if the input data characterize the case as slow transient). A numerical example is given in Chapter 5.

4.1.2. Numerical Solution Method

Figure 4.1 illustrates the time and space discretization and how the liquid holdup for each control volume calculated in the previous time step is used to obtain the liquid holdup in the following time step.

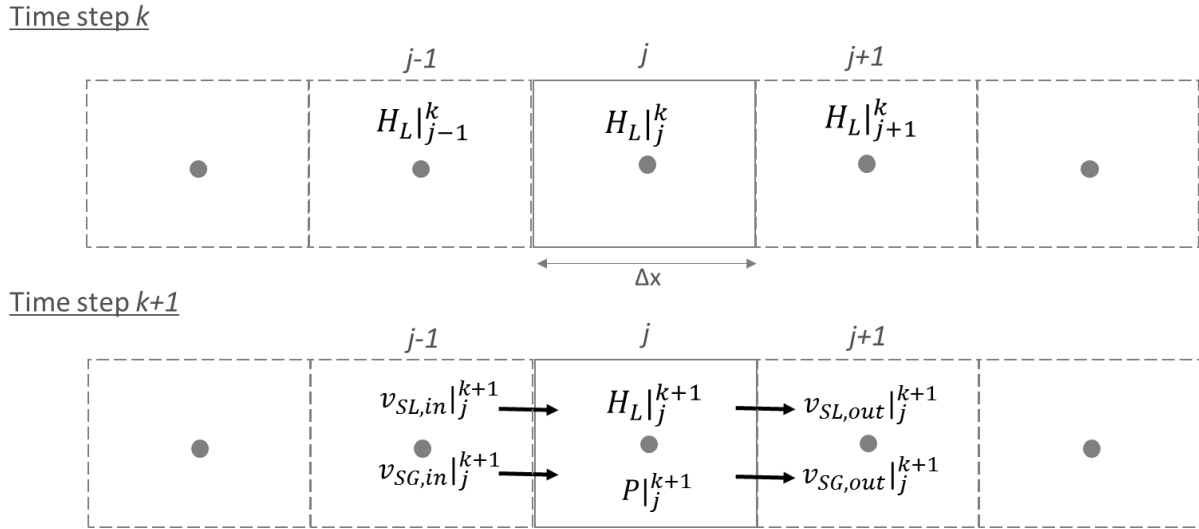


Figure 4.1. Schematic of time and space discretization for the model developed in this work

The numerical solution consists of solving Eqs. (4.2), (4.5) and (4.6) for the superficial velocities of the gas and the liquid and the liquid holdup. This is achieved by first discretizing Eqs. (4.2), (4.5) and (4.6):

$$\frac{H_L|_j^{k+1} - H_L|_j^k}{dt} = \frac{v_{SL,in}|_j^{k+1} - v_{SL,in}|_j^k}{\delta x} \quad (4.12)$$

$$v_{SG,out}|_j^{k+1} + v_{SL,out}|_j^{k+1} = v_{SG,in}|_j^{k+1} + v_{SL,in}|_j^{k+1} \quad (4.13)$$

$$H_L|_j^{k+1} = 1 - \frac{(v_{SG,in}|_j^{k+1} + v_{SG,out}|_j^{k+1})}{2v_G|_j^{k+1}} \quad (4.14)$$

where the index k refers to time step index and j to location index; and then rearranging the equations in a matrix format:

$$\begin{bmatrix} 1 & 0 & \left(\frac{dt}{dx}\right) \\ 0 & 1 & 1 \\ 2v_G|_j^{k+1} & 1 & 0 \end{bmatrix} \begin{bmatrix} H_L|_j^{k+1} \\ v_{SG,out}|_j^{k+1} \\ v_{SL,out}|_j^{k+1} \end{bmatrix} = \begin{bmatrix} H_L|_j^k + \left(\frac{dt}{dx}\right) v_{SL,in}|_j^{k+1} \\ v_{SG,in}|_j^{k+1} + v_{SL,in}|_j^{k+1} \\ 2v_G|_j^{k+1} - v_{SG,in}|_j^{k+1} \end{bmatrix} \quad (4.15)$$

Eq. (4.15) is solved using Gaussian-elimination by multiplying the rows by nonzero scalars, and replacing the rows by the sum of the row and a scalar multiple of another row, until the value of the three unknowns can be obtained. This method is described in more details by Lindfield and Penny (2012).

From the solution of the matrix (Eq. 4.15), the liquid holdup is used to recalculate C_o and v_d , until convergence is achieved for the grid block. Then, the liquid holdup, superficial liquid velocity and superficial gas velocity are used to calculate the parameters necessary for calculating the pressure gradient in the grid block. The pressure gradient is calculated as derived by Eq. (4.9).

The required fluid properties equations were implemented based on the equations of state for water, oil, and gas, fluids density and viscosity, gas compressibility factor, and gas-liquid interfacial tension as given by Brill and Mukherjee (1999). Hydrocabons are assumed as black oil fluids (McCain, 1973).

4.2. Simulator Algorithm

Once the code starts to run, the input data is read from the spreadsheet user interface. The next step consists of discretizing the space and time in order to adopt the simplified transient model criterion given by Eq. (4.11). For the determination of the time step, the Courant-Friedrichs-Lewy criteria (Courant et al., 1967) is used.

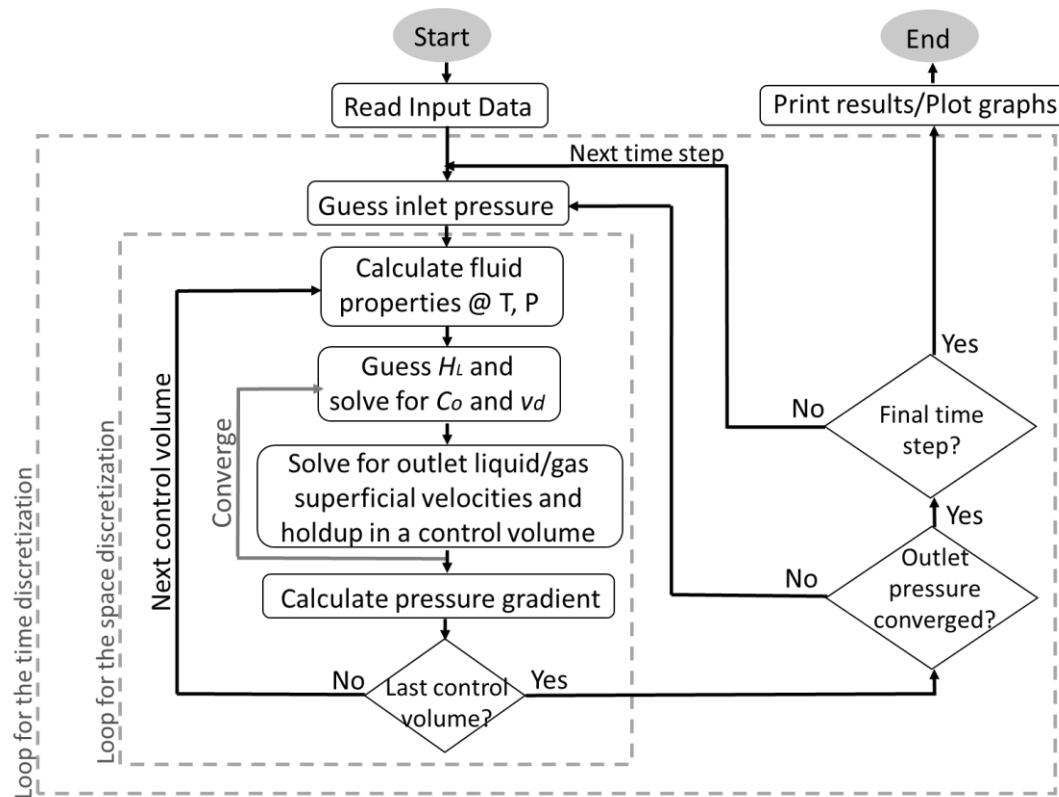


Figure 4.2. Flowchart for the model algorithm

Starting with the steady-state condition preceding the changes in operational conditions, pressure and liquid holdup at each control volume are known. Then, for each following time step, for each control volume in the pipe, the matrix in Eq. (4.15) is solved for $H_L|_j^{k+1}$, $v_{SG,out}|_j^{k+1}$ and $v_{SL,out}|_j^{k+1}$ using the known input velocities at the current time step and the liquid holdup from the previous time step. Once all control volumes have been calculated and convergence has been achieved, the procedure moves on to the next time step. This procedure is repeated until the last time step input by the user. Finally, after the simulation ends, the output module plots the results.

4.2.1. Simulator Input Variables

The input variables are organized in a tabular format in a manner that is very straightforward to use. This section discusses the input data necessary to run the model.

Basic fluid data, temperature and pressure conditions, such as temperature at surface and at bottom hole, temperature and pressure at separator conditions, gas specific gravity and oil API, are input in the first block of variables.

For specifying the well data, the well can be broken down into different sections. For each well section, it is necessary to define the casing inner diameter, tubing inner and outer diameter, roughness of casing and tubing, measured depth (MD) and true vertical depth (TVD) of the bottom of each well section.

The data for the transient simulation is input in a table that conveys the changes in gas and water injection rate and boundary pressure as a function of time. The first time step is the previous steady-state condition prior to the changes in the operational conditions. The user also needs to define a minimum and maximum time step for the calculation.

Once the simulation is initiated, the input module reads the data entered by the user and checks for consistency and completeness. It checks if all the basic input data and data for the well sections and transient points have been correctly entered and if the data is coherent (e.g., outer diameter is not greater than inner diameter).

Figure 4.3 shows the tabular entry format for the required input data discussed in this section and some of the auxiliary messages that show up to guide the user during data input. The table for the transient data shows only 10 rows on Figure 4.3 due to figure size constraints, but it can accommodate 1000 transient data points.

Temperature at surface		deg F
Bottomhole temperature		deg F
Temperature at separator		deg F
Pressure at separator		psi
Gas specific gravity		
Oil API		

Productivity index		[STB/day/psi]
Reservoir pressure		[psi]

Number of Well Sections		Enter the pipe data for each of the well sections below:							
Section	Discretization	Casing ID [in]	Tubing OD [in]	Tubing ID [in]	Roughness csg [in]	Roughness tubing [in]	MD - Y end [ft]	TVD - Y end [ft]	
1	Author: For each section of the well, input the required information (all cells in yellow).	Author: This input guides the code to read the data for the well's sections from the table below it. If Number of Well Sections = 1, then only the data referring to Section 1 on the table will be read.							
2									
3									
4									
5									
6									
7									
8									
9									
10									

Number of transient data points		(Max 1000)		
Transient data				
time step	Time [s]	Gas injection rate [Mscf/day]	Water injection rate [STB/day]	P boundary [psi]
SS	Author: Time step = SS is the previous steady state condition. Holdup is initialized from this condition.			
1				
2				
3				
4				
5				
6				
7				
8				
9				
10				

Minimum time step		[s]
Maximum time step		[s]

Simulation options	
Flow direction	Downward
Geometry	Annulus
<div style="border: 1px solid black; padding: 5px; width: 100px; margin: 0 auto;">RUN</div>	

Author:
Flow direction: choose downward for injection and upward for production. Geometry: either annulus or tubing).

Figure 4.3. Screenshot of the input data section of the simulator developed in this work

4.2.2. Simulator Outputs Results

After the simulation ends, the output module plots the variables of interest both as function of time and as function of measured depth. For graphing the results as a function of measured depth, any of the time steps provided on the transient table can be chosen. For graphing the results as a function of time, the user can choose from the following location options: top, middle or bottom grid block for the pipe. Figure 5.5 shows an example of plotting the results as a function of measured depth at different time steps. Figure 5.6 shows an example of plotting the results as a function of time for the bottom grid block.

5. Model Results and Discussions

In order to validate the model developed in this work, several comparisons were performed using different experimental data sets and synthetic data obtained from the commercial simulator OLGA. The following sections discuss the performance of the simulator implemented in this work for different pipe inclinations: -90° , -45° , 0° , 45° , and 90° , from the horizontal direction.

The main objective of this chapter is to show the comparison study and validation of the simplified transient model proposed in this study to define the conditions for which the model can be used, and verify its limitations.

5.1. Test Well Data for Vertical Downward Flow in the Pipe Annulus

The capability of the simulator in predicting the behavior of gas and liquid flowing downward in pipe annulus was assessed first. For this purpose, the experimental data set from Coutinho (2018) and the commercial simulator OLGA were used. The data set from Coutinho (2018) was obtained using a 2,788 *feet* deep test well, located at the Petroleum Engineering Research & Technology Transfer Laboratory (PERTT Lab) at Louisiana State University. This test well consists of a 5.5 *inch* OD and 4.89 *inch* ID inner casing, and a 2.88 *inch* OD and 2.44 *inch* ID production tubing. A valve is installed at the bottom of the tubing at a depth of 2,716 *feet*. Pressure is measured at the middle of the well (at a depth of 1,648 *feet*), at the bottom of the tubing (at a depth of 2717 *feet*), at the injection line and at the outflow line at the surface (Figure 5.1). There are no measurement devices for liquid holdup.

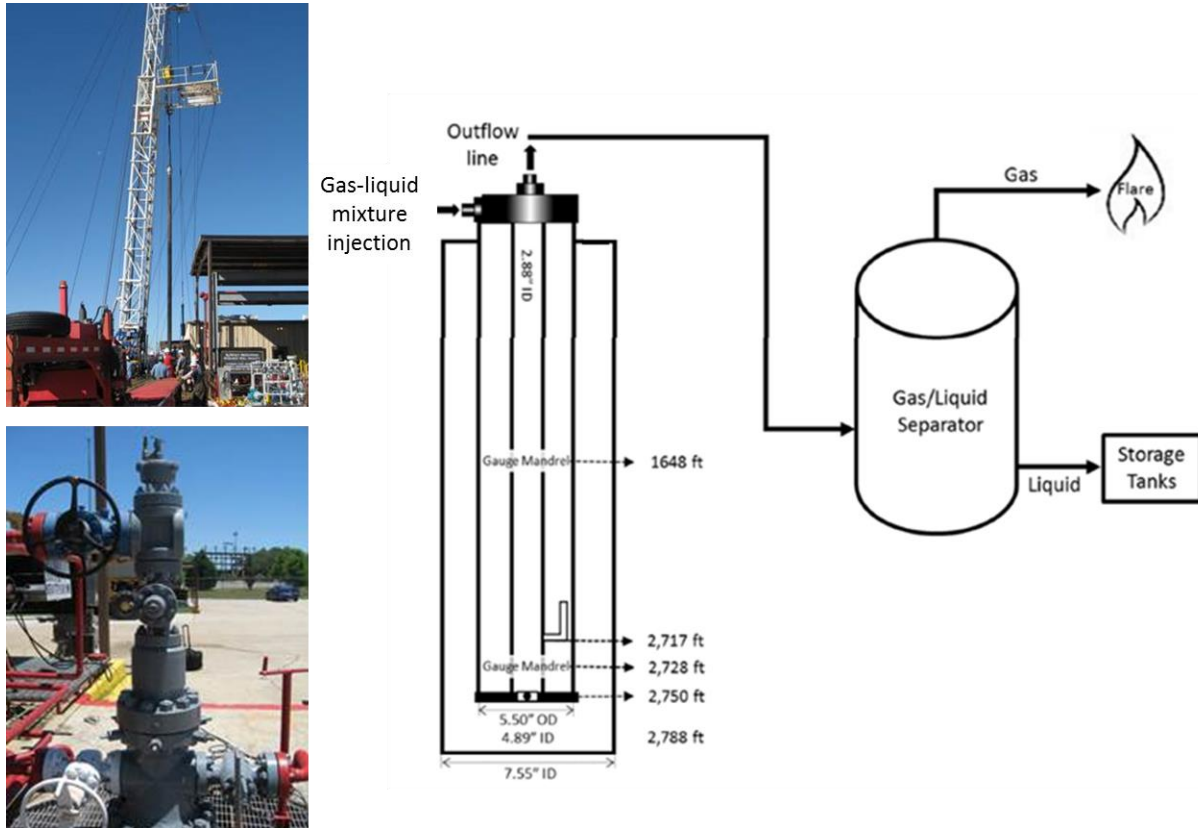


Figure 5.1. Schematic of the field-scale test well used in Coutinho (2018)

The data set consists of 15 experimental runs, for actual volumetric gas rates of 5, 10 and 20 *agpm*, and actual volumetric liquid rates between 20 and 70 *agpm*. The pressure at the injection line ranges from 300 to 1000 *psig*. The fluids used were natural gas and water. In each experimental run, the actual volumetric flow rates injected in the inner tubing-casing annulus were constant. The tests were ended when the gas-liquid mixture reached the bottom of the well. Figure 5.2 presents the test matrix. On Figure 5.2, bubbly, intermittent, and annular flow regimes are represented as triangles, squares, and circles, respectively. Since the flow regime in the well could not be observed, the flow regimes indicated on the graph were predicted using OLGA simulator.

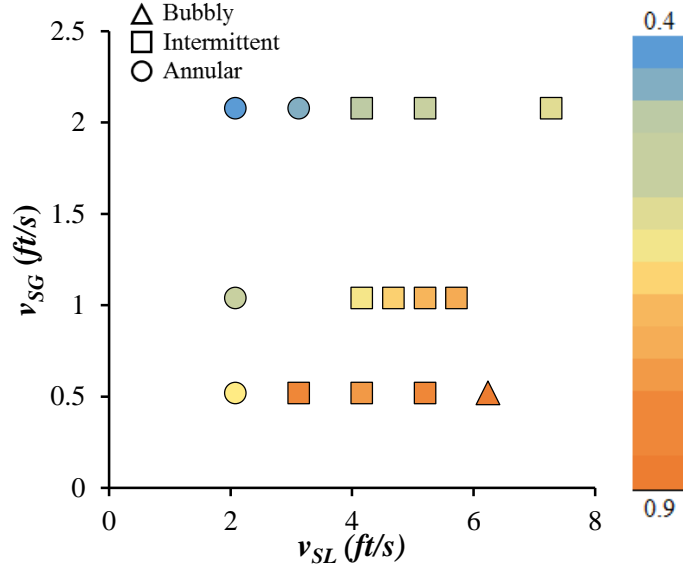


Figure 5.2. Test matrix for Coutinho (2018) experimental data set for downward flow in the annulus.

A model was created in OLGA to represent the test well and generate the results for the comparison. For running the simulations, the pressure at the bottom of the well (measured during the experiments in the test well), the injection liquid flow rate and injection gas flow rate as functions of time are inputted as boundary conditions. Figure 5.3 shows the input data used for a specific run, with actual volumetric gas rate of 20 *agpm*, and actual volumetric liquid rate of 20 *agpm*.

The objective of this comparison was to evaluate the performance of the simplified transient simulator developed in this work, and compare the results obtained with OLGA in terms of injection pressure at the top of the well. Using the boundary conditions shown on Figure 5.3, the injection pressure at the top of the well as a function of time was calculated with the simulator developed in this work and compared to the experimental data and to the results obtained with OLGA. Figure 5.4 summarizes the results.

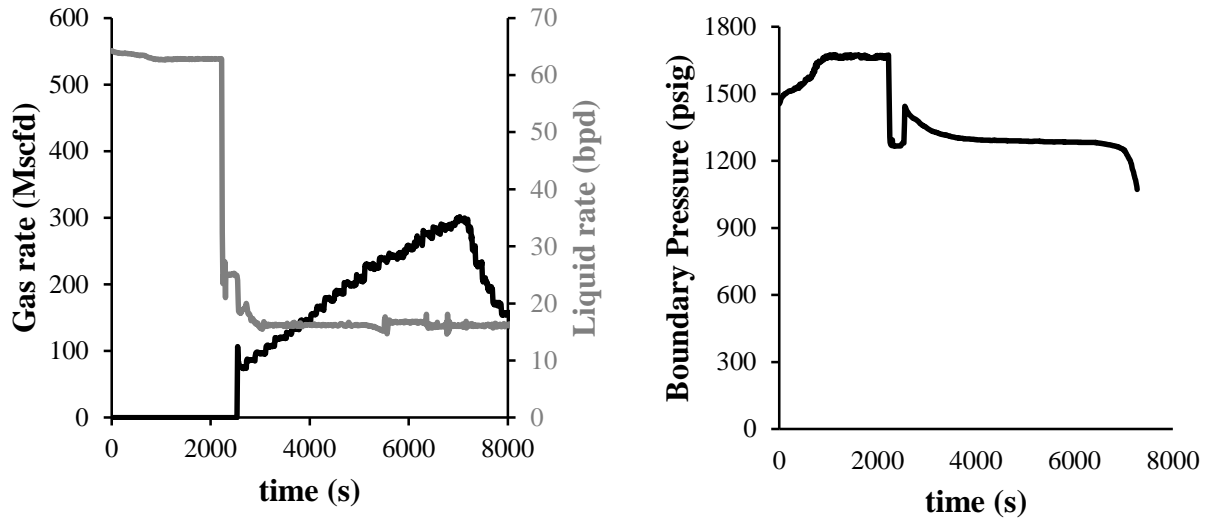


Figure 5.3. Boundary conditions (standard gas and water flowrates and pressure at the bottom of the tubing-casing annulus as a function of time) for a certain experimental run.

Figure 5.4 shows that when the liquid injection rate is decreased at around 2300 *seconds*, the injection pressure decreases. Later, after additional 200 *seconds*, the injection pressure increases because of the increase in the gas injection rate. This happens because the mixture density on the annulus side decreases and thus the difference between the density in the annulus and in the tubing increases. The injection pressure continues to increase until the gas reaches the bottom of the well and flows to the tubing. The moment at which the gas reaches the bottom of the well corresponds to the highest injection pressure. The estimation of this value is important for design and selection of compressors for unloading and gas-lift operations.

Figure 5.4 shows that the model of this work captures the same trend observed in the experiments with reasonable accuracy. OLGA overall also captures the trend, but it over estimates the maximum injection pressure.

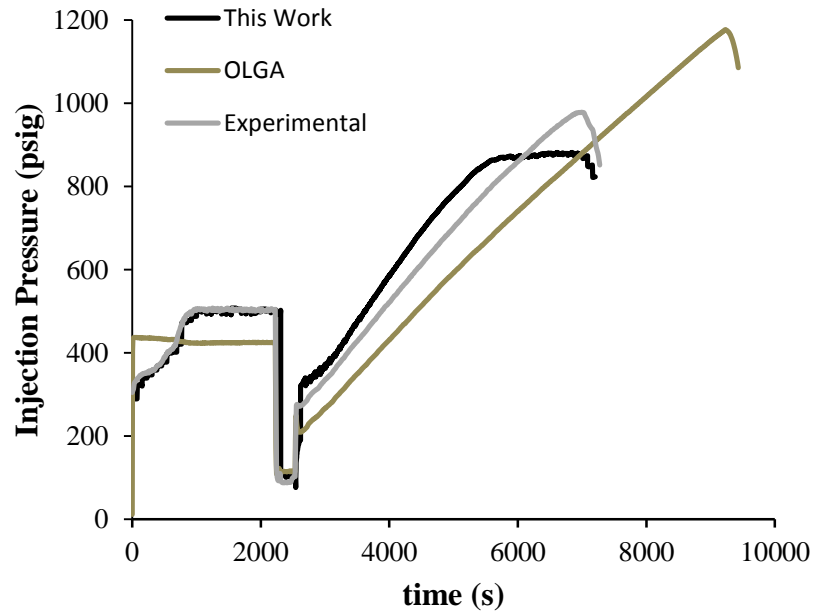


Figure 5.4. Injection pressure as a function of time. Comparison of results from the simulator of this work, OLGA and experimental data from Coutinho (2018).

The capabilities of the output module of the simulator developed in this work allow the user to visualize the migration of the gas along the well and better understand the changes in the injection pressure. Figure 5.5 shows the liquid holdup profile as a function of measured depth at different time steps. It can be seen that gas reaches the bottom of the well at approximately 5389 *seconds*, which is in agreement with the time of maximum injection pressure in Figure 5.4.

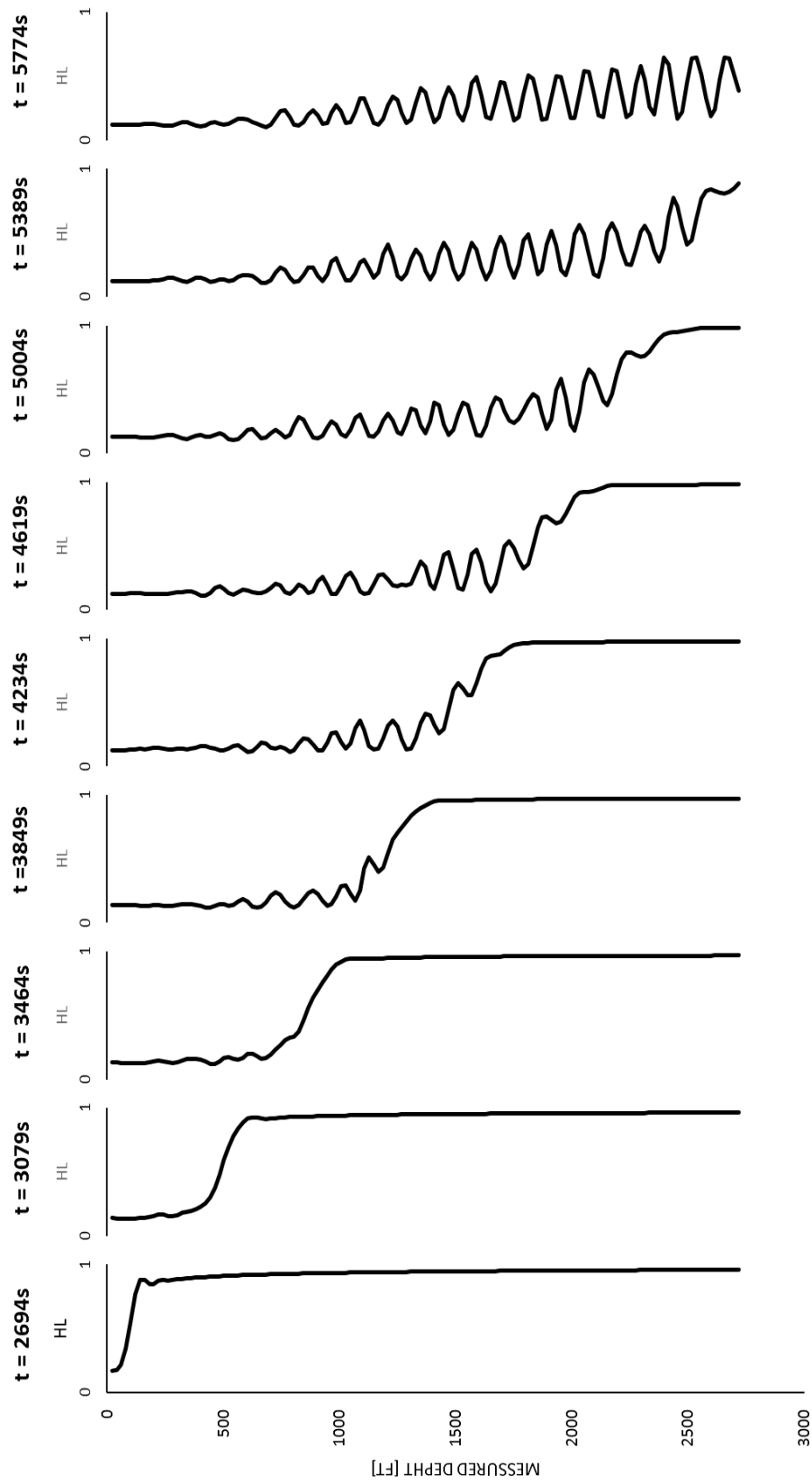


Figure 5.5. Liquid holdup as a function of measured depth at different time steps.

Figure 5.6 shows other graphing option of the output module of the simulator of this work. By plotting the liquid holdup as a function of time at the bottom of the well, the flow regimes may be indicated. In this case, for example, it can be inferred that the flow regime at the end of the transient simulation is intermittent.

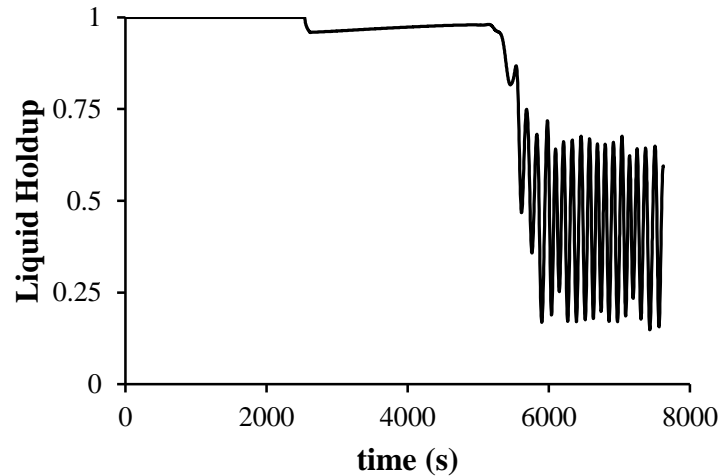


Figure 5.6. Liquid holdup as a function of time at the bottom of the well.

This same comparison was performed for all the 15 runs of the experimental data from Coutinho (2018). Figure 5.7 summarizes the average error for the predicted pressure for the 15 runs. On Figure 5.7, the flow regimes predicted by OLGA at the injection point are represented by different marker types (triangles, squares, and circles, for bubbly, intermittent, and annular flow regimes respectively) and the color of the markers represent the average error. By analyzing the liquid and gas superficial velocities on the X and Y axis on Figure 5.7 and the flow regimes indicated by the markers types, it is possible to estimate the flow regimes transitions.

It can be seen that the average error for injection pressure is small for most of the cases (lower than 20%), which indicates that the model captures the trend observed in the experiments with reasonable accuracy.

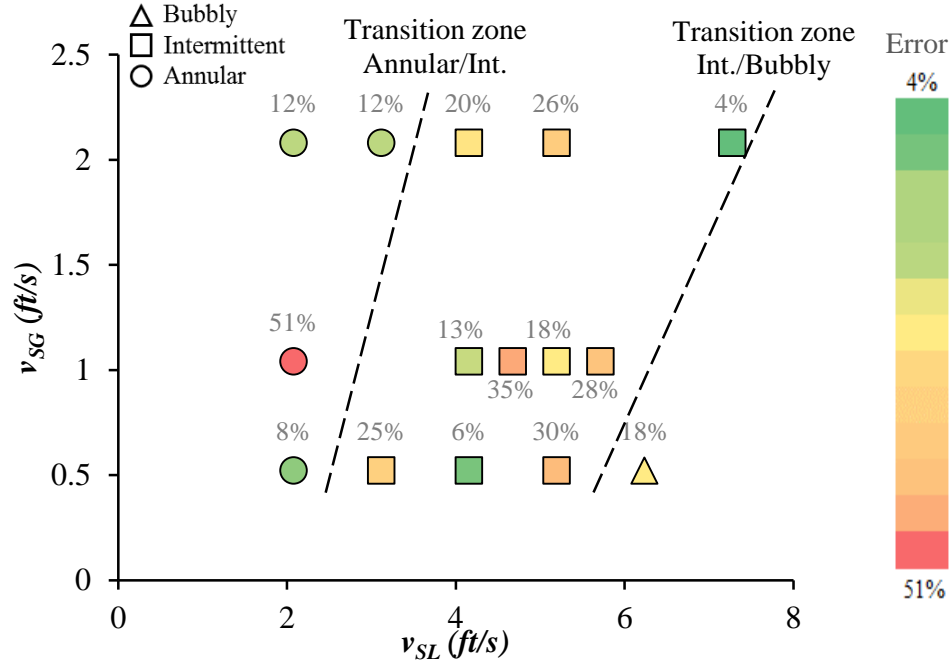


Figure 5.7. Average error for pressure calculated with the model from this work in relation to the experimental data.

Figure 5.8(a) shows the injection pressure as function of time for a case in which the flow regime is predicted as intermittent ($v_{SG} = 0.52$ ft/s, $v_{SL} = 4.1$ ft/s). It can be seen that there is a good match between the pressure predicted in this work and the experimental data. The average error for this case is 6%. As the liquid superficial velocity increases (Figure 5.8(b)), moving the conditions closer to the transition zone between intermittent and bubbly flow ($v_{SG} = 0.52$ ft/s, $v_{SL} = 5.2$ ft/s), the average error increases to 30%. From Figure 5.8 it can be seen that OLGA also does not completely match the experimental pressure for these scenarios (average error of 27% for case (a) and 18% for case (b)).

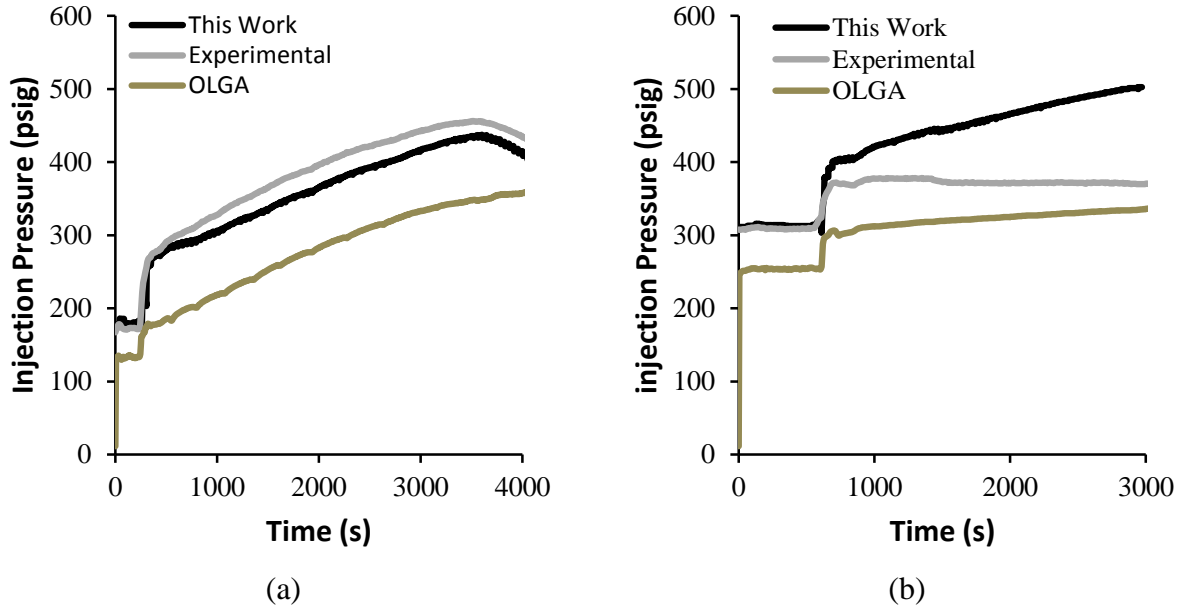


Figure 5.8. Comparison of injection pressure predicted in this work, calculated with OLGA and experimental (Coutinho, 2018) for two different runs: (a) $v_{SG} = 0.52$ ft/s, $v_{SL} = 4.1$ ft/s (b) $v_{SG} = 0.52$ ft/s, $v_{SL} = 5.2$ ft/s.

One of the factors to be considered when evaluating the larger errors in Figure 5.7 is the characteristics of the drift-flux correlation itself. The correlation for the distribution parameter from Bhagwat and Ghajar (2014) has an abrupt change from 2.0 to 1.2 for two-phase Reynolds numbers between 200 and 2000. Since the distribution parameter directly influence the liquid holdup, which affects the pressure calculation, if the input rates change so that between successively time steps the two-phase Reynolds number at a certain location in the well is in the range mentioned, the results for the model would be affected. In addition, as demonstrated by Bhagwat and Ghajar (2014), for flow in annulus, the error for the prediction of the liquid holdup is $\pm 25\%$. Since the error for holdup carries out to the pressure calculation, the error of the model is expected to be at least in the same range.

The rate of change of the liquid and gas volumetric rates is also a factor to be considered in the analysis of the results presented in Figure 5.7. In Section 4.1, the validity of the pseudo-

steady-approach was discussed and Eq. (4.11) was given to indicate the limiting conditions for which the model can be applied. The usefulness of Eq. (4.11) is demonstrated when analyzing the performance of the simulator developed in this work in comparison with the experimental data from Coutinho (2018).

Figure 5.9 illustrates an experimental run from Coutinho (2018) data set for which there is an abrupt change in the injections rates. For this case, in just 11 *seconds* the water injection rate changes from 14 to 2800 *bbl/day*, and gas rate changes from 0 to 92 *Mscf/day*. For the peak rate change, the left-hand-side term of Eq. (4.11) is one order of magnitude greater than the right-hand-side term, violating the criteria of Eq. (4.11).

Figure 5.9 shows that the model is not able to capture the injection pressure accurately for this scenario. Since the model is not able to capture this behavior, it over predicts the injection pressure right at the beginning of the simulation, and, since each time step depends on the results of the previous time step, the error propagates throughout the rest of the simulation.

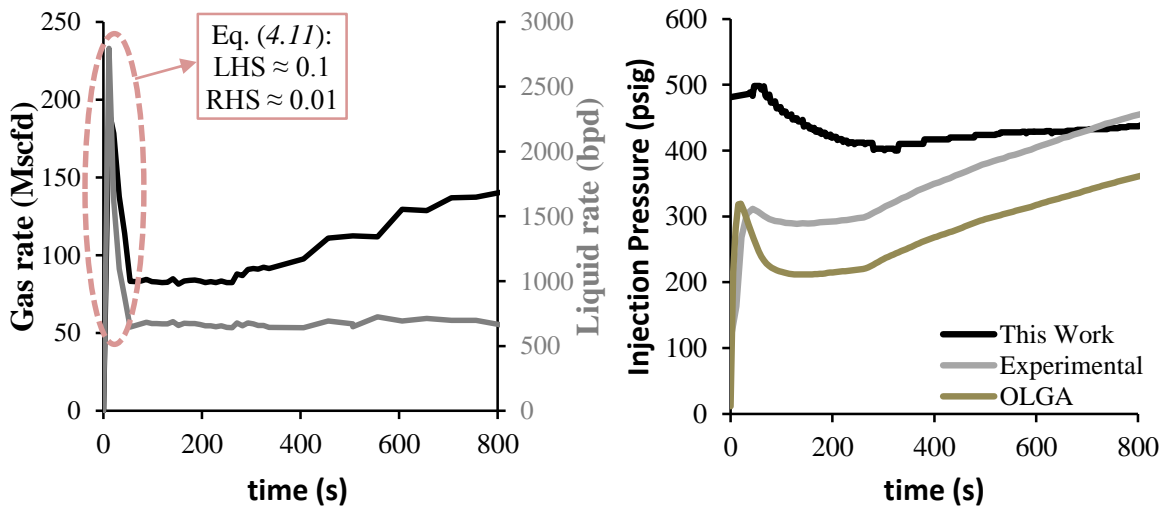


Figure 5.9. Gas and water injection rates for a fast transient case and the comparison of injection pressure predicted in this work, calculated with OLGA and experimental (Coutinho 2018).

From the results discussed above, it can be stated that the simulator developed in this work has a reasonable accuracy on predicting the injection pressure. Even though these are relatively complex cases for a field-scale well in annulus pipe geometry, with many fluctuations on the injections rates and pressure, this simplified transient simulator is able to accurately predict the injection pressure and capture the transient flow behavior of gas and liquid flowing downward in the pipe annulus.

5.2. Large-Scale Flow Loop for Vertical Upward Flow in the Tubing

This sections presents the validation of the simulator developed in this work with experimental data from Waltrich (2012). The data was acquired by the latter author using a large scale flow loop, named TowerLAB, located at the Texas A&M University. The vertical test section is 1.97-*inch* ID, 141-*ft* long, and it is instrumented for measurements of pressure, temperature, and liquid holdup, and has cameras installed at three different axial locations to allow visualization of the flow regime (Figure 5.10). A detailed description of the features of the test section and the instrumentation, visualization and data acquisition system can be found on Waltrich (2012).

Table 5.1 summarizes the conditions of the experiments, which were used as input for the simulator of this work and to obtain the results in OLGA. The cases in Table 5.1 represent upward two-phase flow in vertical pipes for annular and churn flow regimes.

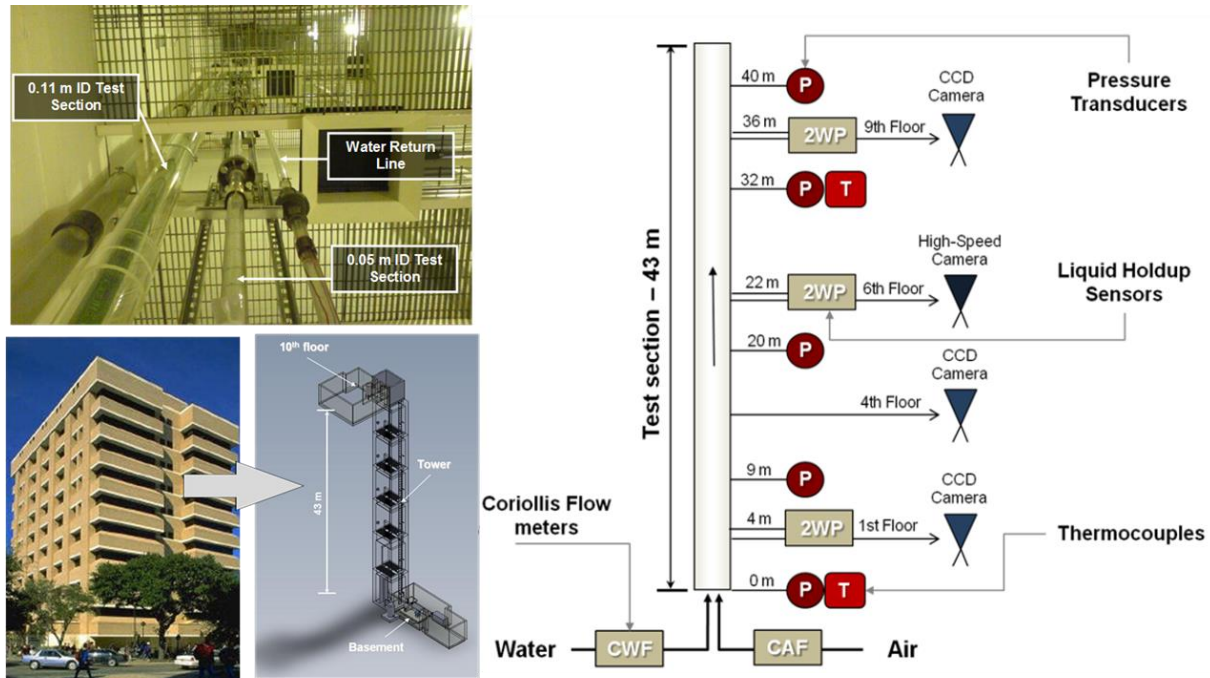


Figure 5.10. Schematic of TowerLab (Waltrich, 2012).

Table 5.1. Experimental conditions of the data from Waltrich (2012)

Case	Injected Air Rate (<i>Mscf/day</i>)		Standard Injected Liquid Volumetric Rate (<i>STB/day</i>)		Boundary Pressure (<i>psia</i>)		Flow Regime	
	Initial	End	Initial	End	Initial	End	Initial	End
1	34.7	21.9	20.8	11.7	16.2	73.5	Annular	Churn
2	30.7	54.8	298.6	365.7	64.3	20.8	Churn	Annular
3	55.6	30.0	390.0	290.0	21.6	74.9	Annular	Churn

Figure 5.11 presents the comparison for liquid holdup obtained experimentally, calculated with the simulator developed in this work and with OLGA, at the top and bottom of the test section for Case 1.

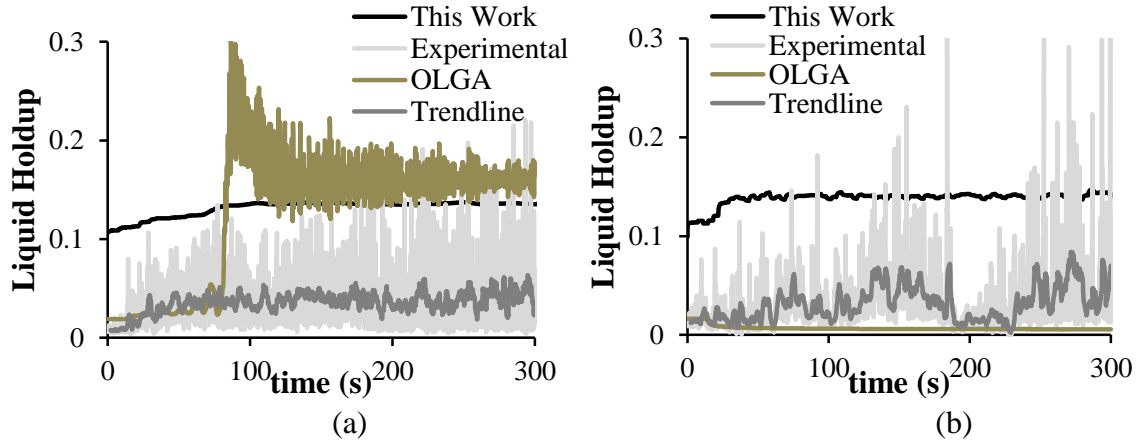


Figure 5.11. Liquid holdup (a) at the top and (b) bottom of the test section - Case 1.

From Figure 5.11, it can be seen that OLGA over predicts the liquid holdup at the top of the test section (Figure 5.11a) when the flow regime changes from annular to churn flow regime, and under predicts it at the bottom of the vertical pipe (Figure 5.11b). The results obtained with the simplified transient simulator developed in this work approximately follow the trend of the experimental data. It is important to mention that the experimental measurement uncertainty of the liquid holdup is at the same order of magnitude for low values of liquid holdup (e.g., lower than 0.1). In addition to that, the drift-flux formulation does not represent well annular flow regimes, as this formulation considers a homogenous gas-liquid mixture which is not the case for annular flow.

Although the error for liquid holdup is high, the pressure at the bottom of the test section calculated with the simplified transient simulator developed in this works presents a reasonable match with the experimental data, as shown in Figure 5.12, with an average error of 10%.

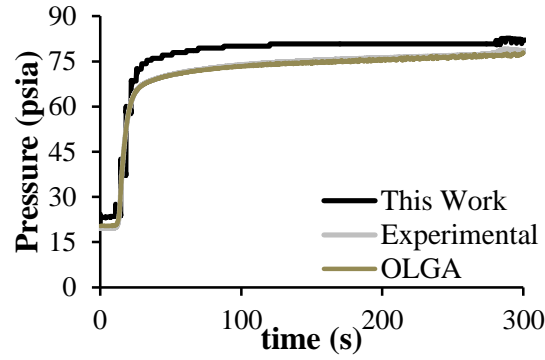


Figure 5.12. Pressure at the inlet of the fluids (bottom of the test section) – Case 1.

This mismatch of liquid holdup, but reasonable agreement with the inlet pressure, is likely due to the fact that the total pressure gradient in annular flow regime is strongly dependent on the friction component, and weakly dependent on the gravitational component.

Case 2 from Table 5.1 represents a scenario of increase in both inflow rates of gas and liquid. From Figure 5.13, the same behavior as in Case 1 is seen, with the results for liquid holdup obtained with the simulator developed in this work following the trend of the experimental data. In this case specifically, OLGA shows a better performance in the prediction of the liquid holdup. However, for the pressure at the bottom of the test section, the average error for the results obtained with the simulator of this work (7%) is lower than that for OLGA (31%), as shown in Figure 5.14.

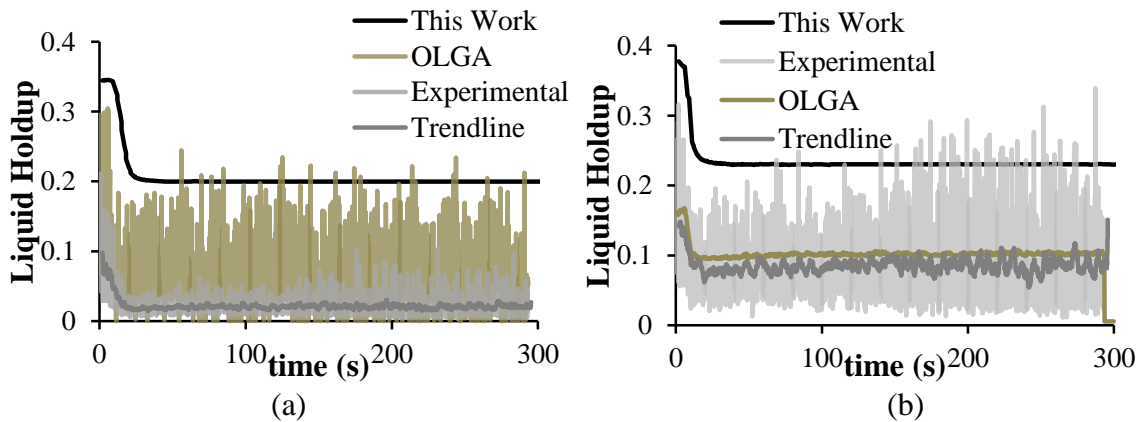


Figure 5.13. Liquid holdup at (a) the top and (b) bottom of the test section – Case 2.

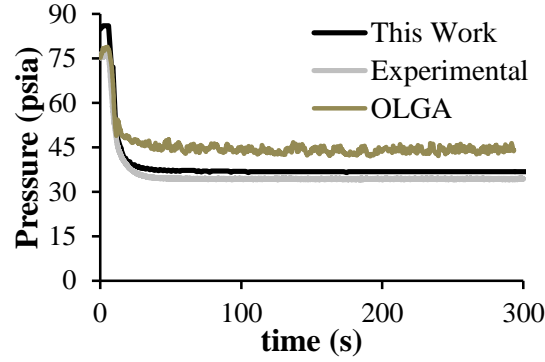


Figure 5.14. Pressure at the inlet of the fluids (bottom of the test section) – Case 2.

Figure 5.15 show the results for Case 3, which represents the scenario of decreasing both inflow rates of gas and liquid. As in the previous cases 1 and 2, it is seen that the liquid holdup follows the trend of the experimental data. The average error for the pressure at the bottom of the test section for this case is 2%, as shown in Figure 5.16.

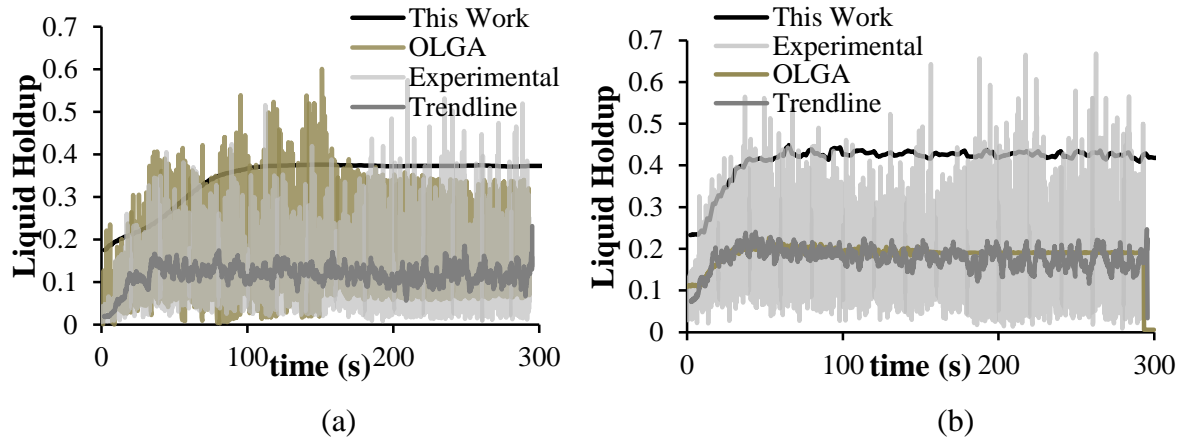


Figure 5.15. Liquid holdup at (a) the top and (b) bottom of the test section – Case 3.

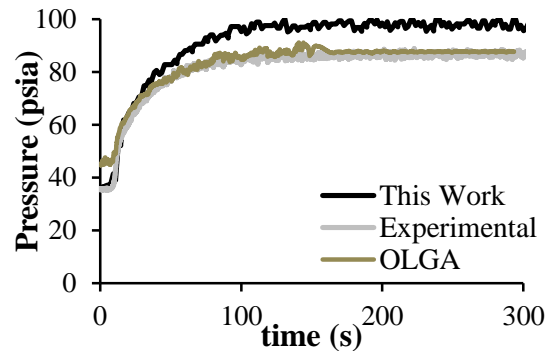


Figure 5.16. Pressure at the inlet of the fluids (bottom of the test section) – Case 3.

The results presented in this section show that the model of this work captures the trend of the experimental liquid holdup, but the results from the model are shifted towards higher liquid holdup values. It is important to note that the liquid holdup for these experimental cases is lower than 0.20, therefore, a small relative difference between the calculated and measured values already results in a high percentage error. In addition, it is difficult to measure with high accuracy the liquid holdup at this level. From the observation of these comparisons, it seems that the prediction of the preceding steady-state condition might be the issue. Therefore, if the prediction of the liquid holdup for these low liquid holdup levels can be improved, a lower error could be achieved. Nevertheless, the simulator developed in this work, presented an overall reasonable match in terms of pressure with the experimental data for annular and churn flow regimes in vertical upward flow.

5.3. Synthetic Data from OLGA Simulator

The previous sections discussed a comparison of the performance of the model developed in this work and the experimental data for vertical downward flow in annulus and vertical upward flow in tubing. Since the available experimental data sets do not cover all flow regimes and pipe inclinations, it was necessary to generate synthetic data, using the commercial simulator OLGA, in order to expand the comparison and cover a wider range of conditions. The synthetic cases generated with OLGA cover superficial liquid velocities from 0.01 *ft/s* to 10 *ft/s* and superficial gas velocities from 0.01 *ft/s* to 60 *ft/s*. For the injection cases (downward flow), the boundary pressure (at bottom hole) range covered in these cases is from 400 to 1100 *psig*. For the production cases (upward flow), the boundary pressure (at wellhead) range covered is from 20 to 100 *psig*.

5.3.1. Vertical Downward Flow

Table 5.2 details the cases run for vertical downward flow in a 1400 *feet* long pipe with a 2 *inch* hydraulic diameter.

Table 5.2. Synthetic cases generated with the commercial simulator OLGA for vertical downward flow.

Pipe Inclination (<i>degrees</i>)		Input Gas Rate (<i>Mscf/day</i>)		Input Liquid Rate (<i>STB/day</i>)		Boundary Pressure (<i>psig</i>) (constant)	Flow Regime
	Case	Initial	End	Initial	End		
-90°	1	1	30	2000	2000	600	Slug
	2	1	30	1000	1000	600	Slug/Annular
	3	5	5	50	250	200	Falling Film
	4	20	20	50	250	200	Falling Film
	5	20	20	2000	4000	1000	Bubbly
	6	500	500	2000	4000	800	Slug
	7	600	600	2000	4000	700	Slug
	8	800	800	1000	2000	400	Annular
	9	8000	8000	3000	4000	1100	Annular

Case 2 (Figure 5.17a) presents very high errors likely because it is very close to the transition to falling film flow regime. For Cases 3 and 4, which are in falling film flow regime, the simplified model developed in this work did not achieve convergence.

For Cases 2, 5, 8, and 9, Figure 5.17b-d illustrate the comparison for liquid holdup and pressure at three locations in the pipe (top, middle, and bottom) as a function of time.

Case 5, (Figure 5.17b), which is in bubbly flow regime, shows good agreement with OLGA, with maximum error for the liquid holdup of 1.2%. Consequently, the results for inlet pressure also present a good match with OLGA results.

As the gas superficial velocity increases and the flow regime changes to slug and then annular, the predictions of the simplified model of this work start to deviate from the results obtained with OLGA, and the maximum error increases.

Figure 5.17c-d show the comparison of liquid holdup and pressure for Cases 8 and 9, which are in annular flow regime. It can be seen that the liquid holdup obtained with the simplified simulator of this work is shifted towards higher values of liquid holdup, in comparison with the results from OLGA. The error on the holdup prediction is propagated to the pressure predictions, with the maximum error around 54%.

Figure 5.18 shows the errors for liquid holdup and pressure at the top, middle and bottom grid blocks for Cases 1, 6, and 7, which are in slug flow regime. The maximum errors for the liquid holdup and pressure are 61% and 54%, respectively. The errors are higher for Case 8, which is closer to the transition between slug and annular flow regimes.

These results, however, are expected, since the formulation of the simplified model is better suited for bubbly and slug flow regimes. Also, it is important to consider the differences in the formulations of OLGA and the simplified model. OLGA is a two fluid model, which is a more rigorous approach and it also has its own flow regime map. As demonstrated in Section 3.1, there are disagreements between the flow regimes predicted by OLGA and experimental observations. The disagreements in flow regime prediction lead to greater errors for liquid holdup and pressure.

Thus, although OLGA results are used as benchmark data in this study, it is still difficult to conclude on the actual accuracy of the simplified model for downward flow.

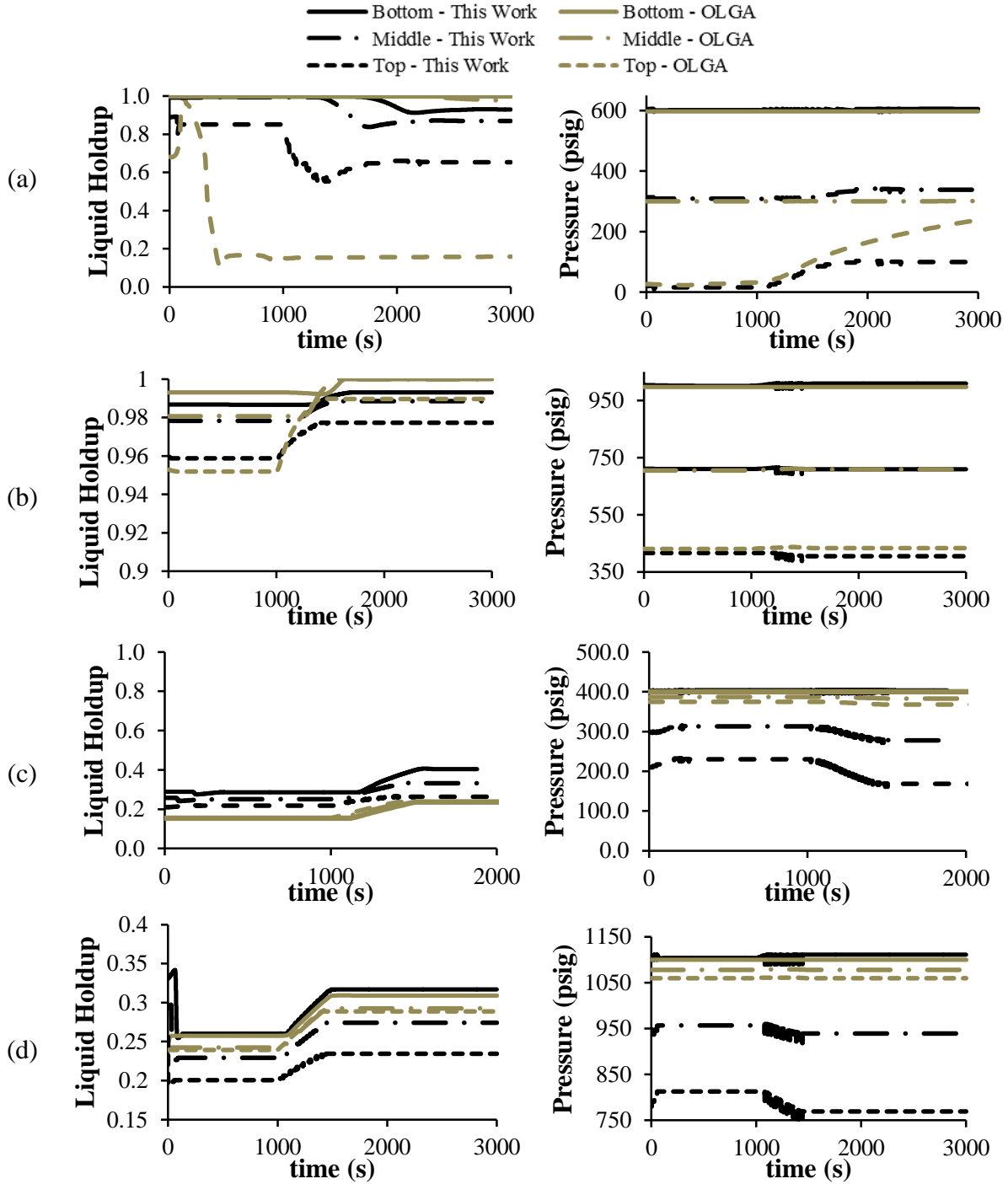


Figure 5.17. Comparison of results using the simulator of this work and OLGA for liquid holdup and pressure at three locations (top, middle and bottom of pipe) as a function of time, for (a) Case 2, (b) Case 5, (c) Case 8, and (d) Case 9, in vertical downward flow in the annulus.

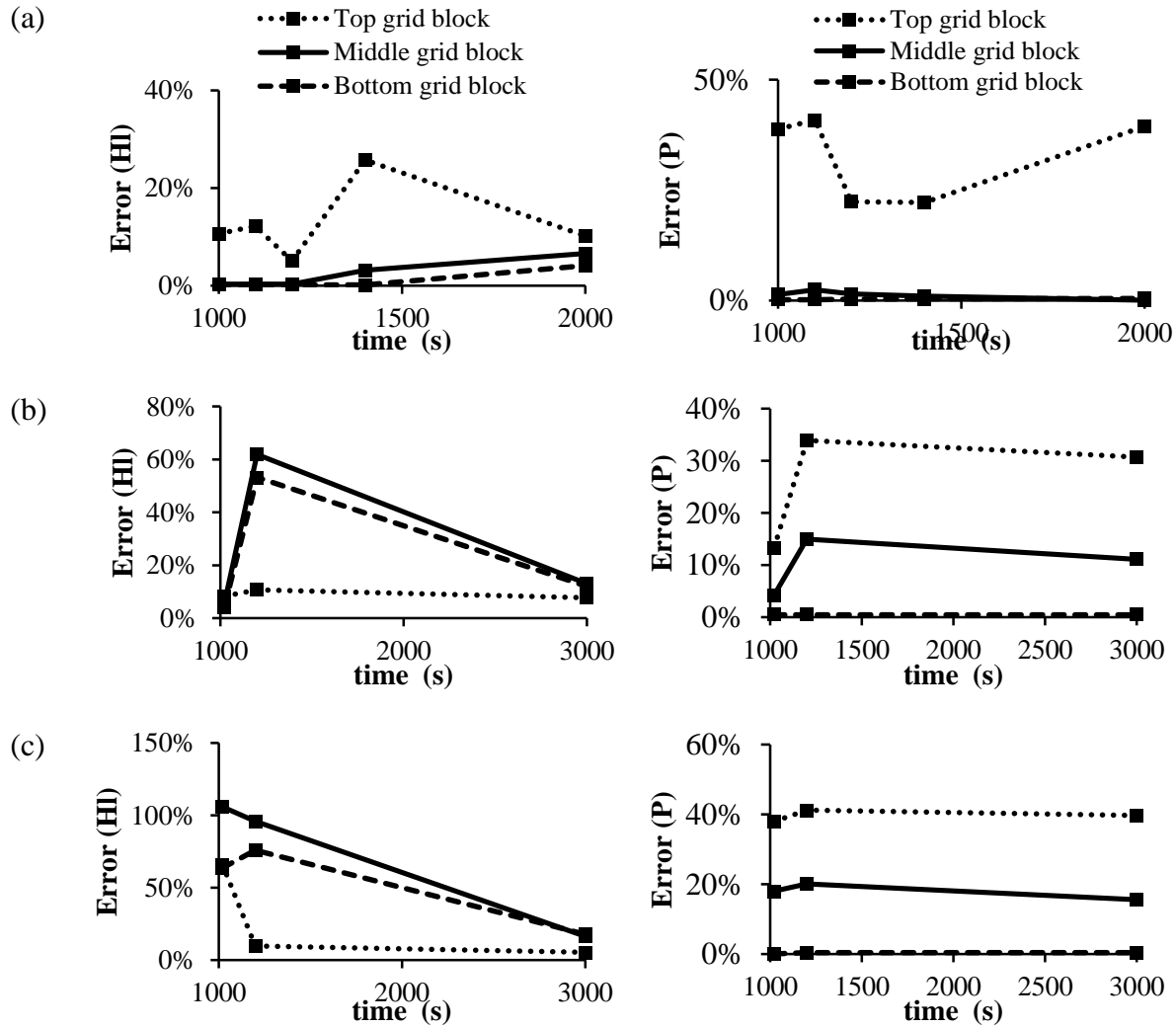


Figure 5.18. Errors for liquid holdup and pressure at the top, middle and bottom grid blocks for (a) Case 1, (b) Case 6, and (c) Case 7.

In Section 2.1, the flow regimes for downward flow were discussed and the falling film flow regime was presented. For low superficial liquid velocities in downward flow, a thin liquid film in free falling movement forms in the walls of the pipe. In order to evaluate the performance of the model for this flow regime, some cases with very low superficial liquid velocity (lower than 0.6 ft/s) were considered. For these conditions, the liquid holdup is approximately in the range of

0.02 to 0.08. The simplified model developed in this work proved not to be adequate for falling film flow regime conditions, and did not achieve convergence for these cases.

Waltrich et al. (2015), in a study on liquid transport during gas flow transients applied to liquid loading, experimentally observed the breakup of liquid film. In their experiments, they observed the behavior of the liquid distribution at three axial positions along the test section (141 *feet* long, 2 *inch* ID). Figure 5.19 presents the snapshots of the video recordings taken during the experiments. At the beginning of the experiment, for annular flow regime, they observed a continuous liquid film flowing upwards. However, after 15 *seconds*, the flow rates changed and the liquid film started to flow downward. At the same time, in other locations of the test section, discontinuities in the liquid film were observed.

Although the study by Waltrich et al. (2015) was performed for upward flow, it provides some indications on the understanding of downward flow in falling film flow regime. For the conditions for which this flow regime appears, the thin liquid film flowing on the walls of the pipe might break up depending on the transient changes, and form liquid film discontinuities. This discontinuities can be seen as not following the one-dimensional assumption of the model of liquid film symmetry for the flowing area. Since the model ignores velocities and accelerations other than those in the axial direction, the model returns a physical inconsistency when used to simulate falling film and does not converge.

Based on the comparisons using the experimental data from Coutinho (2018) and the synthetic data generated with OLGA, the mapping of the error for the simplified model is shown in Figure 5.20 and Figure 5.21. This error mapping aims at providing reference in terms of expected errors for different superficial velocities of liquid and gas for liquid holdup and pressure predictions. On these figures, the size of the markers indicate the average error.

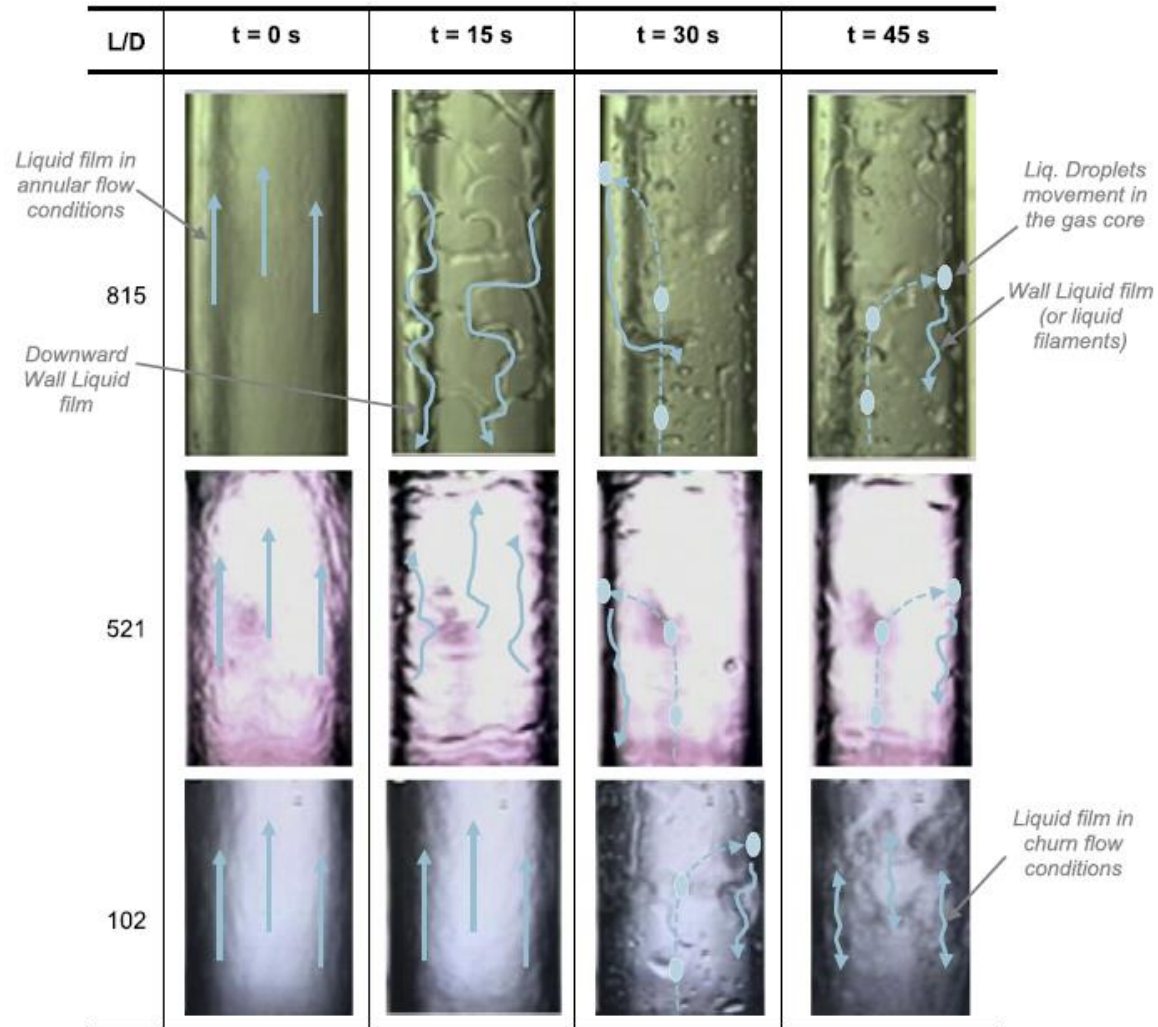


Figure 5.19. Snapshots of the simultaneous video recording from Waltrich (2015) at three different axial locations in the test section at different times. The continuous blue lines indicate the liquid film flow direction and the dashed lines indicate the droplet movement as observed in the video recording.

As it can be seen in Figure 5.20 and Figure 5.21, the predictions of liquid holdup and pressure for bubbly and slug flow regimes are fairly accurate. The same trend of increasing maximum errors when the conditions approach a flow regime transition is observed.

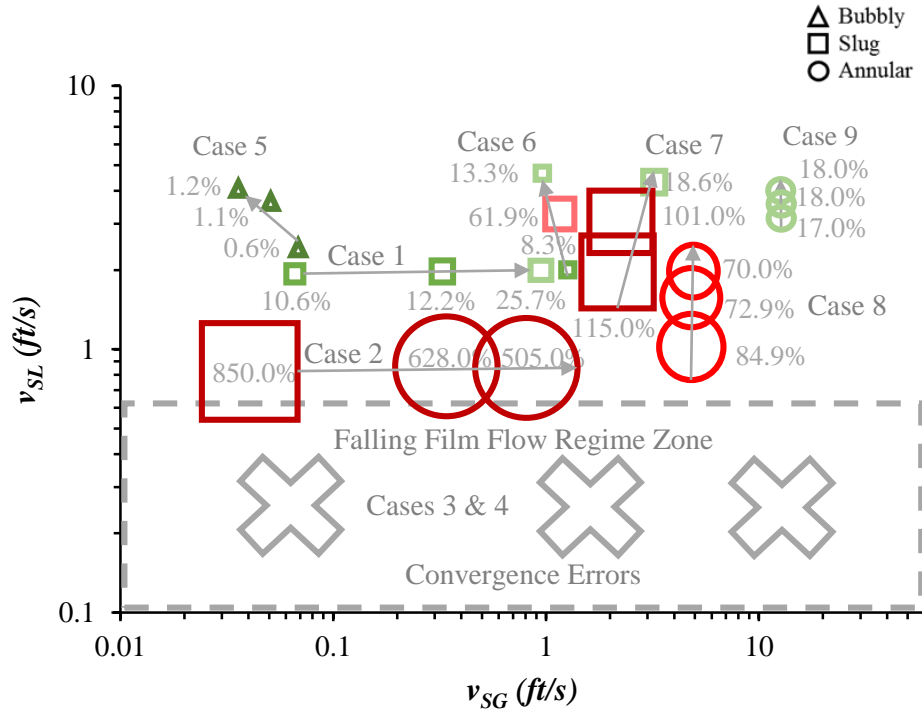


Figure 5.20. Maximum error for liquid holdup predictions for vertical downward flow ($\theta = -90^\circ$). The different flow regimes are indicated by the type of point marker. The size of the markers indicate the average error.

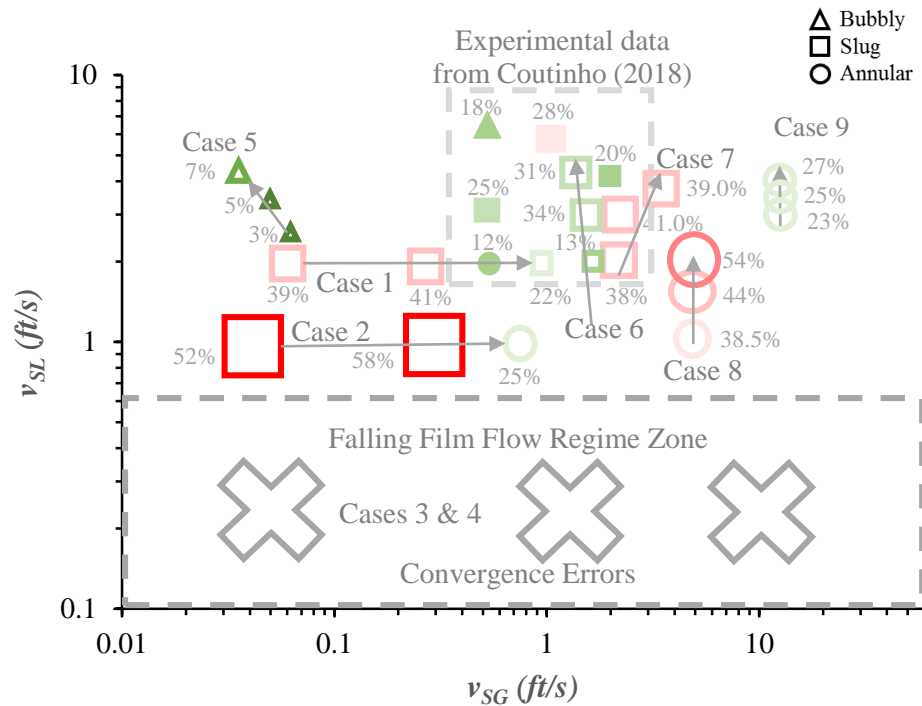


Figure 5.21. Maximum error for pressure predictions for vertical downward flow ($\theta = -90^\circ$). The different flow regimes are indicated by the type of point marker. The size of the markers indicate the average error.

As the liquid superficial velocity approaches 1 *ft/s* and lower, the liquid holdup approach values lower than 0.08, indicating falling film flow regime. For these cases the error of the simplified model for the liquid holdup goes to above 850%. The simplified model is not able to capture the abrupt changes in the liquid holdup that are predicted by OLGA. Also, since the liquid holdup values are small, even a small relative difference yields a high percentage error.

Overall, the conclusions drawn from the comparison with synthetic data generated by OLGA agree with the observations drawn from the comparison with experimental data from Coutinho (2018). Since Coutinho (2018) did not measure holdup experimentally, Figure 5.20 only shows the results for the comparison with synthetic data. The falling film flow regime zone, in which the simplified model does not work, is indicated in Figure 5.20 and Figure 5.21.

5.3.2. Inclined Downward Flow

A similar analysis was performed for downward flow in a -45° inclined pipe. Table 5.3 details the cases run for this pipe inclination. As discussed in Section 2.1, for inclined downward flow, stratified is the predominant flow regime and it was the flow regime predicted for most of the cases analyzed in this section.

Figure 5.22 shows the comparison for liquid holdup and pressure at three locations in the pipe (top, middle, and bottom) as a function of time, using both the simplified model and OLGA simulator, for a bubbly (Case 2) and a stratified (Case 3) flow regime case. The model did not achieve convergence for Cases 4 and 5, due to extremely low liquid holdup level (<0.05). Figure 5.23 shows the error for the liquid holdup and pressure at three location in the pipe for the other cases.

Table 5.3. Synthetic cases generated with the commercial simulator OLGA for inclined downward flow.

Pipe Inclination (degrees)	Case	Input Gas Rate (Mscf/day)		Input Liquid Rate (STB/day)		Boundary Pressure (psig) (constant)	Flow Regime
-45°	1	1	30	2000	2000	600	Stratified/Slug
	2	20	20	2000	4000	1000	Bubbly
	3	800	800	1000	2000	400	Stratified
	4	5	5	50	250	200	Stratified
	5	20	20	50	250	200	Stratified
	6	500	500	2000	4000	800	Stratified
	7	8000	8000	3000	4000	1100	Stratified

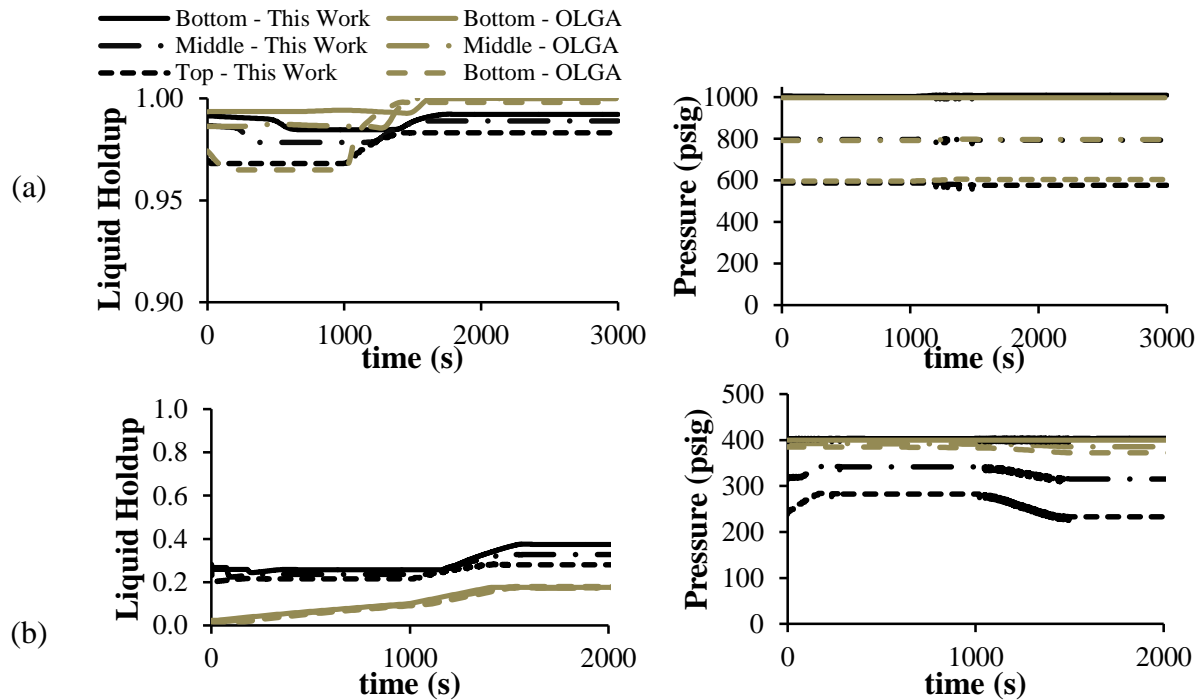


Figure 5.22. Comparison of results using the simulator of this work and OLGA for liquid holdup and pressure at three locations (top, middle and bottom of pipe) as a function of time, for (a) a bubbly flow regime case, and (b) a stratified flow regime case in inclined downward flow in the annulus.

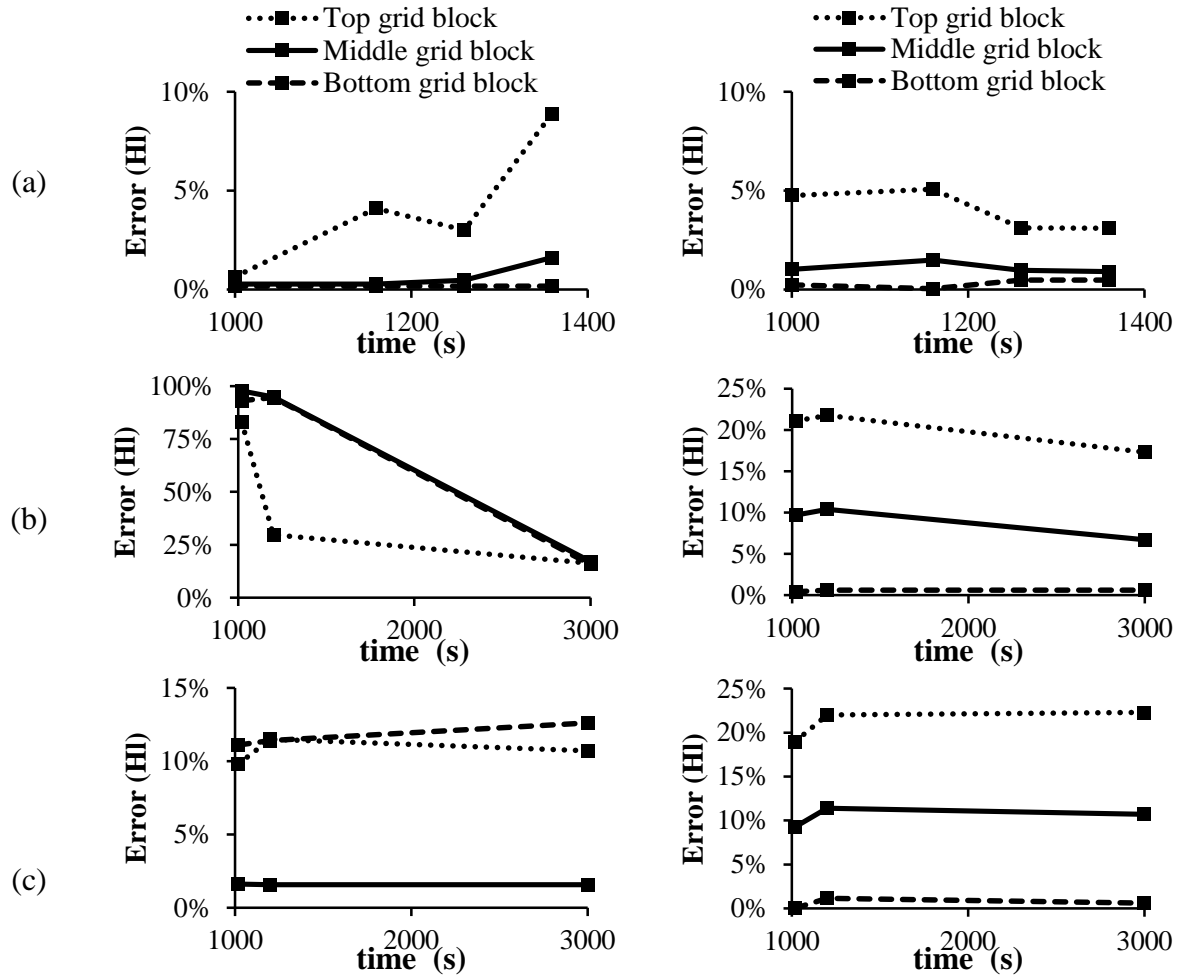


Figure 5.23. Errors for liquid holdup and pressure at the top, middle and bottom grid blocks for (a) Case 1, (b) Case 6, and (c) Case 7.

Figure 5.24 and Figure 5.25 show the maximum errors for liquid holdup and pressure predictions for a -45° inclined pipe. Figure 5.24 shows that the error for the liquid holdup prediction increases as the gas superficial velocity increases and the liquid superficial velocity decreases (see Case 3, for example). The simplified model does not converge for low liquid holdup levels. Overall, the pressure prediction presents a reasonable match with OLGA, with errors lower than 35%.

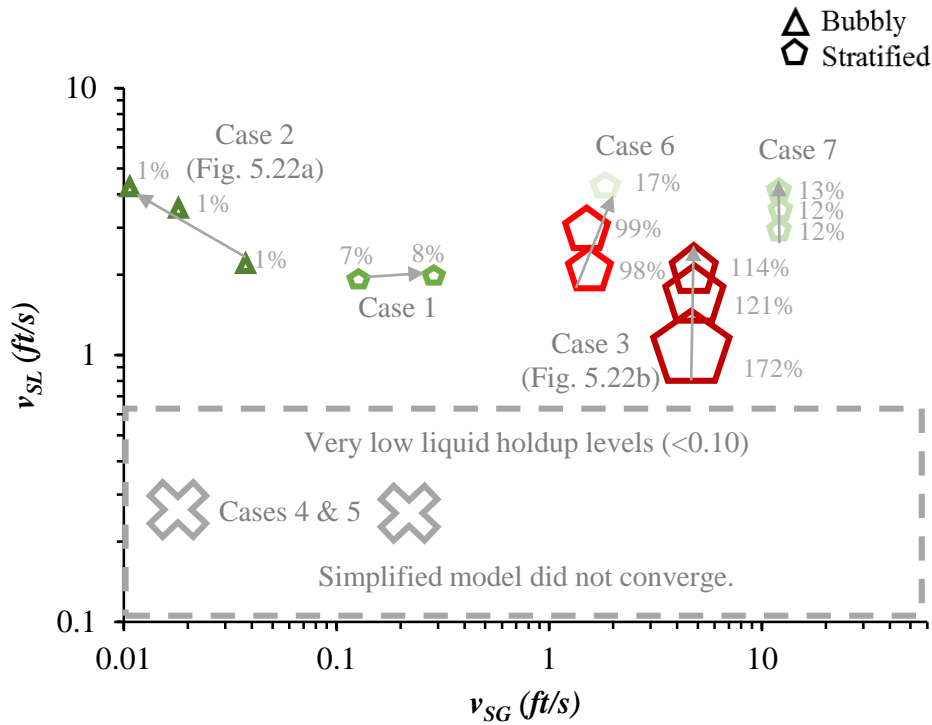


Figure 5.24. Maximum error for liquid holdup prediction for Inclined downward flow ($\theta = -45^\circ$)

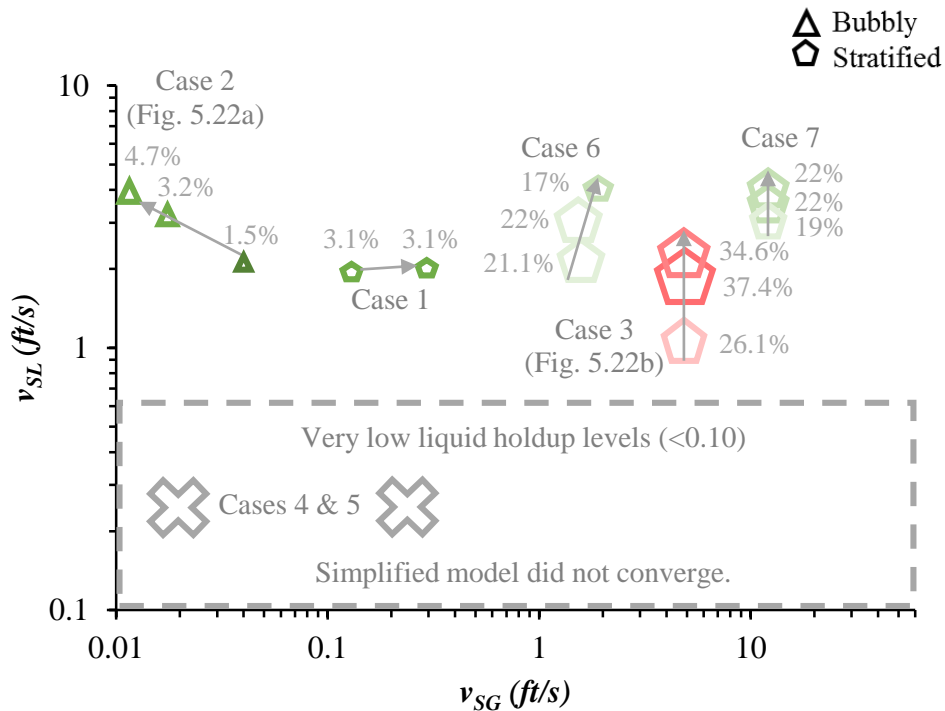


Figure 5.25. Maximum error for pressure prediction for Inclined downward flow ($\theta = -45^\circ$)

5.3.3. Horizontal Flow

In order to analyze the performance of the simplified model for flow in horizontal pipes, synthetic data was generated with the commercial simulator OLGA, as shown in Table 5.4.

Figure 5.26 and Figure 5.27 illustrate the comparison for liquid holdup and pressure at three location in the pipes (inlet, middle, and outlet) as a function of time, using both the simplified model and OLGA, for flow in a 1,378 *feet* long horizontal pipe, with a 3 *inch* diameter.

Table 5.4. Synthetic cases generated with the commercial simulator OLGA for horizontal flow.

Pipe Inclination (<i>degrees</i>)	Case	Input Gas Rate (<i>Mscf/day</i>)		Input Liquid Rate (<i>STB/day</i>)		Boundary Pressure (<i>psig</i>) (constant)	Flow Regime
		Initial	End	Initial	End		
0°	1	29	29	204	1059	40	Slug/Stratified
	2	97	97	206	53	40	Slug/Stratified
	3	280	280	1855	1082	40	Slug
	4	14	14	53	200	40	Stratified
	5	31	31	2138	1132	40	Stratified
	6	5	5	4000	4700	40	Distributed bubble
	7	5	5	200	500	40	Stratified

Cases 1, 2 and 4 (Figure 5.26 a, c, d), which are in slug or stratified flow regimes or in the transition between these two flow regimes, present a maximum error for the liquid holdup of 77% and maximum error for the pressure of 8%. For Case 2 (Figure 5.26 b), which represents a case right at the boundary between stratified and slug flow regimes, it can be seen that OLGA predicted the flow regime to be slug in the beginning of the simulations and stratified after the liquid rate is decreased. However, the simplified model results does not predict this flow regime change, and

under predicts the liquid holdup. Figure 5.26 shows that as the gas and liquid velocity increases, as in Case 3, the maximum error for the liquid holdup decreases to 12%.

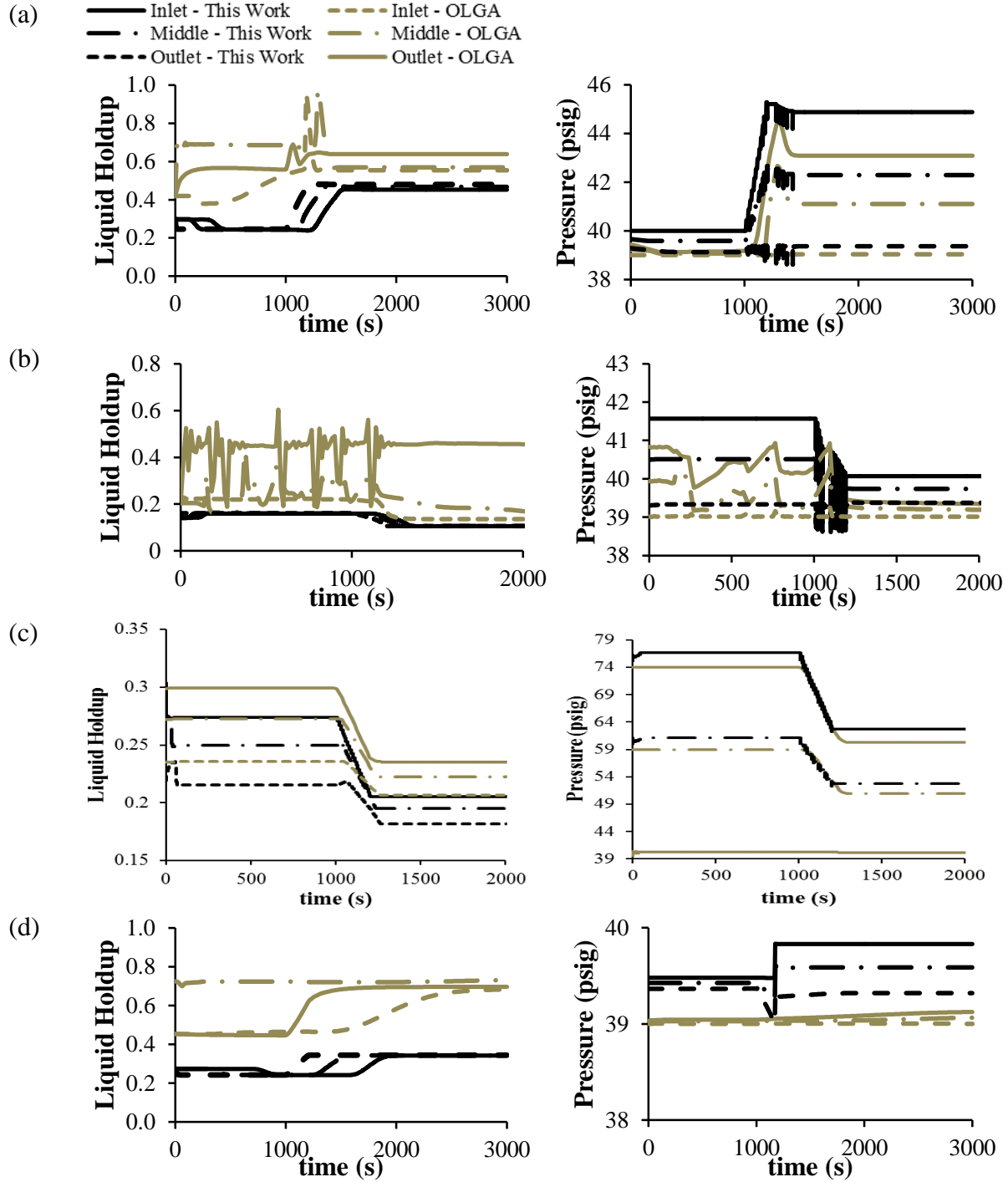


Figure 5.26. Comparison of results using the simplified model and OLGA for liquid holdup and pressure at three locations (inlet, middle and outlet of horizontal pipe) as a function of time, for (a) Case 1, (b) Case 2, (c) Case 3, and (d) Case 4.

Figure 5.27 shows the trend results for the other cases. The simplified model of this work showed a reasonable match with OLGA, with a maximum error for the liquid holdup of 32% and maximum error for the pressure of 7%.

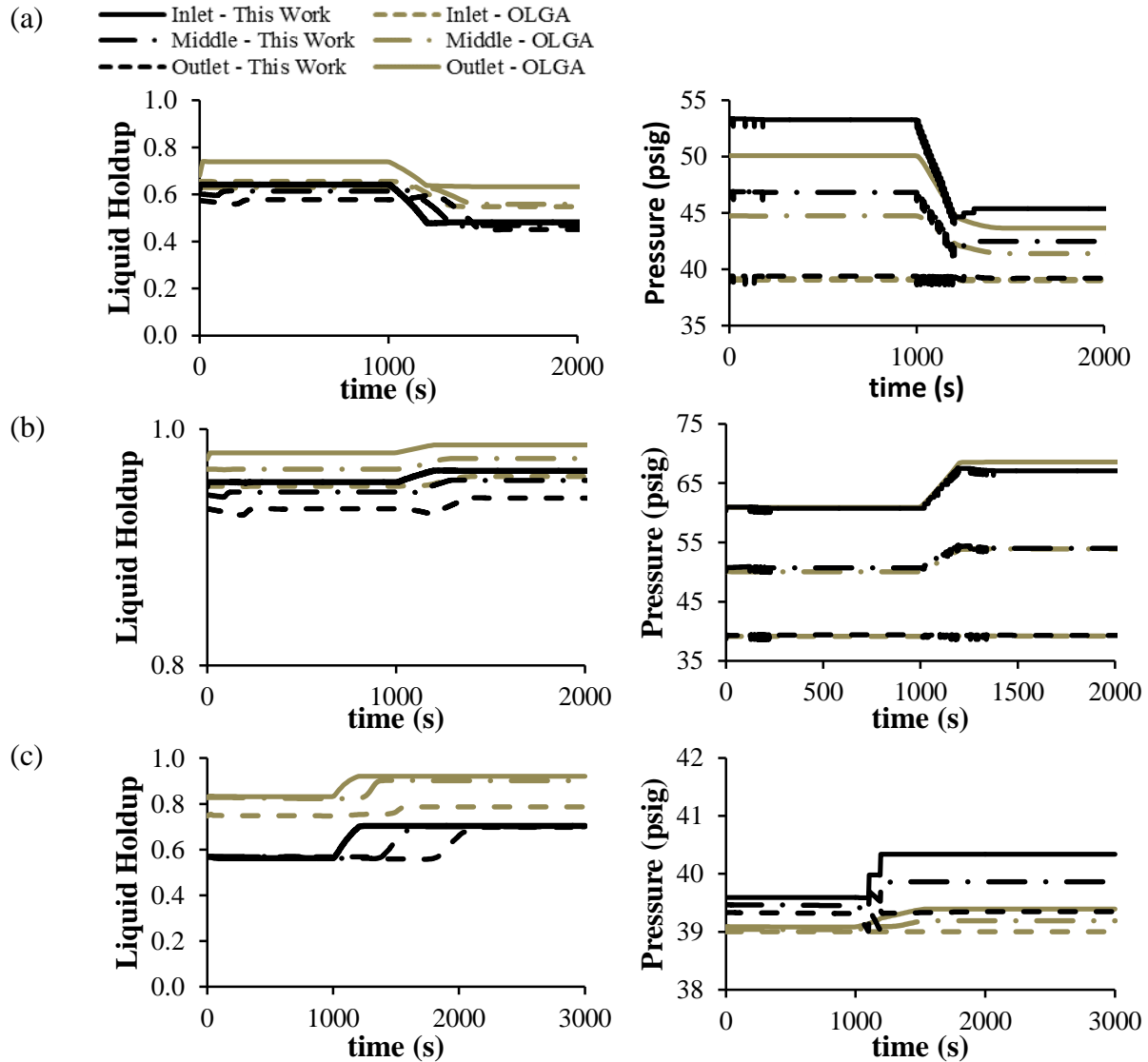


Figure 5.27. Comparison of results using the simplified model and OLGA for liquid holdup and pressure at three locations (inlet, middle and outlet of horizontal pipe) as a function of time, for (a) Case 5, (b) Case 6, and (c) Case 7.

Figure 5.28 and Figure 5.29 show the maximum errors for the liquid holdup and pressure predictions for horizontal flow. As expected, the error for stratified flow regime is higher than for

the other flow regimes, since the formulation in the simplified model adopts a drift-flux simplification, which is not the recommended approach for modelling separated flows such as stratified flow regime.

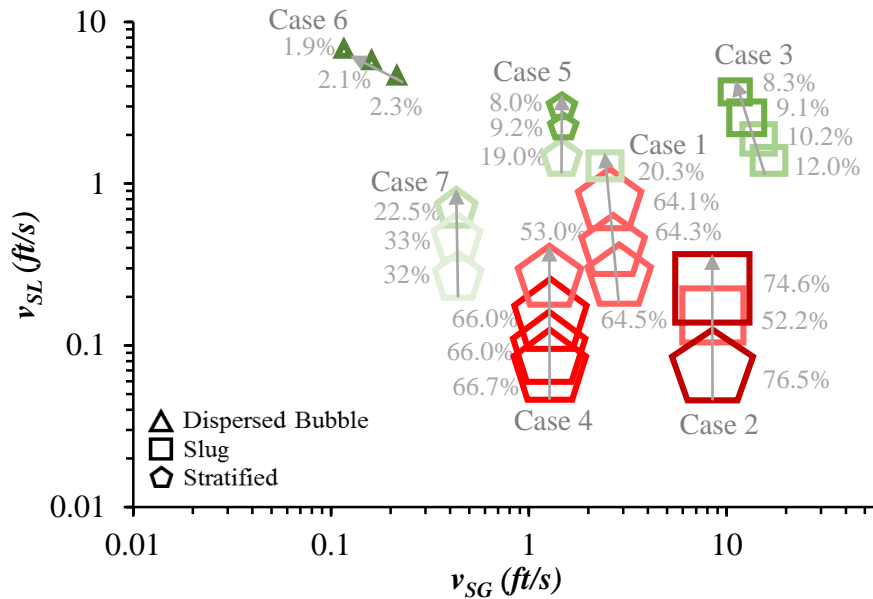


Figure 5.28. Maximum error for liquid holdup predictions for horizontal flow ($\theta = 0^\circ$).

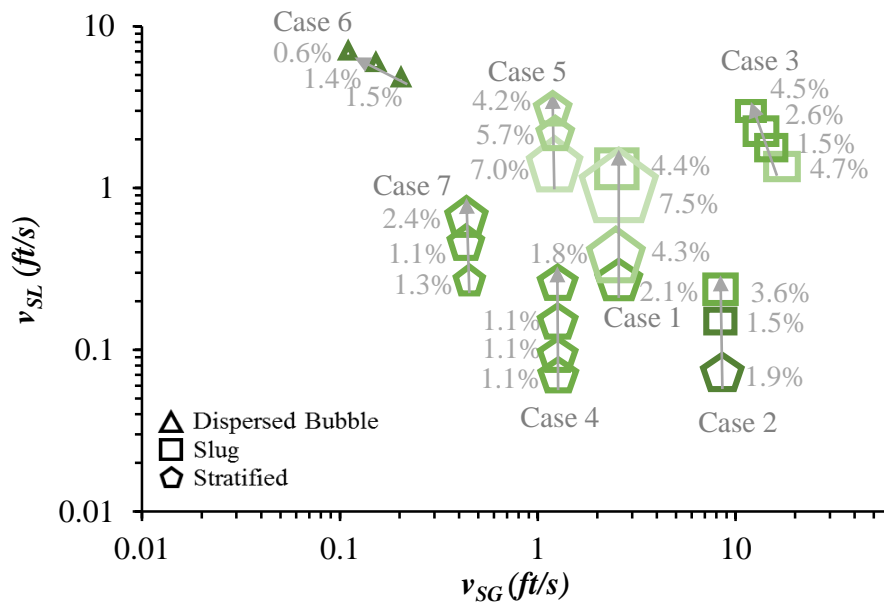


Figure 5.29. Maximum error for pressure predictions for horizontal flow ($\theta = 0^\circ$).

5.3.4. Vertical Upward Flow

Since the experimental data from Waltrich (2012) consisted primarily of churn and annular flow regimes, the commercial simulator OLGA was also used to generate synthetic data for vertical upward flow in bubbly and slug flow regimes, as shown in Table 5.5.

Figure 5.30 and Figure 5.31 show the comparison for liquid holdup and pressure at three locations in the pipe (top, middle, and bottom) as a function of time, using both the simplified model and OLGA simulator.

Table 5.5. Synthetic cases generated with the commercial simulator OLGA for vertical upward flow.

Pipe Inclination (<i>degrees</i>)	Input Gas Rate (<i>Mscf/day</i>)			Input Liquid Rate (<i>STB/day</i>)		Boundary Pressure (<i>psig</i>) (constant)	Flow Regime @ fluid inlet (predicted by OLGA)
	Case	Initial	End	Initial	End		
+90°	1	10	10	100	500	50	Slug/Annular
	2	50	50	1000	5000	60	Slug/Bubbly
	3	20	20	1000	5000	80	Bubbly
	4	5	5	300	700	20	Slug/Bubbly
	5	5	85	20	20	20	Slug

Figure 5.30 shows the case for slug-bubbly flow regime (Case 2). The maximum error for the liquid holdup is lower than 14%, and the maximum error for the pressure is lower than 11%. However, it can be seen that as the simulation runs and the conditions move towards a steady-state condition in the end of the simulation, the error for both liquid holdup and pressure decrease. At the end of the simulation for this case, the error is around 2%.

Figure 5.31 shows a second case for lower liquid velocity (Case 1). For this case, it can be seen that the simplified model does not agree well OLGA results. The beginning of the simulation is predicted as slug flow and then annular flow for the end of the simulation, after the change in flow rate. For this case, the maximum error for the liquid holdup is 61%, and the maximum error for the pressure is 44%

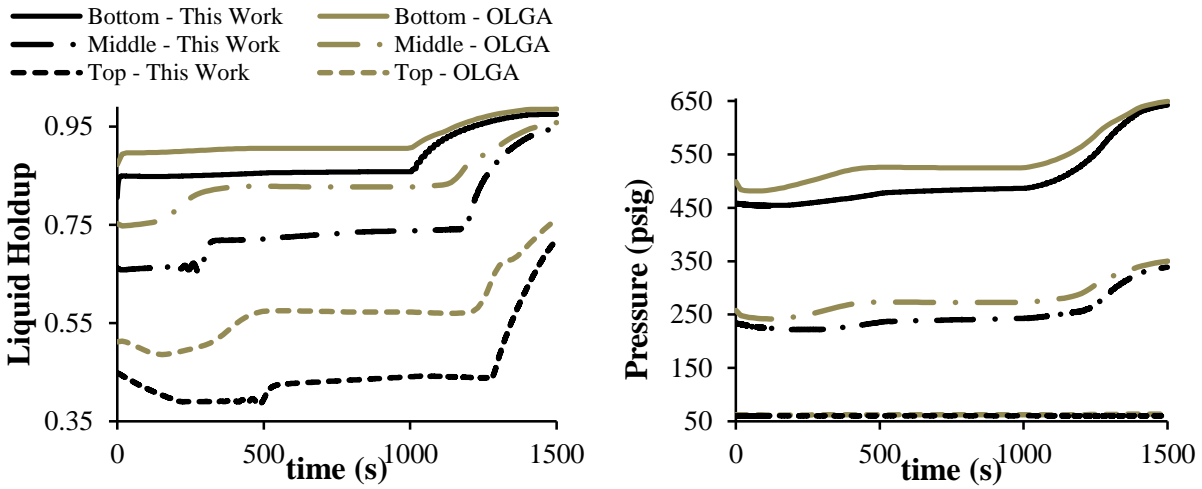


Figure 5.30. Comparison of results using the simulator of this work and OLGA for liquid holdup and pressure at three locations (top, middle and bottom of pipe) as a function of time, for a slug-bubbly flow regime case in vertical upward flow in the tubing.

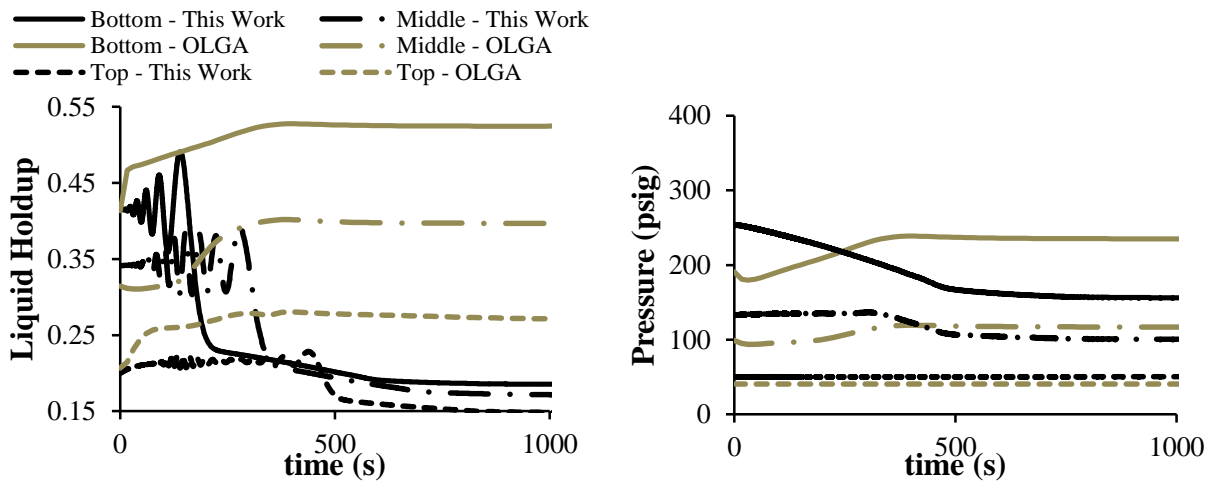


Figure 5.31. Comparison of results using the simulator of this work and OLGA for liquid holdup and pressure at three locations (top, middle and bottom of pipe) as a function of time, for a slug-annular flow regime case in vertical upward flow in the tubing.

Figure 5.32 conveys the information on the trend of liquid holdup and pressure along a vertical tube for Cases 3, 4 and 5, showing the errors for these two variables at the top, middle and bottom grid blocks.

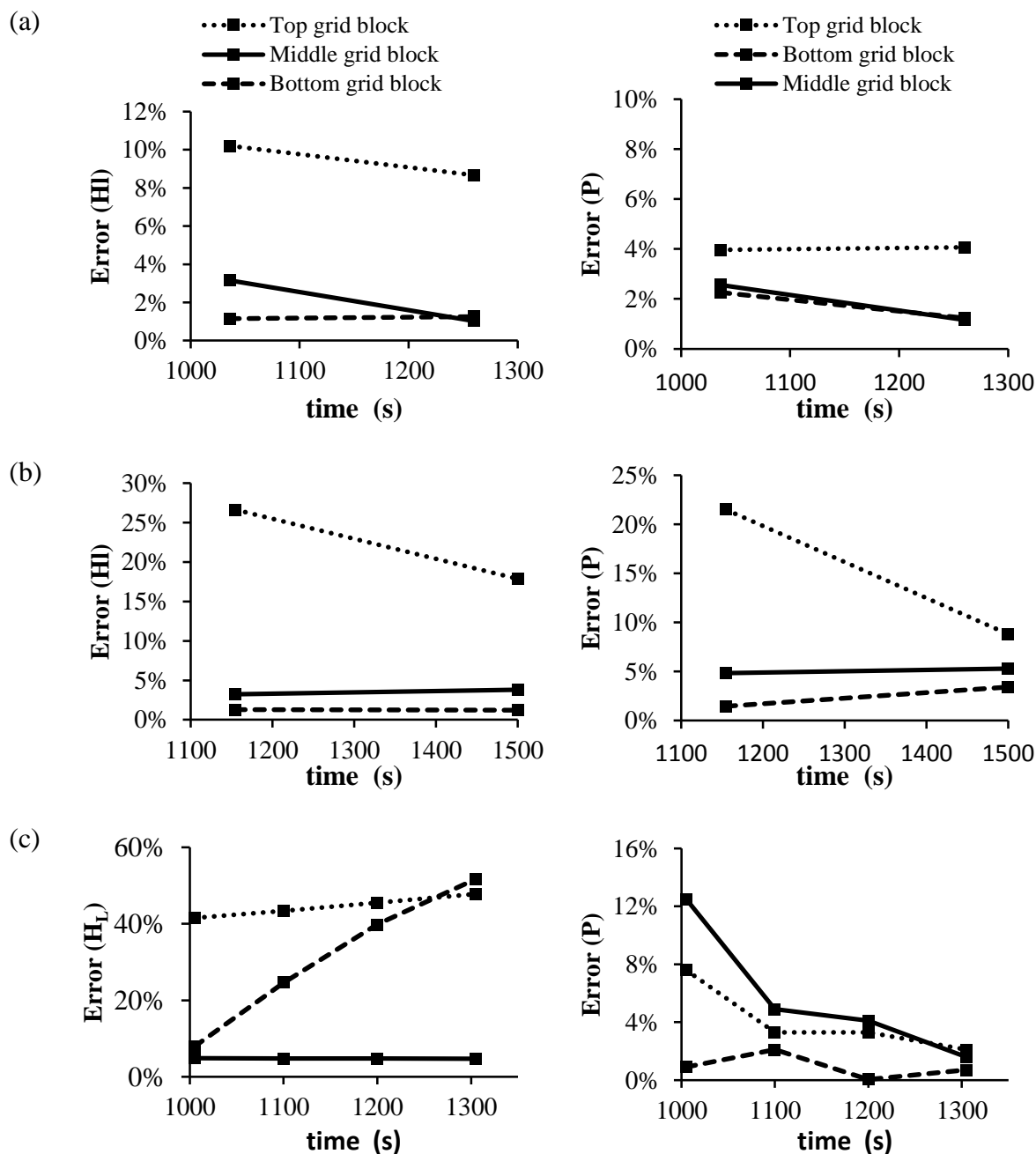


Figure 5.32. Errors for liquid holdup and pressure at the top, middle and bottom grid blocks for (a) Case 3, (b) Case 4, and (c) Case 5.

Based on the comparisons using the experimental data from Waltrich (2012) and the synthetic data generated with OLGA, an error map was also created for vertical upward flow. Figure 5.33 shows the maximum error for the liquid holdup predictions. As can be seen from this figure, the simplified model is fairly accurate in predicting the liquid holdup in bubbly and slug flow regimes, with errors equal or lower than 30% (except for Case 1, which is close to the annular flow regime transition, and Case 5, which is close to the Reynolds number in the range of the discontinuity in the drift-flux parameters correlations). However, Figure 5.34 shows that the maximum error for the pressure predictions is lower than 44% for all flow regimes.

For the experimental data from Waltrich (2012), the error calculated for the liquid holdup in relation to the trend line of the experimental data is extremely high (Figure 5.33), due to the low magnitude of the experimental liquid holdup. The liquid holdup in the cases from Waltrich (2012) is in the range of 0.01 to 0.10. Therefore, a relative difference of 0.01 between the liquid holdup predicted with the model of this work and the experimental value, can represent a percentage error of 100% for the worst case. Since the relative difference is higher than 0.01 for all cases, because the model is not well suited to annular flow regime, the errors are extremely high, reaching more than 300%.

In Figure 5.34, for the case in slug flow regime with the lowest gas and liquid superficial velocities, the Reynolds number is between 200 and 2000. As explained in Section 5.1, for these Reynolds number range, the correlation for the distribution parameter from Bhagwat and Ghajar (2014) has an abrupt change from 2.0 to 1.2. This abrupt change in the distribution parameter is carried out to the superficial velocities and liquid holdup calculated in the model, and consequently to the pressure calculation. This possibly explain why these two cases have a high average error, which is much higher than most of the other cases.

In a nutshell, Figure 5.33 and Figure 5.34 demonstrate that the simplified model shows higher errors as gas and liquid velocities approach annular flow regime.

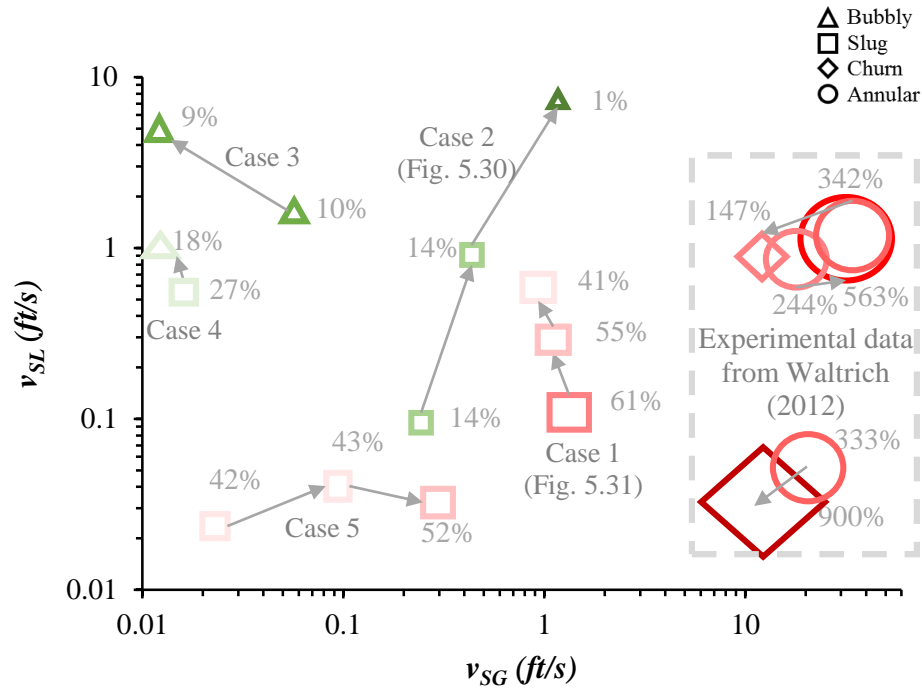


Figure 5.33. Maximum error for holdup prediction for vertical upward flow ($\theta = 90^\circ$).

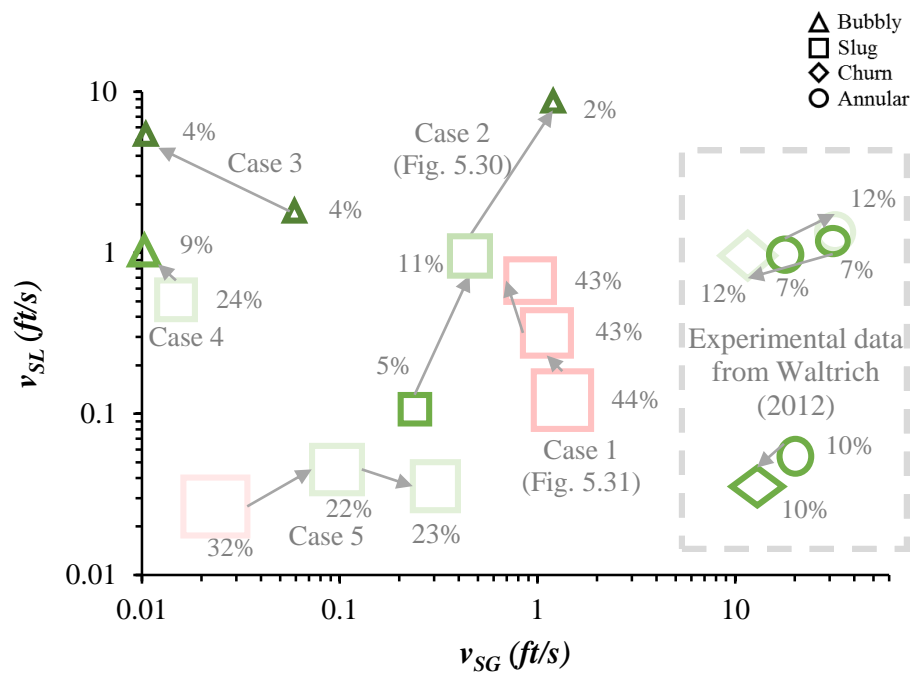


Figure 5.34. Maximum error for pressure predictions for vertical upward flow ($\theta = 90^\circ$).

5.3.5. Inclined Upward Flow

The same analysis was conducted for upward flow in a 45° inclined pipe. Table 5.6 details the cases run for this pipe inclination. Figure 5.35 show the errors for the liquid holdup and pressure at the top, middle and bottom grid blocks, for each case on Table 5.6.

Table 5.6. Synthetic cases generated with the commercial simulator OLGA for inclined upward flow.

Pipe Inclination (degrees)	Input Gas Rate (Mscf/day)			Input Liquid Rate (STB/day)		Boundary Pressure (psig)	Flow Regime @ fluid inlet
	Case	Initial	End	Initial	End	(constant)	(predicted by OLGA)
+45°	1	20	20	1000	5000	80	Slug/Bubbly
	2	5	5	100	500	120	Slug
	3	5	5	1000	2000	120	Bubbly
	4	1000	1000	2000	4000	200	Stratified
	5	1000	1000	100	500	200	Stratified

Figure 5.36 and Figure 5.37 show the maximum errors for the liquid holdup and pressure predictions. It can be seen that the results follow the observations for vertical upward flow, with the difference that for higher gas velocity the stratified flow regime appears, which presents higher errors particularly for the liquid holdup.

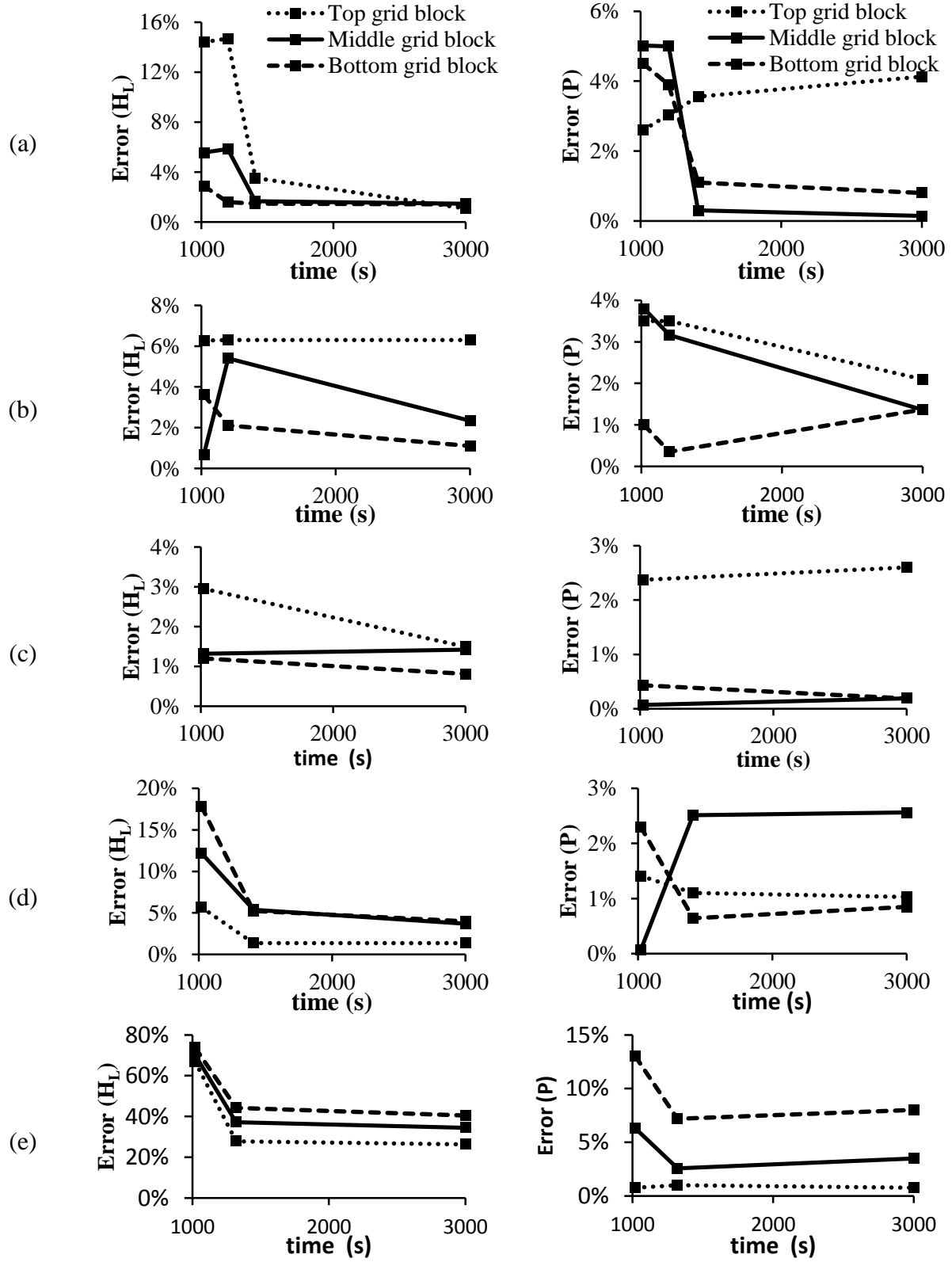


Figure 5.35. Errors for liquid holdup and pressure at the top, middle and bottom grid blocks for (a) Case 1, (b) Case 2, (c) Case 3, (d) Case 4, and (e) Case 5.

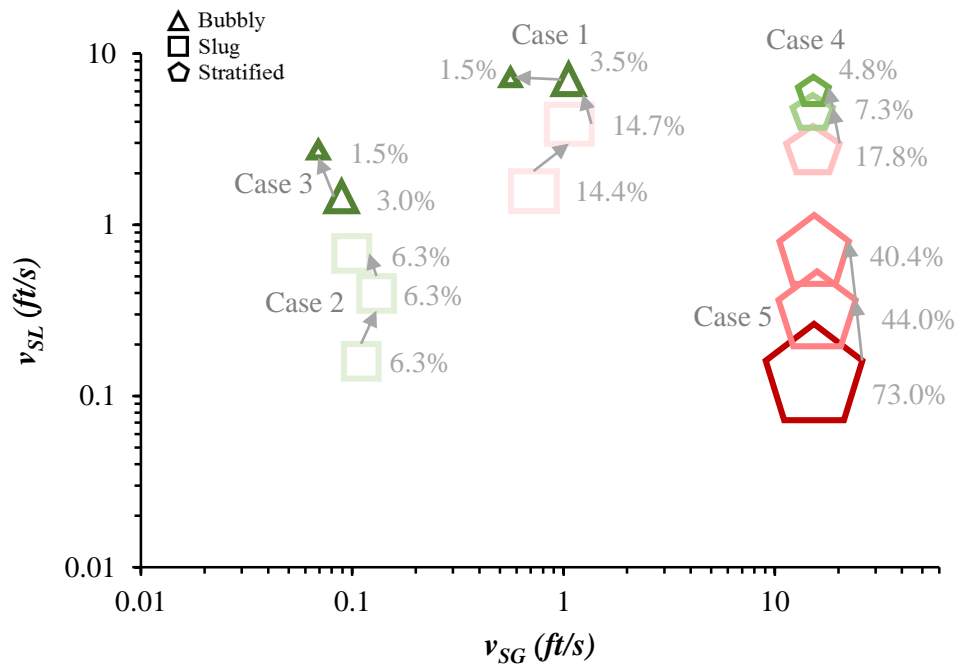


Figure 5.36. Maximum error for the liquid holdup predictions for inclined upward flow ($\theta = 45^\circ$).

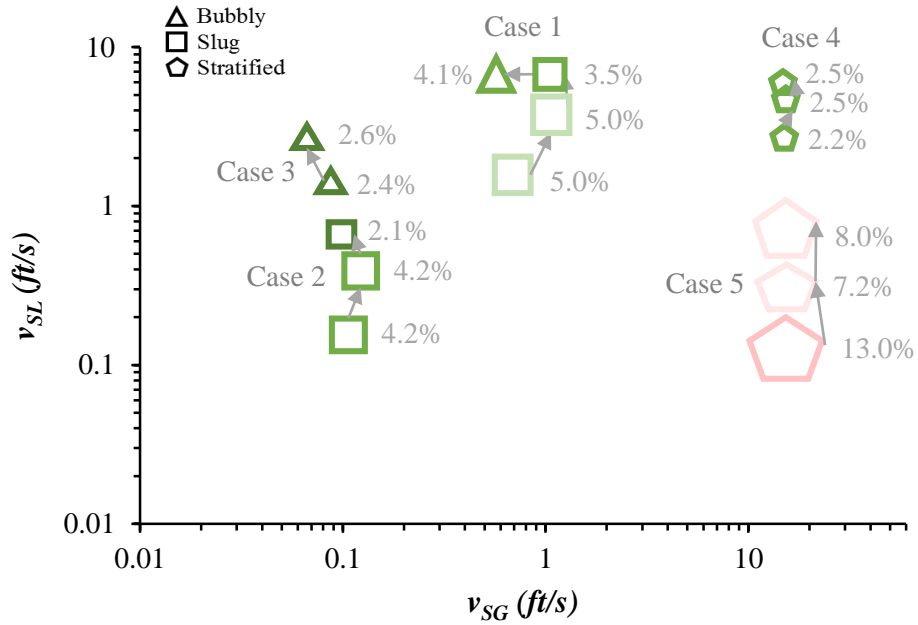


Figure 5.37. Maximum error for pressure predictions for inclined upward flow ($\theta = 45^\circ$).

5.3.6. Summary of the results from the comparison with synthetic data

Figure 5.38 and Figure 5.39 show a summary of the results presented in the previous sections. It can be seen that the results of the simplified model showed an agreement within the range of $\pm 30\%$ for the holdup predictions for 65% of the scenarios, and an agreement within the range of $\pm 30\%$ for the pressure predictions for 82% of the scenarios considered in this work.

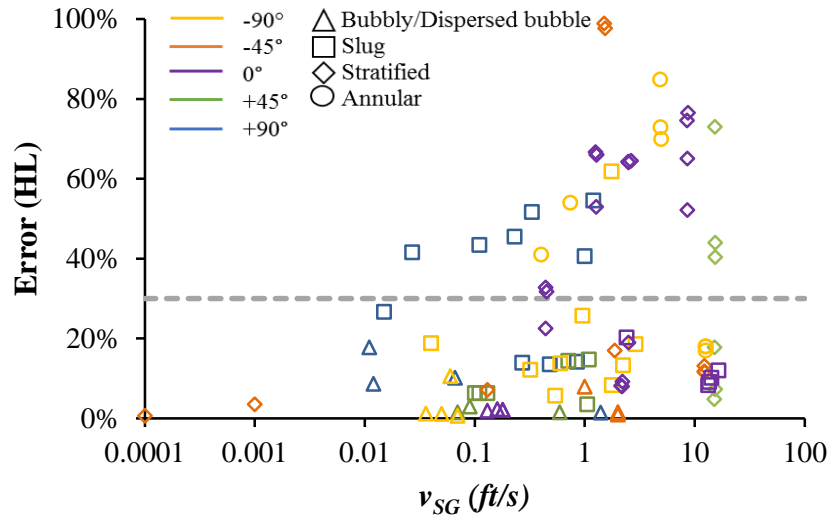


Figure 5.38. Summary of maximum error for liquid holdup for all cases in all pipe inclinations.

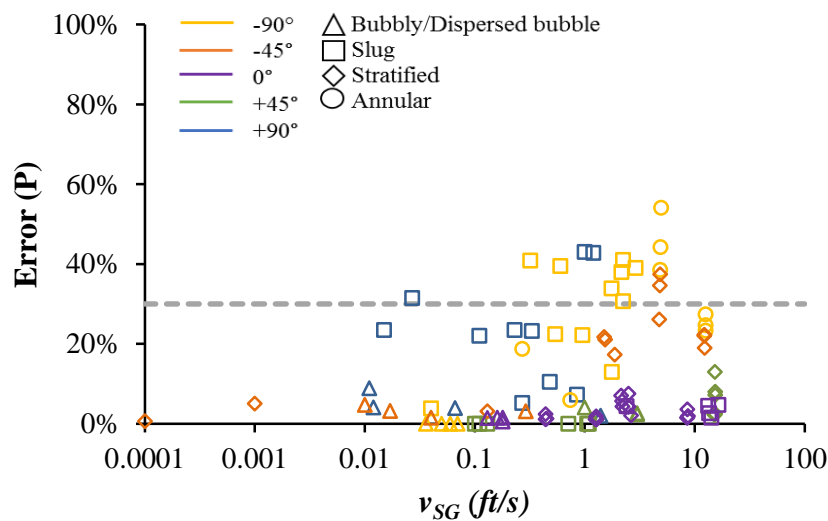


Figure 5.39. Summary of maximum error for pressure for all cases in all pipe inclinations.

Table 5.7 recommends the range of applicability of the simulator develop in this work based on the results presented on this chapter.

Table 5.7. Recommend range of applicability of the simulator developed in this work.

Pipe inclination	Recommend range of applicability
$\theta = -90^\circ$ (vertical downward flow)	$v_{SL} > 2 \text{ ft/s}$ and $v_{SG} < 100 \text{ ft/s}$ For lower liquid superficial velocity, the model doesn't achieve convergence because of the presence of falling film flow regime.
$\theta = -45^\circ$ (inclined downward flow)	$v_{SL} > 0.6 \text{ ft/s}$ and $v_{SG} < 1 \text{ ft/s}$, $v_{SL} > 3 \text{ ft/s}$ and $v_{SG} < 100 \text{ ft/s}$ For $v_{SL} < 0.6 \text{ ft/s}$, the model doesn't converge.
$\theta = 0^\circ$ (horizontal flow)	$v_{SL} < 1 \text{ ft/s}$ and $v_{SG} < 1 \text{ ft/s}$, $v_{SL} > 1 \text{ ft/s}$ and $v_{SG} < 100 \text{ ft/s}$ For conditions outside these ranges - e.g. low v_{SL} and high v_{SG} - high errors incur for the liquid holdup prediction, but not for the pressure prediction. So utilization of the model depends on the user's need.
$\theta = 45^\circ$ (inclined upward flow)	$v_{SL} < 0.01 \text{ ft/s}$ and $v_{SG} < 10 \text{ ft/s}$ $v_{SL} > 3 \text{ ft/s}$ and $v_{SG} > 10 \text{ ft/s}$ For conditions outside these ranges, high errors incur for the liquid holdup prediction as the flow regime approaches stratified, but not for the pressure prediction. So utilization of the model depends on the user's need.
$\theta = 90^\circ$ (vertical upward flow)	$v_{SL} > 0.6 \text{ ft/s}$ and $v_{SG} < 10 \text{ ft/s}$ High errors for the liquid holdup prediction for gas superficial velocity above this limit, as flow regime approaches churn/annular, but not for the pressure prediction. So utilization of the model depends on the user's need.

6. Conclusions and Recommendations for Future Work

This work presented an improvement to the formulation of a simplified transient model from the literature (Choi et al., 2013) and performed a unique and extensive evaluation of the model for a wide range of conditions and pipe inclinations, using different data sets (test well data, experimental data from a flow loop, and synthetic data generated with the commercial simulator OLGA). Envelopes of applicability were provided in order to guide the user on the expected errors of the simplified model. A useful criterion was also derived for the first time from the momentum conservation equation in order to quantitatively differentiate between slow and fast transient phenomena and provide guidance on the employability of the model from this work.

As discussed in the previous chapter, the simplified model developed in this work proved to be fairly accurate at predicting liquid holdup and pressure for transient conditions in bubbly, dispersed bubble, slug and churn flow regimes. For bubbly and dispersed bubble flow regimes the error for liquid holdup and pressure prediction was lower than 17% for all pipe inclinations. For most of the cases in slug and churn flow regimes, the error for the liquid holdup was lower than 45% and the error for the pressure prediction was lower than 24%, for all pipe inclinations. On the other hand, the errors for the cases in annular, stratified and falling film flow regimes, were much higher. However, this was expected, since a drift-flux approach is utilized in the formulation of the simplified transient model, and such approach is not recommended for separated flows.

The objective of implementing the model of this work in a simulator was effectively accomplished. The main advantages of the simulator are:

- Since it is open source, changes can be easily implemented by the user and the code can be modified in order to better suit the needs of the user and to extend the applicability to other flow scenarios. This presents the possibility for continuous improvement.
- Due to its simplicity and the familiarity people have with Microsoft Excel, the simulator is easy-to-use and widely accessible, as it uses a platform (Excel) that is included in most computers nowadays.
- The execution time of the simulator is reasonable. For some of the more complicated cases, the simulator took around 6 *minutes* to run the entire simulation, but simpler cases ran in about 1 *minute*. This is understandable, since Excel VBA is not the most robust language.

Based on the findings presented in Chapter 5 and the points just mentioned, some suggestions for future work include:

- Validation of the model with field data, to confirm the assumption of applicability for hydrocarbon fluids.
- Definition of an improved criteria for comparing the results of the simulator with experimental and synthetic data. A comprehensive comparison is complicated by the number of parameters and dimensions to be analyzed (results in both space and time).
- Using a real-time experimental approach or employing machine learning for obtaining the drift flux parameters and improving the drift-flux correlations for low liquid holdup values, in order to improve the performance of the model for annular and stratified flow regimes.
- In order to improve execution time, the simulator could be switched to other programming language and an interface could be designed just to show the results after the simulation. Or to take advantage of the simplicity of Excel interface for the results, only the code could be saved as an executable in other language.

Appendix A. Bhagwat and Ghajar (2014) Drift-Flux Distribution Parameter and Drift Velocity Correlations

The correlation for the distribution parameter (C_o) is given by:

$$C_o = \frac{2 - (\rho_G/\rho_L)^2}{1 + (Re_{TP}/1000)^2} + \frac{\left[\left(\sqrt{(1 + (\rho_g/\rho_l)^2 \cos\theta)/(1 + \cos\theta)} \right)^{(1-\alpha)} \right]^{2/5} + C_{o,1}}{1 + (Re_{TP}/1000)^2} \quad (A.1)$$

with $C_{o,1}$ is calculated as

$$C_{o,1} = \left(C_1 - C_1 \sqrt{(\rho_g/\rho_l)} \right) [(2.6 - \beta)^{0.15} - \sqrt{f_{TP}}] (1 - x)^{1.5} \quad (A.2)$$

where Re_{TP} is the two-phase mixture Reynolds number, θ is the pipe orientation (measured from the horizontal), α is the void fraction ($1 - H_L$), β is the gas volumetric flow fraction, f_{TP} is the two-phase friction factor (calculated using Colebrook (1939) equation), x is the two-phase flow quality, and C_1 is a constant that assumes the value of 0.2 for circular and annular pipe geometries. For $0^\circ > \theta \geq -50^\circ$ and $Fr_{sg} \leq 0.1$, $C_{o,1}$ assumes a value of zero.

The gas volumetric flow fraction is calculated as:

$$\beta = \frac{v_{SG}}{v_{SG} + v_{SL}} \quad (A.3)$$

The two-phase mixture Reynolds number is calculated as:

$$Re_{TP} = \frac{v_m \rho_L D_h}{\mu_L} \quad (A.4)$$

where v_m is the mixture velocity, D_h is the hydraulic diameter, and μ_L is the liquid phase viscosity.

The distribution parameter takes a value close to 1.2 for vertical bubbly and slug flow, and approaches unity as the flow pattern shifts to annular flow regime. However, for horizontal and near horizontal downward inclined pipe orientations, the distribution parameter is less than unity (Bhagwat and Ghajar, 2014).

The correlation for the drift velocity is given by:

$$v_d = (0.35\sin\theta + 0.45\cos\theta) \sqrt{\frac{gD_h(\rho_L - \rho_G)}{\rho_L}} (1 - \alpha)^{0.5} C_2 C_3 C_4 \quad (\text{A.5})$$

where the variables C_2 , C_3 and C_4 given by:

$$C_2 = \left(\frac{0.434}{\log_{10}(\mu_l/0.001)} \right)^{0.15}, \text{ if } (\mu_l/0.001) > 10 \quad (\text{A.6})$$

$$C_2 = 1, \text{ if } (\mu_l/0.001) \leq 10$$

$$C_3 = (La/0.025)^{0.9}, \text{ if } La < 0.025 \quad (\text{A.7})$$

$$C_3 = 1, \text{ if } La \geq 0.025$$

$$C_4 = -1, \text{ if } (0^\circ > \theta \geq -50^\circ \text{ and } Fr_{sg} \leq 0.1) \quad (\text{A.8})$$

$$C_4 = 1, \text{ elsewhere}$$

where La is the Laplace variable defined as the inverse of the non-dimensional hydraulic pipe diameter:

$$La = \sqrt{\frac{\sigma/g\Delta\rho}{D_h}} \quad (\text{A.9})$$

where σ is the interfacial tension.

The Froude number based on the superficial gas velocity in Eq. (A.8) is given by:

$$Fr_{sg} = \sqrt{\frac{\rho_g}{\rho_g - \rho_l}} \frac{v_{SG}}{\sqrt{gD_h \cos\theta}} \quad (\text{A.10})$$

The drift velocity is maximum for bubbly flow and becomes negligibly small for annular flow.

References

- Almabrok, A. A., Aliyu, A. M., Lao, L., & Yeung, H. (2016). Gas/liquid flow behaviours in a downward section of large diameter vertical serpentine pipes. *International Journal of Multiphase Flow*, 78, 25–43.
- Al-Safran, E.M., & Brill, J.P. (2017). *Applied Multiphase Flow in Pipes and Flow Assurance*. Society of Petroleum Engineers.
- Ambrus, A., Aarsnes, U. J. F., Vajargah, A. K., Akbari, B., & Oort, E. van. (2015). A Simplified Transient Multi-Phase Model for Automated Well Control Applications. *International Petroleum Technology Conference*. doi:10.2523/IPTC-18481-MS
- Ansari, A. M., Sylvester, N. D., Sarica, C. Shoham, O., & Brill, J. P. (1994). A Comprehensive Mechanistic Model for Upward Two-Phase Flow in Wellbores. *SPE Production and Facilities*, 9 (02): 143-152. SPE-20630-PA. <http://dx.doi.org/10.2118/20630-PA>.
- Aziz, K., & Govier, G. W. (1972). *Pressure Drop In Wells Producing Oil And Gas*. Petroleum Society of Canada. doi:10.2118/72-03-04
- Barnea, D., Shoham, O., & Taitel, Y. (1982). Flow pattern transition for downward inclined two phase flow; horizontal to vertical. *Chemical Engineering Science*, 37(5), 735–740.
- Beggs, D. H., & Brill, J. P., (1973). A study of two-phase flow in inclined pipes. *J. Petroleum Technology*. 25 (05), 607-617. SPE-4007-PA. <http://dx.doi.org/10.2118/4007-PA>.
- Bendiksen, K.H., Maines, D., Moe, R., and Nuland, S. (1991). The Dynamic Two-Fluid Model Olga: Theory and Application. *SPE Production Engineering* 6 (2). <http://dx.doi.org/10.2118/19451-PA>.
- Bhagwat, S. M., & Ghajar, A. J. (2012). Similarities and differences in the flow patterns and void fraction in vertical upward and downward two phase flow. *Experimental Thermal and Fluid Science*, 39, 213–227.
- Bhagwat, S. M., & Ghajar, A. J. (2014). A flow pattern independent drift flux model based void fraction correlation for a wide range of gas–liquid two phase flow. *International Journal of Multiphase Flow*, 59, 186–205.
- Brill, J. P., & Mukherjee, H. K. (1999). *Multiphase Flow in Wells*, first printing. Richardson, Texas: Society of Petroleum Engineers Incorporated (Reprint).
- Choi, J., Pereyra, E., Sarica, C., Lee, H., Jang, I. S., & Kang, J. (2013). Development of a

fast transient simulator for gas–liquid two-phase flow in pipes. *Journal of Petroleum Science and Engineering*, 102, 27–35. <https://doi-org.libezp.lib.lsu.edu/10.1016/j.petrol.2013.01.006>

Colebrook, C.F. (1939). Turbulent flow in pipes, with particular reference to the transition between the smooth and rough pipe laws. *Journal of the Institution of Civil Engineers*, 11, 1938–1939.

Courant, R., Friedrichs, K. O., & Lewy, H. (1955). On the partial difference equations of mathematical physics being a translation of *Über die partiellen Differenzengleichungen der mathematischen Physik*. Ithaca, N.Y..

Coutinho, R. (2018). Experimental and Numerical Investigation of Liquid-Assisted Gas-Lift Unloading. LSU Doctoral Dissertations.

Danielson, T. J., Brown, L. D., & Bansal, K. M. (2000). Flow Management: Steady-State and Transient Multiphase Pipeline Simulation. Offshore Technology Conference. doi:10.4043/11965-MS

Duns Jr., H., & Ros, N. C. J. (1963). Vertical flow of gas and liquid mixtures in wells. In 6th World Petroleum Congress, Frankfurt, Germany, 19-26 June 1963.

Fan, Y., & Danielson, T. J. (2009). Use of Steady State Multiphase Models To Approximate Transient Events. Society of Petroleum Engineers. doi:10.2118/123934-MS

Goda, H., Hibiki, T., Kim, S., Ishii, M., & Uhle, J. (2003). Drift-flux model for downward two-phase flow. *International Journal of Heat and Mass Transfer*, 46(25), 4835–4844.

Golan, L. P., & Stenning, A. H. (1969). Two-Phase Vertical Flow Maps. *Proceedings of the Institution of Mechanical Engineers, Conference Proceedings*, 184(3), 108–114.

Hagedorn, A. R., & Brown, K. E. (1965). Experimental study of pressure gradients occurring during continuous two-phase flow in small-diameter vertical conduits. *J. Petroleum Technology* **17** (04), 475-484. SPE-940-PA. <http://dx.doi.org/10.2118/940-PA>.

Hasan, A. R. (1995). Void Fraction in Bubbly and Slug Flow in Downward Two-Phase Flow in Vertical and Inclined Wellbores. Society of Petroleum Engineers. doi:10.2118/26522-PA

Hasan, A. R., & Kabir, C. S. (1988). A Study of Multiphase Flow Behavior in Vertical Wells. Society of Petroleum Engineers. doi:10.2118/15138-PA

Hasan, A. R., & Kabir, C. S. (1988). Predicting Multiphase Flow Behavior in a Deviated Well. Society of Petroleum Engineers. doi:10.2118/15449-PA

Hasan, A.R., & Kabir, C.S. (1990). Performance of a two-phase gas/liquid flow model in vertical wells. *Journal of Petroleum Science and Engineering*, 4(3), 273–289.

Henriot, V., & Pauchon, C. (1997). Tacite: Contribution Of Fluid Composition Tracking On Transient Multiphase Flow Simulation. Offshore Technology Conference. doi:10.4043/8563-MS

Hernandez, A., Gonzalez, L., & Gonzalez, P. (2002). Experimental Research on Downward Two-Phase Flow. Society of Petroleum Engineers. doi:10.2118/77504-MS

Hibiki, T., & Ishii, M. (2002). Distribution parameter and drift velocity of drift-flux model in bubbly flow. *International Journal of Heat and Mass Transfer*, 45(4), 707–721.

Ishii, M. (1977). One-dimensional drift-flux model and constitutive equations for relative motion between phases in various two-phase flow regimes. doi:10.2172/6871478.

Li, J., Teixeira, M. A., & Fan, Y. (2012). Performance Evaluation of a New Simplified Transient Two-Phase Flow Modeling. Society of Petroleum Engineers. doi:10.2118/151034-MS

Lorentzen, R. J., Fjelde, K. K., Frøyen, J., Lage, A. C. V. M., Nævdal, G., & Vefring, E. H. (2001). Underbalanced and Low-head Drilling Operations: Real Time Interpretation of Measured Data and Operational Support. Society of Petroleum Engineers. doi:10.2118/71384-MS

Malekzadeh, R., Belfroid, S. P. C., & Mudde, R. F. (2012). Transient drift flux modelling of severe slugging in pipeline-riser systems. *International Journal of Multiphase Flow*, 46, 32–37.

Masella, J., Tran, Q., Ferre, D., & Pauchon, C. (1998). Transient simulation of two-phase flows in pipes. *Int. Journal of Multiphase Flow*, 24(5), 739–755.

Minami, K. (1991). Transient flow and pigging dynamics in two-phase pipelines. PhD Dissertation, U. of Tulsa.

Minami, K., & Shoham, O. (1994). Transient two-phase flow behavior in pipelines-experiment and modeling. *International Journal of Multiphase Flow*, 20(4), 739–752. [https://doi-org.libezp.lib.lsu.edu/10.1016/0301-9322\(94\)90042-6](https://doi-org.libezp.lib.lsu.edu/10.1016/0301-9322(94)90042-6)

Mukherjee, H., & Brill, J. P. (1985). Pressure Drop Correlations for Inclined Two-Phase Flow. *Journal of Energy Resources Technology*, 107(4), 549.

Nicklin, D.J., Wilkes, J.O., Davidson, J.F., 1962. Two phase flow in vertical tubes. *Transactions of the Institution of Chemical Engineers*, 40, 61–68.

- OLGA Dynamic Multiphase Flow Simulator. 2000. Schlumberger.
- Orkiszewski, J. (1967). Predicting Two-Phase Pressure Drops in Vertical Pipe. Society of Petroleum Engineers. doi:10.2118/1546-PA
- Oshinowo, T., & Charles, M. E. (1974). Vertical two-phase flow part I. Flow pattern correlations. Canadian Journal of Chemical Engineering, 52(1), 25.
- Pauchon, C. L., & Dhulesia, H. (1994, January 1). TACITE: A Transient Tool for Multiphase Pipeline and Well Simulation. Society of Petroleum Engineers. doi:10.2118/28545-MS
- Rassame, S., & Hibiki, T. (2018). Drift-flux correlation for gas-liquid two-phase flow in a horizontal pipe. International Journal of Heat and Fluid Flow, 69, 33–42.
- Shi, H., Holmes, J., Durlofsky, L., Aziz, K., Diaz, L., Alkaya, B., & Oddie, G. (2005). Drift-flux modeling of two-phase flow in wellbores. SPE JOURNAL, 10(1), 24–33.
- Shoham, O. 2006. *Mechanistic modeling of gas-liquid two-phase flow in pipes*. Richardson, TX: Society of Petroleum Engineers (Reprint).
- Taitel, Y., & Dukler, A. E. (1976). Model for predicting flow regime transitions in horizontal and near horizontal gas-liquid flow. AIChE Journal, 22, 47–55.
- Taitel, Y., Barnea, D., & Dukler, A. E. (1980). Modelling flow pattern transitions for steady upward gas-liquid flow in vertical tubes. AIChE Journal, 26(3), 345.
- Taitel, Y., Shoham, O., & Brill, J. P. (1989). Simplified transient solution and simulation of two-phase flow in pipelines. Chemical Engineering Science, 44(6), 1353–1359. [https://doi-org.libezp.lib.lsu.edu/10.1016/0009-2509\(89\)85008-0](https://doi-org.libezp.lib.lsu.edu/10.1016/0009-2509(89)85008-0)
- Usui, K. (1989). Vertically Downward Two-Phase Flow, II – Flow Regime Transition Criteria. Journal of Nuclear Science and Technology, 26(11), 1013–1022. <https://doi-org.libezp.lib.lsu.edu/10.1080/18811248.1989.9734422>
- Usui, K., & Sato, K. (1989). Vertically Downward Two-Phase Flow, I – Void Distribution and Average Void fraction. Journal of Nuclear Science and Technology, 26(7), 670–680. <https://doi-org.libezp.lib.lsu.edu/10.1080/18811248.1989.9734366>
- Vigneron, F., Sarica, C., & Brill, J. (1995). Experimental Analysis of Imposed Two-Phase Flow Transients in Horizontal Pipes. BHR Group Conference Series Publication, 14, 199–218.

- Wallis, G. B. (1969). One-dimensional two-phase flow. New York: McGraw-Hill.
- Yamazaki, Y., & Yamaguchi, K. (1979). Characteristics of Cocurrent Two-Phase Downflow in Tubes: Flow Pattern, Void Fraction and Pressure Drop. *Journal of Nuclear Science & Technology*, 16(4), 245.
- McCain, W. D. (1973). The properties of petroleum fluids. Tulsa: Petroleum Pub. Co.
- Zuber, N., & Findlay, J. A. (1965). Average Volumetric Concentration in Two-Phase Flow Systems. *ASME. Journal of Heat Transfer*, 87(4), 453–468. doi: <https://doi.org/10.1115/1.3689137>
- Waltrich, Paulo (2012). Onset and Subsequent Transient Phenomena of Liquid Loading in Gas Wells: Experimental Investigation Using a Large Scale Flow Loop. Doctoral dissertation, Texas A&M University.
- Waltrich, P. J., Falcone, G., & Barbosa, J. J. R. (2015). Liquid transport during gas flow transients applied to liquid loading in long vertical pipes. *Experimental Thermal and Fluid Science*, 68, 652–662. <https://doi-org.libezp.lib.lsu.edu/10.1016/j.expthermflusci.2015.07.004>
- Shippen, M., & Bailey, W. J. (2012). Steady-State Multiphase Flow—Past, Present, and Future, with a Perspective on Flow Assurance. *Energy Fuels*, 26, 7, 4145-415. <https://doi.org/10.1021/ef300301s>
- Lindfield, G.R., & Penny, J.E.T. (2012). *Numerical Methods* (Third Edition), Academic Press, 67-145, ISBN 9780123869425, <https://doi.org/10.1016/B978-0-12-386942-5.00002-3>
- Tang, H., Bailey, W. J., Stone, T., & Killough, J. (2019). A Unified Gas/Liquid Drift-Flux Model for All Wellbore Inclinations. *Society of Petroleum Engineers*. doi:10.2118/197068-PA

Vita

Ligia Tornisiello received her Bachelor's degree in Petroleum Engineering from Universidade Federal do Ceara (UFC). She was accepted into the LSU Petroleum Engineering program where she anticipates graduating with her Master's degree in December 2019.